DEVELOPMENT OF CARBON FABRIC-REINFORCED POLYLACTIC ACID/ACRYLONITRILE BUTADIENE STYRENE MULTILAYER COMPOSITES

A THESIS SUBMITTED TO
THE GRADUATE SCHOOL OF NATURAL AND APPLIED SCIENCES
OF
MIDDLE EAST TECHNICAL UNIVERSITY

BY

İREM ÖZTÜRK

IN PARTIAL FULFILLMENT OF THE REQUIREMENTS
FOR
THE DEGREE OF MASTER OF SCIENCE
IN
CHEMICAL ENGINEERING

AUGUST 2021

Approval of the thesis:

DEVELOPMENT OF CARBON FABRIC-REINFORCED POLYLACTIC ACID/ACRYLONITRILE BUTADIENE STYRENE MULTILAYER COMPOSITES

submitted by **İREM ÖZTÜRK** in partial fulfillment of the requirements for the degree of **Master of Science** i**n Chemical Engineering, Middle East Technical University** by,

Prof. Dr. Halil Kalıpçılar
Dean, Graduate School of **Natural and Applied Sciences** _____

Prof. Dr. Pınar Çalık
Head of the Department, **Chemical Engineering** _____

Prof. Dr. Göknur Bayram
Supervisor, **Chemical Engineering, METU** _____

Examining Committee Members:

Prof. Dr. Necati Özkan
Polymer Science and Technology, METU _____

Prof. Dr. Göknur Bayram
Chemical Engineering, METU _____

Assoc. Prof. Dr. Erhan Bat
Chemical Engineering, METU _____

Assoc. Prof. Dr. Hande Çelebi
Chemical Engineering, Eskişehir Technical Uni. _____

Assoc. Prof. Dr. Sezer Özerinç
Mechanical Engineering, METU _____

Date: 11.08.2021

I hereby declare that all information in this document has been obtained and presented in accordance with academic rules and ethical conduct. I also declare that, as required by these rules and conduct, I have fully cited and referenced all material and results that are not original to this work.

Name, Last name: İrem Öztürk

Signature :

ABSTRACT

DEVELOPMENT OF CARBON FABRIC-REINFORCED POLYLACTIC ACID/ACRYLONITRILE BUTADIENE STYRENE MULTILAYER COMPOSITES

Öztürk, İrem
Master of Science, Chemical Engineering
Supervisor: Prof. Dr. Göknur Bayram

August 2021, 119 pages

Multilayer composites are in concern of both world of material science and the industry because of providing enhanced mechanical properties with ultra lightweight. Also, there is a growing demand to use of recyclable, biodegradable materials in polymer composites for the sake of environmental health.

In this study, polymer blends were prepared with polylactic acid (PLA) and acrylonitrile butadiene styrene (ABS) with 10, 30, and 50 wt.%. To compatibilize these polymers, styrene-ethylene-butylene-styrene terpolymer grafted with maleic anhydride (SEBS-MAH), ethylene-glycidyl methacrylate copolymer (E-GMA), styrene-maleic anhydride (SMA), and styrene-acrylonitrile-glycidyl methacrylate (SAN-GMA) with 5, 10, and 15 wt.%. were added. The polymer blending was carried out using a co-rotating twin screw extruder. The polymer layers of multilayer composites were prepared with neat PLA, 70PLA/30ABS and 10SAN-GMA/(70PLA/30ABS), and reinforced with one and three layers carbon fabric (CF). The multilayer composites were produced with compression molding process. The

polymer blends and the multilayer composites were mainly characterized in terms of their physical properties and morphologies.

While all binary blends have approximately the same impact strength values, tensile strength of 70PLA/30ABS blend was 40% higher than other binary blends. The addition of 10 wt.% SAN-GMA into PLA/ABS blends resulted in maximum impact strength of 27.0 kJ/m^2 among the ternary blends. Composites with three layers CF exhibited higher mechanical properties than the composites with one layer CF. SAN-GMA compatibilizer was efficient in decreasing the interfacial tension between PLA and ABS. However, it did not yield the same performance when used in the polymer layers of the multilayer composites.

Keywords: Polylactic Acid, Acrylonitrile Butadiene Styrene, Carbon Fabric, Thermoplastic Multilayer Composites, Modification

ÖZ

KARBON KUMAŞ İLE GÜÇLENDİRİLMİŞ POLİLAKTİK ASİT/AKRİLONİTRİL BÜTADİEN STİREN ÇOK KATMANLI KOMPOZİTLERİN GELİŞTİRİLMESİ

Öztürk, İrem
Yüksek Lisans, Kimya Mühendisliği
Tez Yöneticisi: Prof. Dr. Göknur Bayram

Ağustos 2021, 119 sayfa

Çok katmanlı kompozitler, ultra hafif ağırlıkla birlikte gelişmiş mekanik özellikler sağladıkları için hem malzeme bilimi dünyasının hem de endüstrinin ilgisini çekmektedir. Ayrıca çevre sağlığı için geri dönüştürülebilir, biyolojik olarak parçalanabilir malzemelerin polimer kompozitlerinde kullanımına yönelik artan bir talep vardır.

Bu çalışmada, polimer karışımları polilaktik asit (PLA) ve ağırlıkça %10, %30 ve %50 akrilonitril bütadien stiren (ABS) kullanılarak hazırlanmıştır. Bu polimerleri uyumlu hale getirmek için, maleik anhidrit aşılanmış stiren-etilen-bütilen-stiren terpolimeri (SEBS-MAH), etilen-glisidil metakrilat kopolimeri (E-GMA), stiren-maleik anhidrit (SMA) ve stiren-akrilonitril-glisidil metakrilat (SAN-GMA), ağırlıkça %5, %10 ve %15 olarak eklenmiştir. Polimer harmanlama, aynı yönde dönen çift vidalı bir ekstrüder kullanılarak gerçekleştirilmiştir. Çok katmanlı kompozitlerin polimer tabakaları, saf PLA, 70PLA/30ABS ve 10SAN-GMA/(70PLA/30ABS) kullanılarak hazırlanmış, ve bir ve üç katmanlı karbon kumaş ile güçlendirilmiştir. Çok katmanlı kompozitler basınçlı kalıplama prosesi ile

üretilmiştir. Polimer karışımları ve çok katmanlı kompozitler esas olarak fiziksel özellikleri ve morfolojileri açısından karakterize edilmiştir.

Tüm ikili karışımlar yaklaşık olarak aynı darbe dayanımı değeri gösterirken, 70PLA/30ABS karışımının çekme mukavemeti, diğer ikili karışımlara göre %40 daha fazladır. PLA/ABS karışımına ağırlıkça %10 SAN-GMA'nın eklenmesi, üçlü karışımlar arasında en yüksek darbe dayanımı olan 27.0 kJ/m^2 ile sonuçlanmıştır. Üç tabaka karbon kumaş içeren kompozitler, bir tabakalı olanlara göre daha yüksek mekanik özellikler göstermiştir. SAN-GMA uyumlaştırıcısı PLA ve ABS arasındaki arayüz gerilimini düşürmekte etkili olmuştur. Ancak çok katmanlı kompozitlerin polimer tabakalarında kullanıldığı durumda aynı etkiyi sağlayamamıştır.

Anahtar Kelimeler: Polilaktik Asit, Akrilonitril Bütadien Stiren, Karbon Kumaş, Termoplastik Çok Katmanlı Kompozitler, Modifikasyon

To my mom and dad …

Birsen & Şadi ÖZTÜRK

ACKNOWLEDGMENTS

I would like to express my deepest gratitude to my supervisor Prof. Dr. Göknur Bayram for her guidance and enlightenment throughout my research. It was an honor for me to work with her. I appreciate for her positive attitude and kindness in every phase of the study. She always motivated me to go beyond my limits and shared her knowledge. I wish to thank her for her valuable support.

I want to thank my lab mates, Dr. Berrak Erkmen, Dr. Merve Özkutlu and Ümran Aşçı in Polymer Research Laboratory for sharing their experiences and their full of help throughout my experiments.

This work was supported by the Scientific Research Projects Coordination of the Middle East Technical University [Grant number: TEZ-YL-304-2020-10195].

For the procurement of Novodur HD M203FC, Xibond 920 and Xibond 250, Songnox1076 and Songnox1680, I would like to thank INEOS Styrolution, Polyscope and Grolman Kimya Tic. Ltd. Şti., and Biesterfeld, respectively.

This thesis would not have been accomplished without the love and support of my kindhearted friends, Elif Kurt and Çağla Bozcuoğlu. Elif and I have shared every single occasion in life since we attended METU. Without her encouragement, life would be difficult. Çağla entered my life at the beginning of my master's study but she taught me that what matters is not the number of years that spent together but the sincere friendship. I feel very lucky to have you, girls. Thank you!

My special thanks go to my sister and brother, Zeynep Öztürk Yurt and Hünkar Kemal Yurt. They gave me endless love and support in all parts of my life. They taught me that distance means nothing when the hearts are together.

I would like to express my sincere appreciation to my beloved family. I always feel grateful for having such supportive and lovely mom and dad, Birsen Öztürk and Şadi Öztürk. They always remind me that there are more important things in life than academic records and provide me every opportunity to succeed in life. I am very proud of being your daughter!

TABLE OF CONTENTS

APPENDICES

LIST OF TABLES

TABLES

LIST OF FIGURES

FIGURES

LIST OF SYMBOLS

SYMBOLS

σ	Engineering stress, MPa
σ_f	Flexural stress, MPa
F	Force, N
A	Cross-sectional area, mm^2
E	Tensile modulus or Young's modulus, MPa
ΔL	Change in gauge length, mm
L	Length of the specimen until the break /Support span, mm
L_0	Initial length of the specimen, mm
P	Load at any point on stress-strain curve, N
b	Width of the specimen, mm
d	Depth of the beam, mm
ε_f	Flexural strain, mm/mm
ε	Engineering strain, mm/mm
D	Maximum deflection of the center of beam, mm
T_g	Glass transition temperature, °C
T_m	Melting temperature, °C
wt.%	Weight percent
X_c	Degree of crystallinity
ΔH_m	Heat of melting, J/g
w_p	Weight fraction of crystalline polymer
$H_m°$	Heat of fusion, J/g

LIST OF ABBREVIATIONS

ABBREVIATIONS

ABS	Acrylonitrile butadiene styrene
BSA	Benzene sulfonamide
CF	Carbon fabric
CFRP	Carbon fiber-reinforced polymers
DSC	Differential scanning calorimetry
E-GMA	Ethylene-glycidyl methacrylate copolymer
EPR-MAH	Maleic anhydride grafted ethylene propylene rubber
FTIR	Fourier transform infrared spectroscopy
MW	Molecular weight
N6	Nylon6
NMR	Nuclear magnetic resonance
PC	Polycarbonate
PEEK	Polyetheretherketone
PE-Epoxy	Epoxy terminated polyethylene
PEG	Polyethylene glycol
PLA	Polylactic acid
P_LLA	Poly(L-lactic acid)
PS	Polystyrene
PVC	Polyvinyl chloride
SAN-GMA	Styrene acrylonitrile glycidyl methacrylate copolymer
SAN-MAH	Maleic anhydride grafted styrene-acrylonitrile copolymer
SEBS-MAH	Styrene-ethylene-butylene-styrene terpolymer grafted with maleic anhydride
SEM	Scanning electron microscopy
SMA	Styrene-maleic anhydride
TGA	Thermogravimetric analysis

CHAPTER 1

INTRODUCTION

Researches on polymer-based multilayer composites play an important role on development of materials science. The produced materials are widely used in aerospace, electronics and automotive industries. The demand on these polymer-based multilayer composites is due to their enhanced mechanical and thermal properties. However, the polymers used are mostly the petroleum-based products that have irreversible effect on natural sources. To solve this problem, use of bio-based thermoplastic polymers gains interest.

Polylactic acid (PLA) which is an aliphatic polyester, is a promising candidate with its biodegradable nature, and it is obtained from renewable sources such as sugarcane and corn starch [1]. Although it is a polymer with high tensile strength, it is highly brittle, and its impact properties are low. The mechanical properties of PLA can be improved with modifications through blending with another polymer. The strong mechanical properties of two distinct polymers can be combined through polymer blending method. Since PLA provides high tensile strength but low impact properties, to obtain a blend with optimum mechanical properties, it can be blended with Acrylonitrile Butadiene Styrene (ABS) having high impact properties. In this case, compatibility between the constituents becomes another important issue. When the polymer constituents are miscible, it is possible to reveal a homogeneous blend. However, when the natures of polymers are significantly different, they form immiscible two-phase polymer blend. The immiscible blends require an additional operation to compatibilize the two naturally different polymers. Using

compatibilizers that can form a bridge between functional groups of polymers is expected to result in a single-phase blend.

Multilayer composites are the combination of matrix and reinforcement layers, forming a single composite structure. Superior mechanical properties of the reinforcement layers are combined with the properties of the matrix layers. The layer-by-layer construction provides excellent mechanical properties with low weight to strength ratio. There are several researches on the use of PLA matrix in multilayer composites. However, there are limited studies on the application of blends of PLA that enhanced through polymer blending. It is possible to obtain multilayer composites having more favorable properties by modifying the polymer layer of the composite.

The delamination problem is mostly encountered in multilayer composites. It occurs at the interface between the fabric and polymer layer due to lack of adhesion [2]. The insufficient adhesion between layers can be attributed to totally different chemical and physical nature of reinforcement and matrix material. To overcome this problem, several methods including use of electrospun films, surface treatments of reinforcement layer, the use of compatibilizers, etc. are available [3].

In this thesis, the objectives are to improve the properties of PLA with certain modifications through polymer blending and to produce a multilayer composite with enhanced mechanical and thermal properties. For this purpose, ABS is selected as the constituent of polymer blend. The reason of choosing ABS is its high impact properties that can compensate the weakness of PLA. The blends were prepared in three different weight ratios as 90/10, 50/50 and 70/30 to determine the optimum content. Since ABS and PLA are both physically and chemically different polymers, the blend requires compatibilizer which is expected to provide homogeneous structure in the matrix. Several types of compatibilizers were mixed with PLA/ABS blend in 5-10-15wt.%. The polymer blending was carried out using a co-rotating twin screw extruder. The produced blends were characterized through thermal and

mechanical tests. The mechanical test specimens for impact and tensile tests were prepared using an injection molding machine. SEM and FTIR analyses were carried out to understand the effect of compatibilizer on the morphology and chemical structures of the blends. The multilayer composites were prepared using carbon fabric as reinforcement material, and neat PLA, PLA/ABS blend and Compatibilizer/(PLA/ABS) blend as matrix materials. Compression molding process was used to produce multilayer composites with one and three carbon fabric layers. The produced composites were cut into test samples with water jet, and then, were characterized in terms of mechanical tests (tensile and flexural tests) and SEM analysis.

CHAPTER 2

BACKGROUND

2.1 Thermoplastic Polymers

Thermoplastic polymers are a group of polymers that can melt when heated and solidify under cooling so that they can be reshaped. Once it melts it can be molded into desired shape using commercial techniques as extrusion, injection molding and compression molding. The thermoplastic polymers can be reshaped when they are melted due to their irregular chain distribution. Forming regular crystalline structure from irregular chains requires high energy. Even though fully amorphous thermoplastics are available, thermoplastics are generally composed of semi crystalline structures which are composed of amorphous and crystalline regions. While amorphous parts provide elasticity due to irregular chain distribution, the crystalline parts provide strength to the polymer. The crystalline content can differ from polymer to polymer and expressed in terms of degree of crystallinity.

2.1.1 Polylactic Acid

Polylactic acid (PLA) is a biodegradable aliphatic polyester. Due to its renewable nature, it is a promising polymer that can be used instead of petroleum-based polymers. PLA is obtained by direct polycondensation and ring opening polymerization reaction of raw materials called lactic acid and lactide, respectively. The natural origins of PLA are mostly sugarcanes and potatoes [4]. It is suitable for the extrusion, injection molding and compression molding processes depending on its thermoplastic nature. PLA already exists in daily life in the forms of packaging

materials of foods, medical implants and short shelf life milk bottles. The demand on PLA in polymer science and industry stems from its mechanical properties such as high strength and high stiffness with a reasonable price. Comparing with petroleum-based polymers, it is possible to achieve the required specifications by means of mechanical properties in a more environmental friendly and economical way with the use of PLA. In addition to these promising properties, there are some weaknesses of PLA which are open to further developments. These drawbacks are high brittleness, low extensibility, lack of processability and lack of thermal stability at high temperatures.

2.1.2 Acrylonitrile Butadiene Styrene

Acrylonitrile butadiene styrene (ABS) is an engineering thermoplastic copolymer that is synthesized by the polymerization styrene and acrylonitrile in presence of polybutadiene. The content of sub polymers may differ from product to product. The nitrile groups provide polar attraction between the chains so that the copolymer becomes more durable than neat polystyrene (PS). Styrene provides processability and rigidity while the butadiene content provides toughness due to its rubbery nature. ABS is a commercially used hard and light weight polymer that is processed by extrusion and molding processes. There is a wide range of application areas of ABS from construction industry to production of daily life needs as automotive parts, protective helmets and lego toys [5].

2.2 Compatibilization of Polymers

The commercial blends are generally composed of highly chemically dissimilar polymers that are mixed to combine their promising properties into single material [6]. This immiscibility causes macroscopic phase separations due to high interfacial tension. In this case it becomes impossible to obtain optimized properties for the blend. There occurs a need to an additional material which builds a bridge between

polymers. The additives having similar structure or high affinity to the blend components are used as compatibilizers or interfacial modifiers. The main purpose of using these compatibilizers is to reduce interfacial tension and to stabilize the blend by promoting the dispersion of one phase into another. They are generally random and block copolymers that stabilize the phase morphology. There are two subcategories for compatibilizers as reactive and non-reactive compatibilizers [7]. Non-reactive ones promote the miscibility having similar units to the polymers of the blends. The use of non-reactive compatibilizers can be categorized into three cases. Firstly, the compatibilizer may be miscible with both phases. Secondly, a functional group of the compatibilizer can be miscible with one component, and another functional group of the compatibilizer may be miscible with the other component of the blend. Lastly, the compatibilizer can also be used as impact modifier. Reactive compatibilizers are composed of functional groups that are capable of reacting with the side groups of blend components. The reactions may form a graft, block or lightly cross-linked copolymer. In some cases, the reaction may lead to formation of ionic bonds in the structure. Since the blending of reactive compatibilizers is a mechanochemical process, new copolymers may be generated due to chain breakage and recombination [8]. Both reactive and non-reactive compatibilizers lead to enhanced interfacial adhesion, non-coalesced phased, reduced domain size, and improved mechanical properties and morphology when compared to uncompatibilized blend.

2.3 Thermal Stabilizers

One of the major problems that is encountered during processing of polymers with low heat stability is degradation. Depending on the process conditions there are several types of degradation that may occur such as hydrolysis, thermal decomposition and thermo oxidative degradation. To prevent degradation, thermal stabilizers can be blended with polymers through mixing process. The thermal stabilizers are classified into two major groups, primary and secondary antioxidants.

Primary antioxidants are generally phenolic antioxidants that are capable of scanveging radicals so distrupting the closed loop mechanism of thermo oxidative degradation. Primary antioxidants provide long term stabilization. The secondary ones are phosphate based antioxidants that are capable of decomposing hydroperoxides to alcohols [9].

2.4 Multilayer Composites

Multilayer composites are composed of multiple layers of oriented or randomly oriented reinforcement material and matrix material that bound fibers to combine their desirable properties [10]. A schematic drawing is given in Figure 2.1. There are many types of multilayer composites depending on the purpose of use. Carbon fabric, glass mat, aramid fabric are some examples for reinforcement material. As matrix material, there are polymeric, ceramic and metallic matrices. The polymeric matrix is commonly used in industry due to its ease of processing and light weight for the applications at application temperature of 250°C maximum [11]. There is a wide use of woven carbon fibers reinforcements when ultimate strength is required. Glass fibers are not as stiff as carbon fibers but they are impact resistant, so they are used to replace heavier part in end-market applications. Aramid fibers are mainly preferred for ballistic applications [12]. Different fiber orientations which are significant on determining isotropic behavior, may be used to produce multilayer composites.

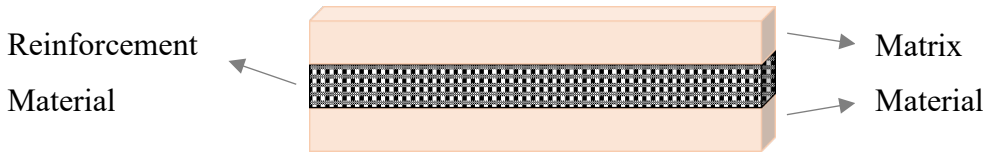

Figure 2.1 Physical Representation of Multilayer Composite.

Most attractive advantage of multilayer composites is their high-strength-to-weight ratio. Especially for automotive and aerospace industry when optimum performances are goaled with limited energy consumption, it becomes a critical issue. Other advantages are that they are applicable to complex shapes and have excellent fatigue, corrosion resistance and high mechanical properties in longitudinal direction [13]. Since the matrix and the reinforcement materials have chemically different natures, they are generally incompatible with each other. The problem is called delamination which means failure at the interface of matrix and reinforcement material due to stress gradient. As a result, delamination causes to low mechanical properties in transverse direction.

2.5 Carbon Fiber-Reinforced Polymers

Carbon fiber-reinforced polymers (CFRP) is a type of composite material that is composed of carbon fibers providing strength and stiffness to the material and polymer phase as matrix that holds the fibers together and provide toughness [14]. Two types of carbon fiber are present in industry as short carbon fibers and long carbon fibers. Depending on the intention of use, both short and long carbon fibers are preferred in industry. Short carbon fiber reinforcements are popular where isotropy is more critical parameter than strength or stiffness and for complex shapes due to ease of processing. Use of long fiber reinforced composites are more complicated and it is not applicable to complex surfaces but due to high aspect ratio, they are highly strong and stiff materials and that is why they are much more preferred for the manufacturing of parts in aerospace and automotive industry. Long fibers are also known as continuous fibers and several forms are available in market as roving, yarns, woven roving (fabric) and woven yarns. Yarns are the collection of twisted fibers. Roving is the collection of untwisted and parallel fibers. They can be woven in several configurations forming fabrics. In production of multilayer

composites, fabrics are preferred due to ease of processing. Commercial CFRP have the matrix phase that is generally thermoset material such as unsaturated polyester, epoxy, etc. But there are also applications and growing interest to thermoplastic matrix composites. The other types of fibers such as glass and aramid fibers are available in markets but the demand on carbon fibers is higher because of the combination ultra-light weight and high strength. They are also applicable to parts for which conductivity and corrosion resistance are required but it is not a low cost material [15].

2.6 Processing Techniques for Thermoplastic Matrix Multilayer Composites/Blends

2.6.1 Extrusion

Extrusion is a common process in plastic industry that is used to process polymers by mixing with the additives, fillers, colorants, or another polymer. It requires melting process to produce homogeneous blends. Extrusion is generally carried out for thermoplastic materials due to melting characteristic under heating but there are applications for thermoset materials at temperatures lower than the curing temperature. In addition to mixing, it is also used for the purpose of removing volatile content of the polymeric materials [16]. Depending on the number of screw and operating conditions, various types are available in the market. During an extrusion process the blends may be directly shaped after mixing or it may be just used for melting and mixing purposes before the blend is shaped with a molding technique. An extruder is composed of seven main parts including feeder, hopper, heating zones, die, cooler, puller and removal part. A schematic of an extruder can be seen in Figure 2.2.

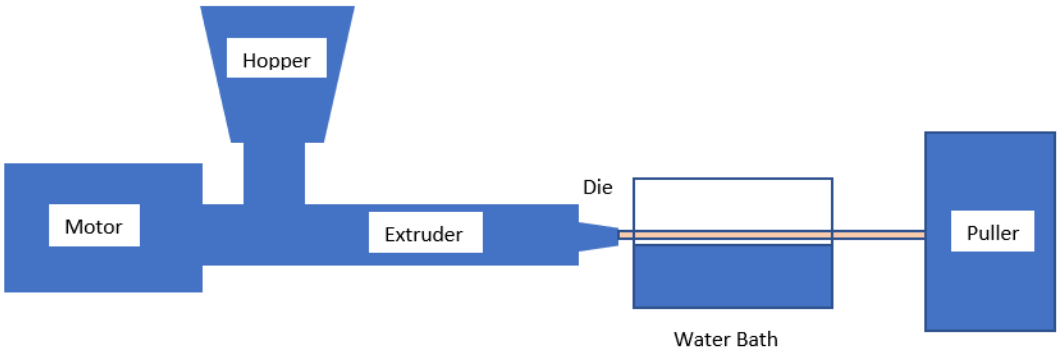

Figure 2.2 Schematic of Extruder.

The working principle of an extruder can simply be explained in some steps. First the raw materials in form of pellets, powder or granules are fed into the feeder and it moves from hooper to cylindrical chamber heated to the temperature that the raw materials can melt. While mixing takes place, the blend moves through the extruder with the help of screws. Depending on the extruder type, the number of screw and operation principle may change. At the end of the extruder, the molten blend is pushed through a constant cross section called die, and reached to cooling section. The cooling process can be achieved with the use of either air or water. Since the extrusion is a continuous process, it requires a puller for the materials cooled down and shaped. The removal part may include cutting process of the material into desired shape or storage of the material [17].

2.6.1.1 Twin Screw Extrusion

The types of extruders vary depending on number of screws that convey and mix the polymer pellets through heating zones of extruder. The single screw extruders are common in industry due to low cost, simplicity and reliability. On the other hand, single screw extruders are not recommended for heat sensitive materials as polyvinyl chloride (PVC) since they provide mixing and pumping due to the friction between

resin and barrel of the extruder. Twin screw extruders include intermeshing screws that provide more homogeneous mixing with less heat formation when compared to single screw extruders. With the intermeshing screws due to the relative motion of one inside channel of another, the extruder behaves like a pump resulting less friction and less heat dissipation. By this way the heating zones of the extruders can be controlled and set to desired temperatures without affected by the screw speed [18]. The twin screw extruders may be classified due to relative motions of screws as co-rotating and counter-rotating twin screw extruders [18]. The motions of screws are shown in Figure 2.3.

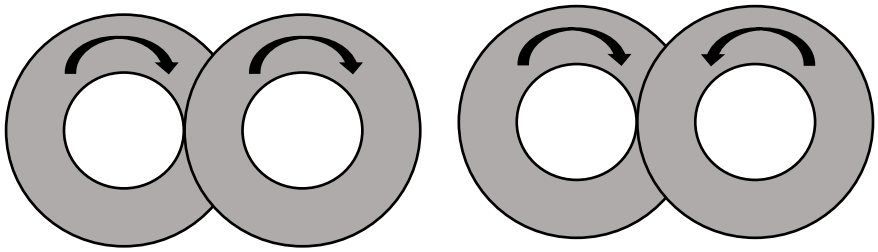

Figure 2.3 Co-rotating and Counter-rotating Screws.

2.6.2 Injection Molding

Injection molding is a basic manufacturing process for plastic materials. The working principle of an injection molding machine can simply be described as shaping of the molten plastic by pumping through cavities of the mold and cooling until it solidifies. This process is applicable to mass production and for complicated shapes. Injection molding process is composed of five main steps as clamping, injection, cooling, mold opening and removal of the products [19]. First the polymer in the form of pellet or granules are fed through a hopper to barrel where the melting occurs. After melting is completed, the molten polymer is injected through the mold cavities with adjusted injection pressure. The mold temperature is adjusted to be lower than the

glass transition temperature of the polymer in order to solidify by taking the shape of the mold. Clamping holds the parts of mold while injection and solidify the specimen. Mold opening process is responsible for the ejection of molded parts.

2.6.3 Compression Molding

Compression molding is another molding technique commonly used for both thermoset and thermoplastic materials. Compared to injection molding, the operation procedure is rather simple. Basically, it is a shaping process that occurs by charging polymers in form of granules or pellets into mold cavity and applying heat and pressure to make polymer fulfill the mold and solidify. The parameters of compression molding process are mold temperature, pressure profile and preheating time [20]. It is normally used for high production volume as automotive parts. A compression molding machine and its parts are illustrated in Figure 2.4.

The process takes place between two movable, heated plates. The movement occurs with the help of slide rods which are controlled with hydraulic press placed at the bottom of the machine. Depending on type of the machine, the press can be provided with a pump, fully automatic or semiautomatic systems.

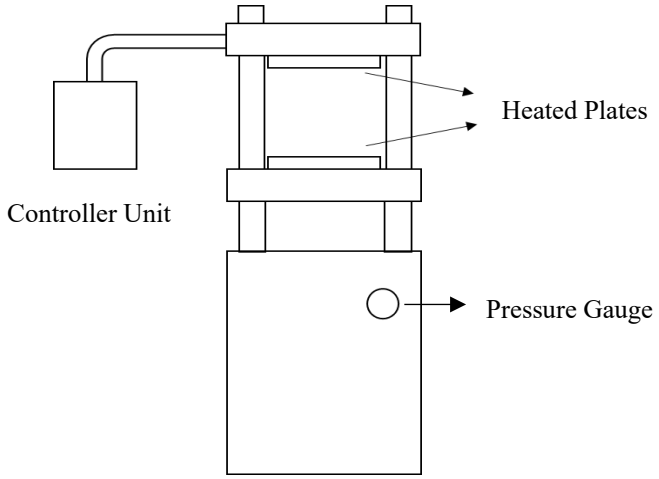

Figure 2.4 Schematic of Compression Molding Machine.

2.7 Characterization Methods for Polymer Blends and Composites

2.7.1 Mechanical Tests

Characterization based on the mechanical properties are significant for determining the properties of materials. It is crucial in developing enhanced materials. Depending on operational or environmental conditions, the materials are exposed to loads, and it is desired for materials to satisfy the safety considerations under these loads. Various types of mechanical tests are available to determine the behavior of the material under different circumstances. Some of these tests are tensile, impact, compressive and fatigue tests.

In this study, the materials including neat polymers, blend and composites are mechanically characterized with tensile, flexural and impact tests.

2.7.1.1 Tensile Test

Tensile test is a mechanical test that the test specimen is exposed to one directional tensile force until it breaks. The results show how the material behaves under certain loads and give data for quality control processes and material characterization studies.

Test configuration basically includes two aligned grips, one is movable, and one is fixed on the test machine. This test enables to obtain direct information on maximum tensile strength and elongation at break values. The dimensions of test specimens are determined by certain standards depending on the material and type of the composite structure. The standards are ISO 527-2 [21] and ISO 527-4 [22] for molding and extrusion plastics, and fiber reinforced composites, respectively. The specimens are attached to the grips of tensile test machine and tensile force is applied until it breaks. During the test, data of the amount of elongation with respect to applied force are collected.

Engineering stress (σ) can be evaluated with Equation 1 below.

$$\sigma = \frac{F}{A} \tag{1}$$

where F is force applied by the grips and A is the cross-sectional area of the specimen.

Engineering strain (ε) can be evaluated with data provided by the test using Equation 2 below.

$$\varepsilon = \frac{\Delta L}{L_0} = \frac{L - L_0}{L_0} \tag{2}$$

where $L, L_0, \Delta L$ are length of the specimen just before the break, initial length and the difference between initial and last lengths of the specimen, respectively.

A typical tensile stress versus strain curve is given in Figure 2.5. From this stress-strain curve certain properties as tensile strength, tensile modulus or Young's modulus and percent elongation can be obtained.

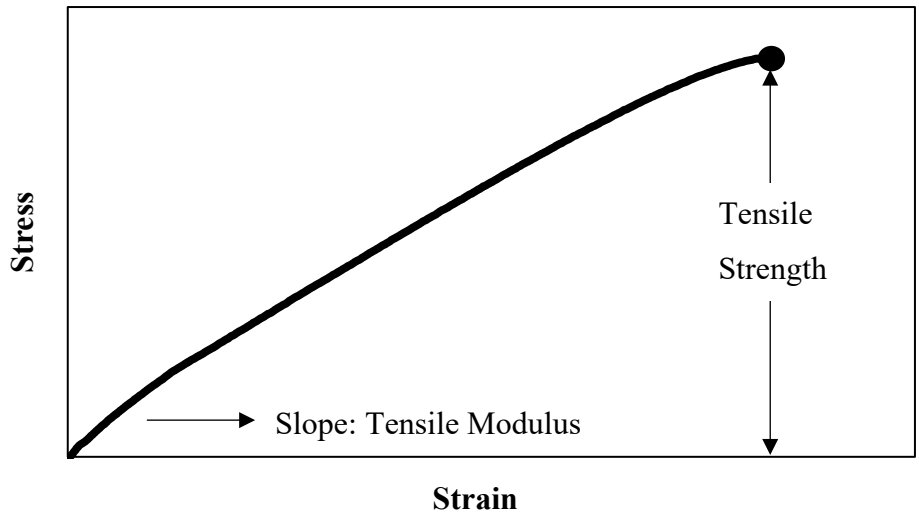

Figure 2.5 Typical Stress-Strain Curve.

Tensile strength is the ratio of the maximum load that the material can withstand to the initial cross-sectional area. In other words, it is the maximum stress that the material undergoes until break up.

Tensile Modulus or Young's Modulus (E) is the initial slope of the curve expressed by Equation 3 below. It is also known as proportionality factor in Hooke's law.

$$E = \frac{\sigma}{\varepsilon} \tag{3}$$

Elongation at break is the ratio between the changed length of the material to its initial length just before it ruptures.

2.7.1.2 Impact Test

Impact test is applied to investigate the behavior of material under rapid loads. By the impact test, the toughness value can be evaluated. Test machine records the

energy absorbed by the material considering the energy loss of the hammer. The impact strength is the energy absorbed by the material divided by the cross-sectional area where the deformation takes place. Depending on hammer type and its movement, there are two types of impact test as izod impact test and charpy impact test that are commonly used. The working principles are approximately the same. Main difference between these two types is the striking point. In charpy impact testing the hammer strikes to the middle of the sample that is placed flat on the test bed while in izod impact test, the striking point is the middle of the sample that is placed in vertical position [23]. The difference and a schematic of an impact test machine are shown in Figure 2.6.

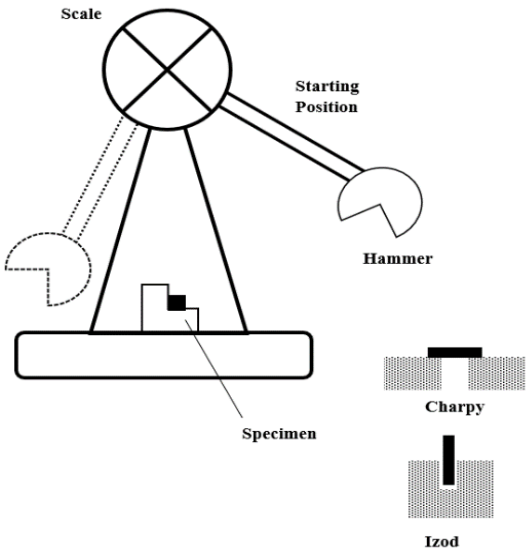

Figure 2.6 Schematic of Impact Test Machine.

2.7.1.3 Flexural Test

Flexural test is a mechanical characterization method to determine the behavior of plastics, composites, etc. under beam loading. It is also known as 3-Point bending test and transverse beam test. The test method is available in ASTM D790 standard that describes standard test methods for flexural properties of unreinforced and reinforced plastics and electrical insulating materials [24]. This test method enables to measure flexural strength and flexural modulus of the material from stress-strain data. A common test configuration is given in Figure 2.7.

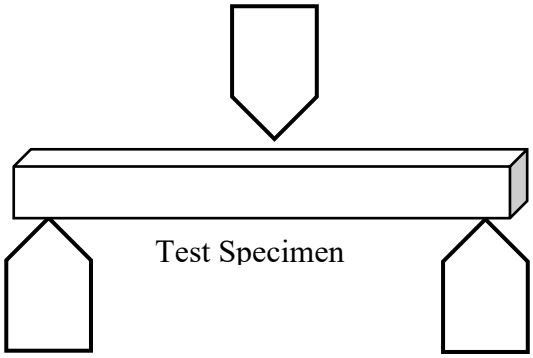

Figure 2.7 Schematic of Flexural Test.

During flexural testing, the maximum stress occurs at the outer middle surface of the specimen. The flexural stress (σ_f) value can be evaluated through loading depending on Equation 4 below.

$$\sigma_f = \frac{3PL}{2bd^2} \tag{4}$$

P is the load at any point on stress-strain curve and L is the support span. b and d are the width and the depth of the test specimen. The flexural modulus (E_f) is equal to the slope of stress-strain curve.

The flexural strain (ε_f) is calculated using Equation 5.

$$\varepsilon_f = \frac{6Dd}{L^2} \tag{5}$$

D, d and L represent the maximum deflection of the center of beam, depth of the specimen and support span, respectively.

2.7.2 Thermal Tests

2.7.2.1 Differential Scanning Calorimetry Analysis

Differential scanning calorimetry (DSC) analysis is a thermoanalytical technique to observe the phase transition behavior of materials while they are exposed to constant temperature change. Some properties that can be determined by this technique are heat capacity, crystallization kinetics and transitions of polymers. The principle of this analysis is to measure the heat flow associated with endothermic and exothermic transitions or reactions [25].

In power compensated DSC analysis, two pans in total are used for reference sample and the sample material. The instrument is programmed to keep the pans at the same temperature while increasing the temperature at the same rate. The transition

temperature is determined when heat is required to keep the pans at the same temperature. A typical DSC curve is given in Figure 2.8.

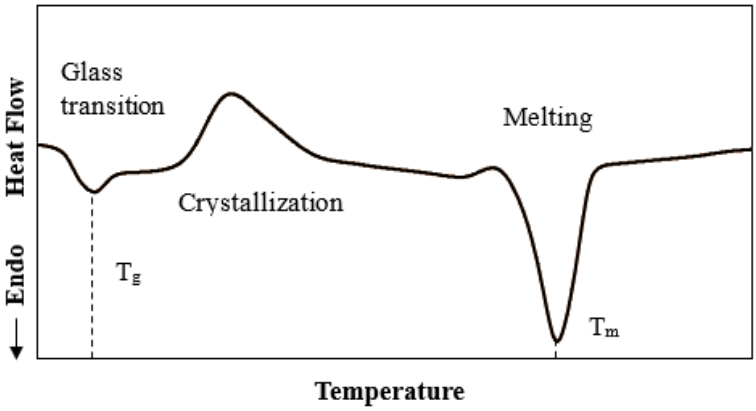

Figure 2.8 Typical DSC Curve.

When glass transition temperature (T_g) of the material is reached, the heat capacity increases so that the heat required to keep the sample pan at the same temperature with reference pan increases. Since it is an endothermic heat flow, it results in a decrease in DSC curve.

Temperature of melting is represented with T_m. Since the crystal structures in the material melt at constant temperature, large amount of heat is required. So, it can be observed as an endothermic peak.

Crystallization is an exothermic reaction. Since heat is released from the material at crystallization temperature, the amount of required heat supplied by the instrument decreases. The crystallization peak can be observed as an exothermic peak in opposed to melting and glass transition peaks.

2.7.2.2 Thermogravimetric Analysis

Thermogravimetric analysis (TGA) is a thermal characterization method which measures the weight loss of the sample as a function of both temperature and time. The weight loss may be originated from several processes such as decomposition, dehydration, etc. By this method, the degradation temperature and certain amount of weight losses at corresponding temperatures can be measured.

The analyzer gives the data that are taken from two sample holders, one has an empty pan as reference and one is for sample pan. Before the sample is placed, the pan on the holder is tared. Then, the initial weight of the sample is recorded by the analyzer. The weight loss of the sample is measured relative to reference holder. Sample pan is heated at predetermined heating rate, and the weight loss is measured.

2.7.3 Fourier Transform Infrared Spectroscopy Analysis

Fourier transform infrared spectroscopy (FTIR) analysis is based on the absorbance and transmittance capability of analyzing material to infrared waves. The absorbance occurs in case the bonds within the molecule vibrates and the molecules start to move around with the infrared waves provided with the equipment. The infrared waves are absorbed if the molecule has changeable dipole moment [26]. The functional groups, bonding positions and the aliphatic, aromatic structures in solid and liquid phases can be detected with FTIR spectroscopy.

2.7.4 Scanning Electron Microscopy Analysis

Scanning electron microscopy (SEM) analysis is a type of electron microscopy analysis that scans the surface of sample with focused electron beam. By interacting with the atoms on the surface of the sample, electrons provide information on topography and composition of the sample. The chemical composition, orientation

of materials, morphology and crystalline structure can be observed by SEM analysis. The images are created depending on the position of electron beam and the corresponding signal. A typical SEM enables to reach high resolutions more than 1 nanometer. The dry and conductive surfaces can be detected with these microscopes under high vacuum [27]. The SEM analysis can be carried out for non-conducting materials when conductive coating such as gold palladium alloy is applied.

2.8 Literature Survey

2.8.1 Polymer Blends

When compared to other biopolymers, PLA has better elastic modulus and processability. However, it is highly brittle, and the impact strength is relatively low. At temperatures higher than 200°C, thermal degradation of PLA becomes a problem. To develop these properties, several strategies are available in literature [29, 30]. Blending polymers with other polymers that have better impact properties is one of the most common strategy.

Hamad and his colleagues [28] applied polymer blending method for preparation binary and ternary blends of PLA, PS and ABS. The rheological and mechanical properties depending on the blend composition were investigated. The blends were prepared in single screw extrusion process at temperature around 150°C and the tensile test specimen were shaped in injection molding process with barrel temperature of 200°C and molded at room temperature. Considering the mechanical properties, the addition of ABS to PLA/PS blends improved the elongation at break values. Especially for PLA/PS blend with 30 wt.% PLA, the elongation at break value was increased to 1.4 times of the binary blend by adding 20 phr ABS. While improving the impact properties with polymer blending method, keeping the modulus constant was a significant issue. It was also stated in this study that modulus of ternary blends were higher than the binary blends and with the addition of 5 phr

ABS to PLA/PS blend with 50wt.% PLA, it was possible to maintain the modulus of neat PLA during blending [28].

In another research, Thongpin et al. [29] investigated the change in properties of PLA when it is in-situ reinforced with Nylon 6 (N6). Blends in various compositions were prepared with twin screw extruder at 160-230°C. Since the melting points of N6 and PLA are significantly different, N6 was plasticized with benzene sulfonamide (BSA) so the melting point was decreased in order to process at the same temperature. The degradation temperature was increased up to 5 wt.% N6. At contents higher than 5 wt.% N6, the N6 particles started to agglomerate. This heterogeneous structure of N6 particles in PLA matrix decreased thermal properties. Since N6 and PLA are not compatible with each other and there is lack of interfacial adhesion, so the tensile strength and modulus were lowered with the addition of N6. Specifically, at the 5 wt. % content of N6, there was minor increase in tensile strength and modulus due to elastic behavior of N6. It was expected for N6 to improve the elongation at break value of PLA since it is elastic polymer when compared to PLA. For contents higher than 5 wt.% N6, the expectation was true. However, at high process temperature there was a decrease in elongation at break value of blend with 5 wt.% N6. This was because of the degradation of PLA at high temperatures [29].

One of the major problems that is encountered during processing of PLA is degradation. There are several types of degradation that may occur depending on the process conditions. Some of the mostly observed situations are hydrolysis, thermal decomposition and thermo-oxidative degradation. Degradation due to hydrolysis of PLA takes place at around 200°C following the random chain scission mechanism [30]. At this process condition, it is possible to obtain products with hydroxyl and carboxyl end groups. At higher temperatures (around 250°C), free radicals started to be formed by degradation mechanism.

Blending polymers with thermal stabilizers are one of the methods to enhance thermal stability of polymers. To overcome the lack of thermal stability of PLA,

Burlet et al. [31] conducted a research on the effect of tris(nonylphenyl) phosphate (TNPP) and its concentration on thermal stability of poly(L-lactic acid) (P_LLA). TNPP and P_LLA were mixed in an internal mixer at process temperature of 180°C under nitrogen atmosphere. Then, the mixture was introduced to compression molding process again at 180°C. Test specimens for rheological properties were prepared using compression molding. As a result, it was stated that TNPP has two competing effects on P_LLA as both chain scission and chain extension depending on the concentration. To maintain the thermal stability, TNPP concentration of 35 wt.% was found to be an optimum value for high molecular weight P_LLA.

2.8.2 Compatibilization of Polymers

While blending two different polymers, compatibility becomes another important issue. To combine the desired properties of selected polymers, there need to have certain level of attraction between the functional groups of polymers. In the absence of attraction, several types of compatibilizers are available depending on couple of selected polymers.

Zhang et al. [32] studied PLA/ABS/polyethylene glycol (PEG) blends where PEG was used as compatibilizer. The experiments were carried out with PEG having two distinct molecular weights (MWs) as PEG800 and PEG6000. The purpose was to improve the interfacial adhesion between PLA and ABS and to enhance both thermal and mechanical properties. The sample preparation was carried out following the stages; drying of polymers in shape of pellets, the extrusion process at temperature ranges from 100°C to 190°C from hopper to die and screw speed of 350 rpm/min, and lastly the injection molding process at temperatures from 40°C to 190°C from feeder to die in the extruder part and mold temperature of 25°C. In morphology analysis, it was concluded that the introduction of PEG into PLA/ABS blend caused an increase in free volume of PLA that provided new places for interaction with ABS. Since it was easier for low MW PEG to scatter in polymer matrix, it resulted

in better interfacial adhesion and a homogeneous blend. Presence of PEG decreased the thermal stability so the degradation temperature was independent of MWs of blend. This was even less than both degradation temperatures of PLA and ABS. With the addition of PEG, the movability of molecular chains increased and the molecular interactions became weaker so that the modulus of the blend decreased. The tensile strength of PLA/ABS blend increased from 18.68 MPa to 31.93 MPa and 36.59 MPa with the addition of PEG800 and PEG6000, respectively. This was explained by the phenomenon that the presence of PEG improves the miscibility of PLA and ABS by creating free volumes between chains of PLA and ABS. The elongation at break of PLA/ABS blend was improved by the addition of PEG due to the increased free volume. It was easier for PEG800 to interfere between the molecular chains so it increased the free volume more than PEG6000 and it was chosen to be used as compatibilizer [32].

In another study carried out by Yeon Jong Ryu and coworkers [33], the aim was to decrease ABS content of car consoles and to substitute ABS with PLA. However, impact strength of PLA is significantly low when compared to ABS. The desired impact strength for car consoles is 80 J/m. Initially a blend with 50PLA/50ABS ratio was prepared and the impact test resulted in 22 J/m while the impact strength of neat ABS was around 480 J/m. The drop was because of the lack of compatibility between polymers. To overcome this problem several compatibilizers including polycarbonate (PC), epoxy terminated polyethylene (PE-Epoxy), maleic anhydride grafted ethylene propylene rubber (EPR-MAH), styrene acrylonitrile glycidiyl methacrylate copolymer (SAN-GMA) and maleic anhydride grafted styrene-acrylonitrile copolymer (SAN-MAH) were introduced into blend with proportions of 10 wt.%, 50 wt.% and 40 wt.%. SAN-GMA resulted in the highest tensile and impact strength as 12 MPa and 29.3 J/m, respectively due to interaction between epoxy group of compatibilizer and carboxyl, hydroxyl groups of PLA. For further enhancements, SAN-GMA with concentration of 5, 10, 15, 20 phr was introduced into the blend with 50 wt.% PLA and ABS. The target value of 80 J/m for impact

strength was reached. Moreover, higher impact strengths as 91.6 J/m and 92.3 J/m were obtained with the addition of 15 phr and 20 phr of SAN-GMA, respectively. The 15 phr and 20 phr of SAN-GMA also enhanced the tensile strength of the blend from 37.3 MPa to around 50 MPa.

2.8.3 Multilayer Polymer Composites

The term 'multilayer polymer composite' means the merging of several reinforcements in fabric form and polymer layers to combine their promising properties in a single material. There are several researches on preparing and developing the multilayer composite structures to achieve desired mechanical strength, flexibility and stiffness, etc. for various applications. The studies are mostly about the thermoset matrix multilayer composites such as epoxy-based carbon fabric composites but there is a growing interest in thermoplastic matrix multilayer composites.

In a study carried out by Galatas et al. [34], the carbon fiber-reinforced polymer (CFRP)-ABS multilayer composites were prepared to be used in unmanned aerial vehicle applications. The aim was to enhance the poor mechanical strength and elastic modulus of neat ABS. ABS resin was transferred between the layers of woven carbon fiber by 3-D printing method. Since the CFRP involved thermoset materials, they were left for curing after the application of ABS layers. The analysis showed that the failure modes of composites were fiber pullout and delamination. It was observed that with increasing number of CFRP layer, the specific strength and elastic modulus of multilayer composite was improved. When the two layers of CF were used, the Young's modulus was increased about 16 times while the ultimate strength was improved by 9 times compared to neat ABS.

The multilayer composites are open to crack initiation and possible failures due to poor interfacial attraction between polymer matrix and reinforcement material. To overcome failures, hybrid composite is an alternative solution. In an article written

by Pathak et al. [13], carbon fabric-reinforced graphene oxide-epoxy composites were prepared to observe the effect of contribution of graphene oxide on mechanical properties of multilayer composite. The epoxy resin was first modified with different graphene oxide amounts between 0.1-0.6 wt.%. The carbon fabric was impregnated by matrix material via compression molding procedure. Through several analyzing methods including FTIR, NMR, etc., it was observed that graphene oxide has some functional groups that attract with both carbon fabric and epoxy resin. Depending on this fact, when the graphene oxide content was equal to 0.3% by weight, the flexural strength and flexural modulus of multilayer composite were increased by 66% and 72%, respectively. Also, the interlaminar shear strength were improved by 25% due to interlocking function of graphene oxide.

To improve mechanical properties of multilayer polymer composites, the enhanced interlaminar strength is crucial. Several methods are available to strengthen the interlaminar adhesion including modification of polymer layer and surface treatment of reinforcement material. In a study carried out by Sharma et al. [35], polyetheretherketone (PEEK) multilayer composites were prepared with treated and untreated carbon fabric. PEEK is a specialty thermoplastic polymer with high thermal and mechanical resistance. Cold remote nitrogen–oxygen plasma was used for the treatment of carbon fabric. When the mechanical test and SEM results of treated and untreated PEEK/carbon fiber composites were compared, it was concluded that the treatment improved the mechanical properties of composites by 10-15%, while increasing the wear properties of composites by 22-25%.

2.9 Motivation of Thesis

Polymer-based multilayer composites are promising materials in the view of industry and polymer science. They provide excellent mechanical performances and weight reduction solutions. Various types of polymer-based multilayer composites are

available in the market. In addition, there is a growing demand on the use and development of polymer-based multilayer composites.

There are several types of multilayer composites depending on the matrix and reinforcement material. Carbon fabric-reinforced polymer composites are widely used in industry due to high strength of carbon fibers. The polymer type varies depending on the intent of use. The polymers can be categorized basically into two groups as thermosets and thermoplastics. In literature, there are significant knowledge on the modifications and characterization of thermoset polymers and their use in multilayer composites. However, the use of thermoset materials is opposed to environmental concerns. Today, since the terms 'recyclability' and 'biodegradability' gain interest, the thermoplastic polymers have been preferred to thermoset polymers. The thermoplastic polymers are highly recyclable and have remolding capabilities while providing high impact resistance [36].

PLA is a thermoplastic polymer with biodegradable nature and high tensile strength. However, PLA has low thermal stability and high brittleness. There are researches to overcome the weaknesses of PLA with different methods as polymer blending. ABS is an amorphous thermoplastic copolymer with high impact properties. While blending PLA and ABS, it has been expected to combine their superior properties. Due to their significantly different nature, they are incompatible. To enhance the properties of blends of PLA and ABS, there are researches available in literature. However, there are limited studies on the development of the blends of PLA and ABS to be used in multilayer composites.

In this thesis, the blends of PLA and ABS with different concentrations were prepared and characterized with SEM analysis, thermal and mechanical tests. After the PLA/ABS ratio was determined, thermal stabilizers with different combinations were blended with PLA/ABS and characterized in case of lack of thermal stability. To achieve miscibility, four chemically different compatibilizers with three different concentrations were introduced to PLA/ABS blends. The most effective

compatibilizer were determined considering FTIR, SEM and mechanical test results. The polymer layers of the multilayer combination were prepared and used together with one and three layers of carbon fabric. SEM analysis, flexural and tensile tests were carried out for the characterization purposes of multilayer composites.

The motivation of this thesis is to develop biodegradable and recyclable multilayer composites and to form a perspective in order to minimize the use of petroleum-based thermoset polymers in multilayer composites. For this purpose, it was aimed to contribute to literature on the development of PLA/ABS-based blends and to extend their application in multilayer composites.

CHAPTER 3

EXPERIMENTAL

3.1 Materials

Materials used in the preparation of multilayer composites were polylactic acid (PLA), acrylonitrile butadiene styrene copolymer (ABS) and carbon fabric (CF). While preparing ABS-PLA blends, maleic anhydride grafted linear triblock copolymer based on styrene and ethylene/butylene (SEBS-MAH), ethylene glycidyl methacrylate copolymer (E-GMA), styrene maleic anhydride random copolymer (SMA) and styrene glycidyl methacrylate random copolymer (SAN-GMA) were also used as compatibilizer.

3.1.1 Polylactic Acid

Polylactic acid (PLA) was used as main matrix material and it was obtained from the NaturePlast company with a trade name of PLI 005. It is a thermoplastic material and biodegradable polymer which is produced from renewable sources [37]. PLA is highly brittle and transparent polymer that is suitable for injection molding process. The functional groups of PLA are hydroxyl and carbonyl groups. The chemical structure and the physical properties of PLA are given in Figure 3.1 and Table 3.1, respectively.

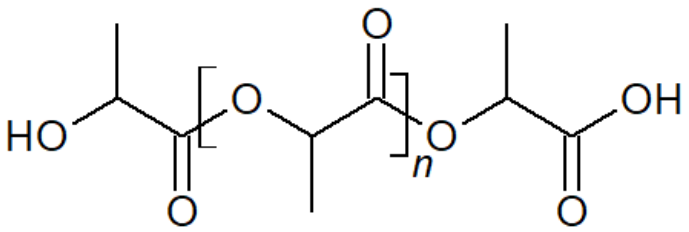

Figure 3.1 Chemical Structure of PLA.

Table 3.1 Physical Properties of PLA.

Property	**Unit**	**Value**
Melt Flow Index (MFI) at 190°C/2.16 kg	g/10 min	10 - 30
Specific Gravity	g/cm³	1.20 - 1.30
Degradation Temperature	°C	240 - 250
Melting Point	°C	145 - 155
Tensile Strength	MPa	47
Tensile Elongation at Break	%	3.0
Tensile Modulus	MPa	3300
Impact Strength (Unnotched, Charpy)	kJ/m²	21

3.1.2 Acrylonitrile Butadiene Styrene Copolymer

Acrylonitrile butadiene styrene (ABS) copolymer was introduced to PLA matrix in polymer blending process. The ABS with a trade name of Novodur HD M203FC was supplied by the Ineos Styrolution. It is special for injection molding process with high flowability. The usage areas are medical applications, inhaler housings and insulin pens. The acrylonitrile part forms polar attraction, provides heat stability and chemical resistance. In addition, the butadiene content is the reason for the toughness of the copolymer with high impact strength. The rigidity and the ease of processing of ABS is due to its styrene content. The chemical structure is illustrated in Figure 3.2, and the properties based on technical datasheet are listed in Table 3.2.

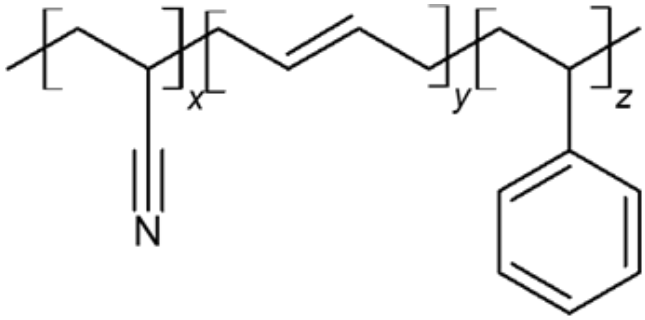

Figure 3.2 Chemical Structure of ABS.

Table 3.2 Physical Properties of ABS.

Property	Unit	Value
Melt Volume Rate at 220°C/10 kg	cm^3/10 min	31
Density	kg/m^3	1050
Vicat Softening Temperature at 50 N,120 °C/h	°C	101
Tensile Stress at Yield	MPa	46
Elongation at Break	%	> 15
Tensile Modulus	MPa	2400
Impact Strength (Unnotched, Charpy)	kJ/m^2	110

3.1.3 Carbon Fabric

Carbon fabric (CF) was used as reinforcement material for multilayer composites. The fabric is twill woven. It was supplied by Metyx Composite with a trade name of CW 245 B- Carbon 3K 2x2 Twill Woven. It has areal density of 246 g/m^2.

3.1.4 Compatibilizers

Several compatibilizers were introduced to binary blend of PLA and ABS. The compatibilizers were chosen depending on their functional groups.

3.1.4.1 Maleic Anhydride Grafted Styrene-Ethylene-Butylene-Styrene Terpolymer

Maleic anhydride grafted linear triblock copolymer based on styrene and ethylene/butylene (SEBS-MAH) was obtained from Kraton Company with a trade name of FG1901 GT. The reason of choosing this terpolymer was the possibility of interaction between the maleic anhydride group and hydroxyl, carboxyl groups of PLA and with ABS. Styrene and butylene parts are also miscible with ABS. The chemical structure and physical properties of SEBS-MAH are given in Figure 3.3 and Table 3.3, respectively.

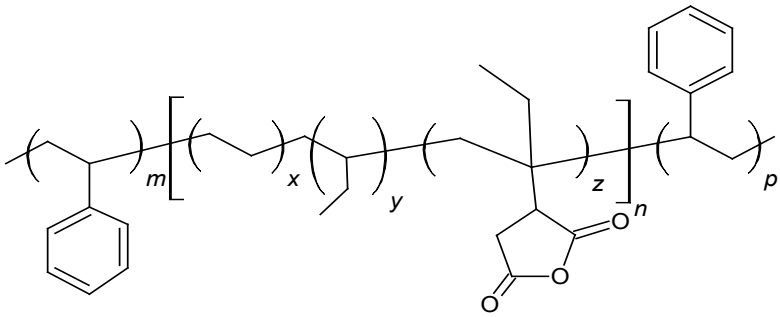

Figure 3.3 Chemical Structure of SEBS-MAH.

Table 3.3 Physical Properties of SEBS-MAH.

Property	Unit	Value
Melt Flow Index (MFI) at 230°C/5 kg	g/10 min	14 - 28
Relative Density at 20°C	-	0.88 - 0.95
Specific Gravity	g/cm³	0.91
Maleic Anhydride Bound	wt.%	1.4 - 2.0
Tensile Strength	MPa	34.5
Tensile Elongation at Break	%	500

3.1.4.2 Ethylene-Glycidyl Methacrylate Copolymer

Ethylene-glycidyl methacrylate (E-GMA) copolymer was chosen as a compatibilizer due to its glycidyl methacrylate content because the epoxy functional group is potentially interactive with -OH and -COOH groups of PLA. The compatibilizer was supplied by Arkema Company with a trade name of LOTADER AX8840. The chemical structure and physical properties of E-GMA are given in Figure 3.4 and Table 3.4, respectively.

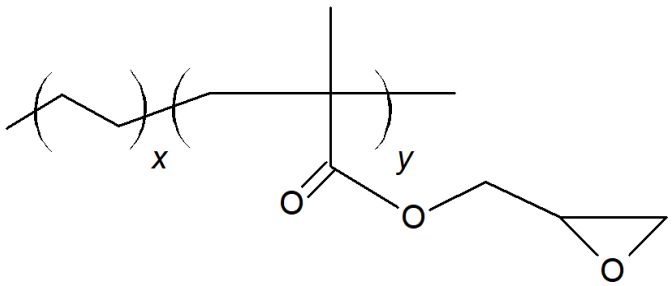

Figure 3.4 Chemical Structure of E-GMA.

Table 3.4 Physical Properties of E-GMA.

Property	Unit	Value
Melt Flow Index (MFI) at 190°C/2.16 kg	g/10 min	5
Density at 23°C	g/cm³	0.94
Glycidyl Methacrylate Content	wt.%	8
Melting Point	°C	105
Tensile Strength	MPa	8
Elongation at Break	%	420
Tensile Modulus	MPa	104

3.1.4.3 Styrene-Maleic Anhydride

Styrene-maleic anhydride (SMA) is a random copolymer of styrene and maleic anhydride. It is an additive which can be used as being compatibilizer, surface modifier, etc. In this study, the purpose of using SMA is to compatibilize two immiscible polymers. It was purchased from Polyscope Company with a product name of Xibond 250. The chemical structure and physical properties are shown in Figure 3.5 and Table 3.5, respectively.

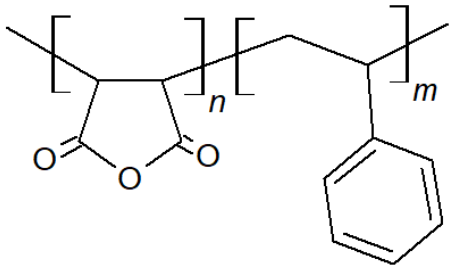

Figure 3.5 Chemical Structure of SMA.

Table 3.5 Physical Properties of SMA.

Property	Unit	Value
Molecular Weight	g/mole	10000
Acid Value	mg KOH/g	285
Glass Transition Temperature	°C	130
Kinematic Viscosity	cSt	0.7
Thermal Stability 10°C/min, N_2 at 1% loss	°C	240
Maximum Processing Temperature	°C	290

3.1.4.4 Styrene-Acrylonitrile-Glycidyl Methacrylate

Styrene acrylonitrile glycidyl methacrylate (SAN-GMA) was procured from Polyscope Company with a product name of Xibond 920. It is a random copolymer that may be used as chain extender, compatibilizer, etc. As compatibilizer, it improves the interfacial adhesion and optimizes the morphology [38]. The reason of choosing this compatibilizer is due to its high epoxy content of glycidyl methacrylate phase that interacts with functional groups of PLA. In addition, the styrene acrylonitrile phase is miscible with SAN phase of ABS. The chemical structure and properties are shown in Figure 3.6 and Table 3.6, respectively.

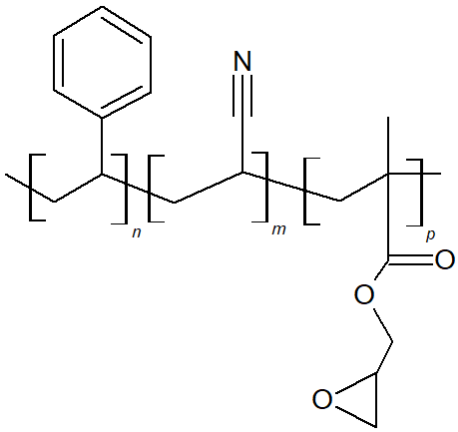

Figure 3.6 Chemical Structure of SAN-GMA.

Table 3.6 Physical Properties of SAN-GMA.

Property	Unit	Value
Molecular Weight	g/mole	50000
Glycidyl Methacrylate Content	wt.%	20
Glass Transition Temperature	°C	95
Thermal Stability 10°C/min, N_2 at 1% loss	°C	265
Maximum Processing Temperature	°C	230

3.1.5 Thermal Stabilizers

In this study, two types of thermal stabilizers as phenolic and phosphite antioxidants were used. The stabilizers were procured from Biesterfeld Company. As phenolic antioxidant, Octadecyl-3-(3,5-di-tert-butyl-4-hydroxyphenyl) propionate with trade name of Songnox1076 was preferred and as phosphite antioxidant, Tris (2,4 di tert butylphenyl) phosphite with trade name of Songnox1680 was chosen. The phenolic and phosphite antioxidants were represented by TS-1 and TS-2, respectively. The properties in technical data sheets are listed in Table 3.7.

Table 3.7 Properties of Thermal Stabilizers [39, 40].

Thermal Stabilizer Type		**Songnox1076**	**Songnox1680**
Property	**Unit**	**(TS-1)**	**(TS-2)**
Melting Point	°C	50 - 55	181-187
Volatile Loss	%	< 0.20	< 0. 30
Molecular Weight	g/mol	531	647

3.2 Experimental Methodology

This section includes the methodology for the preparation of polymer blends, multilayer composites and the modifications for polymer blends of the study.

3.2.1 Drying

Prior to processing, all polymers and compatibilizers were dried in vacuum oven at 90˚C for 24 hours.

3.2.2 Determination of PLA/ABS Ratio

To improve the properties of PLA, it was blended with ABS with different PLA/ABS ratios using twin screw extruder. The extruder process conditions are given in Part 3.3.1. The PLA/ABS ratios were varied as 90PLA/10ABS, 70PLA/30ABS and 50PLA/50ABS by weight. The optimized PLA/ABS ratio was chosen depending on their mechanical properties and processability.

3.2.3 Determination of Compatibilizer Type and Content

Four different compatibilizers (SEBS-MAH, E-GMA, SMA and SAN-GMA) with three different concentrations as 5, 10, 15 wt.% were mixed with 70PLA/30ABS using a twin-screw extruder. The blend names associated with corresponding compatibilizer and compatibilizer concentrations are listed in Table 3.8.

Table 3.8 Sample Codes and Corresponding Compatibilizer Ratios.

Sample Codes	Compatibilizer Types	Compatibilizer Concentrations (wt.%)	Binary Blend
5SEBS-MAH	SEBS-MAH	5	70PLA/30ABS
10SEBS-MAH		10	
15SEBS-MAH		15	
5E-GMA	E-GMA	5	
10E-GMA		10	
15E-GMA		15	
5SMA	SMA	5	
10SMA		10	
15SMA		15	

Table 3.8 Sample Codes and Corresponding Compatibilizer Ratios (continued).

5SAN-GMA	SAN-GMA	5	70PLA/30ABS
10SAN-GMA		10	
15SAN-GMA		15	

3.2.4 Determination of Process Temperature

Extrusion and molding processes were carried out at two different operation temperatures as 200°C and 230°C. The process temperatures for PLA and ABS were considerably different. So, the purpose of this analysis was to determine the optimum temperature to process these two polymers at the same time. The assessment was based on mechanical, thermal tests and SEM analysis.

3.2.5 Preparation of Multilayer Composites

During the preparation of multilayer composites, first the polymer layers were prepared from their pellets with different weights according to different number of carbon fabrics as 1 and 3 layers in composite structure. Then, the carbon fabrics, and polymer layers were compressed together using compression molding machine with operation parameters given in Tables 3.11 and 3.12, in Section 3.3.3. The amounts of polymer layers were determined keeping the carbon fiber content of multilayer composites proportional to number of carbon fabric and trying to produce all composites with thickness at 2 +0.4 mm. The composites were prepared with three different polymer matrixes as neat PLA, 70PLA/30ABS, and 10SAN-GMA/(70PLA/30ABS) layers which were selected according to their optimum properties and for the comparison purposes. The carbon fabrics were positioned with hand lay-up method considering the fibers to be placed in same direction. For 1CF and 3CFs composites, 40 grams and 20 grams of polymer layers were produced,

respectively. The weights of polymer layers were determined considering a relative increase in CF content from 1CF to 3CFs. Schematic representations for 1CF and 3CFs composites are illustrated in Figure 3.7.

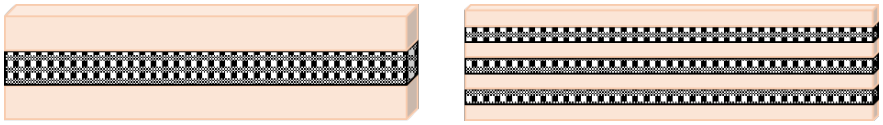

Figure 3.7 Schematic Representation of 1CF and 3CFs Multilayer Composites.

All polymer layers and multilayer composites were prepared using metal frames. The purpose of using frames was to cover the polymer pellets and form them in shape of layer. For composites, metal frames prevented the slippage of carbon fabric and enabled to reach desired thickness. The dimensions of metal frames for 40 gr, 20gr polymer layers and multilayer composites were 18×18×0.2 cm^3, 18×18×0.1 cm^3 and 20×20×0.2 cm^3, respectively. The theoretical calculation for carbon fiber content is available in Appendix A.

3.3 Experimental Methods for Processing

3.3.1 Extrusion

A co-rotating twin screw extruder (Thermoprism TSE-16-TC) was used for polymer blending process and for introducing additives and compatibilizers to polymer blend. The specifications are listed in Table 3.9.

Table 3.9 Specifications of Twin Screw Extruder.

Property	Unit	Value
Twin Bore Diameter	mm	16
Screw Diameter	mm	15.6
Maximum Screw Speed	rpm	500
Barrel Length (24 D)	mm	384
Die Length (1 D)	mm	16
Maximum Torque	N.m	12

The feed rate was chosen as 25 g/min and the screw speed was kept at 80 rpm. The extruder was operated at two different temperature profiles as 190-200-200-200-200°C for all polymer blends and 200-230-230-230-230°C for polymer blends with 10wt.% compatibilizer to determine optimum process temperature. A photograph of extruder that was used in this study is shown in Figure 3.8.

Figure 3.8 Photograph of Twin Screw Extruder [70].

3.3.2 Injection Molding

Injection molding process was carried out for the preparation of tensile and impact test specimens of neat polymers and their blends. The process was carried out using a DSM Micro 10 cc Injection Molding Machine in compliance with ASTM D 638 standard [41]. A photograph of the machine is shown in Figure 3.9.

Figure 3.9 Photograph of Injection Molding Machine [70].

The molding parameters are listed in Table 3.10 for two different process conditions that were used to determine the optimum process temperature. For the blends in which ABS content is equal and greater than 30%, the mold temperature of 55°C was used in molding process in order to remove the specimens from the mold easily. However, 55°C molding temperature for the blend with 90wt.% PLA was not used because specimens do not solidify enough to take out of mold. This was again due to difference between process temperature of PLA and ABS. The mold temperature of 50°C was used for 90PLA/10ABS blend.

Table 3.10 Injection Molding Parameters.

Property	Unit	Value
Barrel Temperature	°C	200 / 230
Mold Temperature (for lower than 30% ABS content)	°C	50
Mold Temperature (for 30% ABS content and higher)	°C	55
Time for Melting	min	4
Injection Pressure	bar	13

3.3.3 Compression Molding

The polymer layers and multilayer composites were prepared using a hydraulic compression molding machine. A photograph of the machine is given in Figure 3.10.

Figure 3.10 Photograph of Compression Molding Machine.

The compressions of polymer blends and multilayer composites were carried out between two metal plates and the materials were placed between two Teflon plates to prevent adhesion. Since the chemical nature of matrix materials are significantly different, the compression parameters were variant for polymer layers and multilayer composites. The process parameters and mold dimensions are listed in Tables 3.11 and 3.12, respectively. The process temperature was kept at 200°C. Since it was expected for materials to cover the molds and the behaviors of neat polymer and blends under heat were significantly different, there were distinct compression molding procedures applied for each sample.

Table 3.11 Compression Molding Parameters of Polymer Layers.

Sample Code	**Weight (gr)**	**Compression Molding Procedure**
Neat PLA	40	7 min no pressure 2 min 50-200 bar
	20	7 min no pressure 2 min 50-100 bar
70PLA/30ABS	40	7 min no pressure 2 min 100-280 bar
	20	7 min no pressure 2 min 10 bar
10SAN-GMA	40	7 min no pressure 2 min 50 bar
	20	7 min no pressure 2 min 50-250 bar

Table 3.12 Compression Molding Parameters of Multilayer Composites.

Sample	Number of Carbon Fiber Layer	Compression Molding Procedure
Neat PLA	1CF	5 min no pressure 2 min 30-60-90 bar
	3CFs	5 min no pressure 2 min 30-60-90-120 bar
70PLA/30ABS	1CF	5 min no pressure 2 min 30-60-90-120 bar
	3CFs	5 min no pressure 2 min 30-60-90-150 bar
10SAN-GMA	1CF	5 min no pressure 2 min 30-60-90-120 bar
	3CFs	5 min no pressure 2 min 30-60-90-150 bar

3.4 Characterization Methods

3.4.1 Tensile Test

Tensile test was used to determine tensile strength, modulus and elongation at break values of polymer blends that were previously injection molded and multilayer composite specimens that were prepared by compression molding. For this purpose, a Shimadzu Autograph AG-IS 100 kN universal tensile testing instruments was used. A photograph of the instrument is given in Figure 3.11.

Figure 3.11 Photograph of Tensile Test Machine.

The cross-head speeds were chosen as 3 mm/min for tensile test specimens of neat polymer and blends and 2 mm/min for tensile test specimens of carbon fabric-reinforced polymer composite specimens. The tests were carried out at room temperature. The tensile strength, modulus and elongation at break values were calculated depending on stress-strain data. In the calculation of the strain, the gauge length was taken as initial distance between the grips, L in Figure 3.12 for polymer blend specimens and it was taken as length of narrow parallel sided portion, L_1 in Figure 3.13 for multilayer composites.

The dimensions of tensile test specimens were determined based on the ISO 527-2 standard [21], type 5A specimen and ISO 527-4 standard [22], type 1B specimen for polymer blends and carbon fabric-reinforced polymer composites, respectively. The schemes of specimens are given in Figures 3.12 and 3.13 for type 5A specimen and

type 1B specimen, respectively. The dimensions are shown in the Tables 3.13 and 3.14.

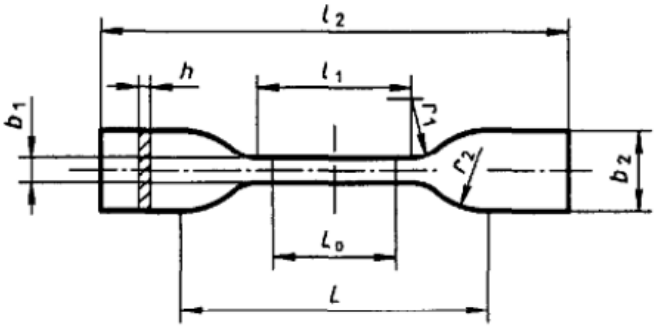

Figure 3.12 ISO 527-2 standard Type 5A Specimen [21].

Table 3.13 Dimensions of ISO 527-2 standard Type 5A Specimen [21].

Dimension	**Value, mm**
L_2 – Overall length, minimum	75
b_2 – Width at ends	12.5
L_1– Length of narrow parallel-sided portion	25
b_1 – Width of narrow parallel- sided portion	4
L – Initial distance between grips	50
L_0 - Gauge Length	20
h- Thickness, minimum	2

Since the mold of injection molding machine was standard for tensile and impact test specimens, they were ready for testing just after processing. But for multilayer composites, the specimens were cut using water jet machine in Peyar İnşaat Dekorasyon Ltd. Şti. with dimensions illustrated in Figure 3.13 and given in Table 3.14.

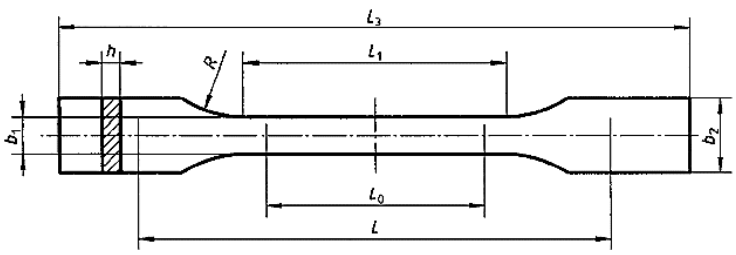

Figure 3.13 ISO 527-4 Standard Type 1B Specimen [22].

Table 3.14 Dimensions of ISO 527-4 Standard Type 1B Specimen [22].

Dimension	**Value, mm**
L_2 – Overall length, minimum	150
b_2 – Width at ends	20
L_1– Length of narrow parallel-sided portion	60
b_1 – Width of narrow parallel- sided portion	10
L – Initial distance between grips	115
L_0 - Gauge Length	50
h- Thickness, minimum	2-10

3.4.2 Impact Test

Impact test of neat polymers and their blends with compatibilizers were carried out using a Ceast Resil Impactor 6967 device according to ISO 179 [42]. The charpy test was applied with hammer of 7.5 J. An image of the test device is given in Figure 3.14. The specimen (unnotched) dimensions are listed in Table 3.15.

Figure 3.14 Photograph of Impact Test Machine [71].

Table 3.15 Dimensions of Impact Test Specimen.

Dimension	**Value, mm**
Overall Length	80
Width	10
Thickness	4

3.4.3 Flexural Test

Flexural test was used to determine the flexural strength and modulus of the produced carbon fabric-reinforced polymer composites. To observe delamination behavior of the multilayer composites, Shimadzu Autograph AG-IS 100 kN universal tensile testing instrument was used in applying 3-point bending test. The test was carried out according to the ASTM D790 standard [24]. The crosshead speed was selected as 3 mm/min. The span to depth ratio was chosen as 16:1. Dimensions of test specimens are listed in Table 3.16.

Table 3.16 Dimensions of Flexural Test Specimen.

Dimension	**Value, mm**
Overall Length	80
Width	10
Thickness	≈ 2

3.4.4 Thermogravimetric Analysis

The maximum temperature at degradation and the temperatures at 10% weight loss were measured using a Shimadzu DTG-60H Thermogravimetric Analyzer. The weights of the specimens were between 5-10 mg and they were heated up to 600°C from room temperature at a rate of 10°C/min under nitrogen atmosphere.

3.4.5 Differential Scanning Calorimetry

DSC is one of the thermal characterization methods for neat polymers and their blends. In this thesis, the glass transition temperature and melting temperature were determined using a Shimadzu DSC-60A differential scanning calorimeter.

Before the analysis samples were placed into an aluminum pan and compressed covering the sample. The analyses were carried out for samples having 5-10 mg weight with two heating scans and one cooling scan. The samples were heated from 50°C to 250°C under nitrogen atmosphere at a heating rate of 10°C/min, and cooled spontaneously to room temperature. The results were reported from the second heating scan. From the data taken, the degree of crystallinity of the samples were evaluated by Equation 6 [43].

$$X_c(\%) = \frac{\Delta H_m}{w_p \times H_m^\circ} x100 \quad (6)$$

where $X_c(\%)$ is the degree of crystallinity of the blends or neat polymers, w_p is the weight fraction of crystalline polymer in the blend, ΔH_m is the heat of melting (J/g) and H_m° is the heat of fusion of fully crystalline polymer which is 93.6 J/g for PLA [44].

3.4.6 Fourier Transform Infrared Spectroscopy

FTIR analysis was done to observe possible interactions between polymers and compatibilizers. Perkin Elmer FTIR-ATR instrument was used for FTIR analysis with 4000-500 cm^{-1} wavelength range, 4 cm^{-1} resolution and 64 number of scans.

3.4.7 Scanning Electron Microscopy

SEM analysis was performed with a QUANTA 400 F Field Emission High Resolution Scanning Electron Microscope in METU Central Laboratory. SEM images of the impact and tensile fractured surfaces were taken in various magnifications. To provide conductivity, the samples were coated with gold palladium alloy before the analysis.

3.4.8 Ash Content Analysis

Ash content analysis was carried out using a furnace to determine experimentally the carbon fiber content of multilayer composites. Analysis was carried out according to ASTM D5630-13 [45]. The furnace was set at 650°C to lose all the polymer with less than 4% loss in carbon fiber [46]. First the crucibles were cleaned and left in the furnace for 30 minutes. Then, the crucibles were put in desiccator to cool for 15

minutes. After that, the empty crucibles were weighted (w_1). Approximately 2 grams of multilayer samples were prepared and put in the crucibles and reweighted (w_2). The crucibles with samples were left in the furnace for 20 minutes and then left for cooling in the desiccator for 15 minutes. After cooling, the crucibles were weighted (w_3). The percent carbon fiber content was calculated with the following equation below. The theoretical calculations and the results of ash content analysis are given in Appendix A and Table B.1. in Appendix B, respectively.

$$\text{Ash Content (\%)} = \frac{w_3 - w_1}{w_2 - w_1} \times 100 \tag{7}$$

CHAPTER 4

RESULTS AND DISCUSSION

4.1 Characterization of Polymer Blends

4.1.1 Effect of PLA/ABS Ratio and Thermal Stabilizer on Morphology, Thermal and Mechanical Properties

In this part, the results of morphology analysis, thermal and mechanical tests of PLA/ABS and Thermal Stabilizer/(PLA/ABS) blends are discussed. Several PLA/ABS ratios such as 90/10, 70/30, 50/50 were studied to observe the effect of ABS on PLA matrix and to determine the optimum blend content. These ratios were selected to keep the PLA as the main matrix material. The thermal stabilizers were introduced to the PLA/ABS blend to detect if there is a negative effect of process temperature (200°C) on material properties and to eliminate thermal degradation.

4.1.1.1 Blend Morphologies

The morphology analysis was carried out to figure out the behavior of ABS in PLA matrix. Analysis results of neat PLA and 90PLA/10ABS, 70PLA/30ABS, 50PLA/50ABS samples are shown in Figure 4.1. The images were taken from the impact fractured surfaces of samples.

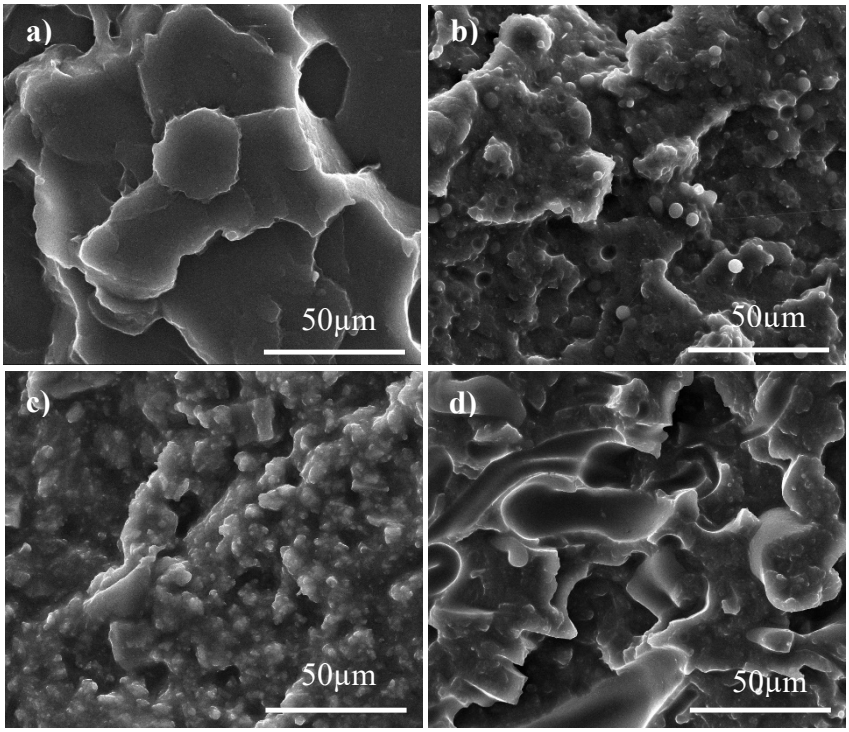

Figure 4.1 SEM Images of a) Neat PLA b) 90PLA/10ABS c) 70PLA/30ABS d) 50PLA/50ABS Blends.

Neat PLA shows smooth and continuous surfaces while in 70PLA/30ABS sample ABS is the irregularly dispersed phase in PLA matrix. ABS forms spherical phases in PLA matrix which can be attributed to two main reasons. Firstly, the process temperature which is 200°C may be insufficient for ABS to melt. Since degradation temperature of PLA which is between 240-250°C [37], is approximately equal to melting temperature of ABS which is between 240-260°C [47], it is difficult to keep PLA without degradation while melting ABS. The effect of process temperature on morphology was studied and discussed in Section 4.2. The second reason is the incompatibility between these polymers that forms distinct boundaries causing interfacial tension. In this case as the content of the dispersed phase increases, they are likely to form coalescence. When the volumetric ratio comes close to the viscosity ratio, the discontinuous phase transfers to the co-continuous phase. Since the viscosity of ABS is higher than PLA, as the ABS content increases, the co-

continuous phase morphology is observed. It can be seen from the SEM image of 50PLA/50ABS blend that ABS domains are no more the dispersed phase in PLA matrix.

The effect of thermal stabilizers on morphology of 70PLA/30ABS blend was investigated as a preliminary study of the thesis. SEM images of 70PLA/30ABS blend with 1% TS-1, 1% TS-2 and 0.5% TS-1+0.5% TS-2 can be observed from Figure 4.2. For all configurations, there are distinct phase separations and there is not any developing effect of thermal stabilizer on morphology. To prevent the excess use of additional material and formation of impurities, and as there is not any enhancement in the mechanical properties of the binary blends (Section 4.1.1.2), the thermal stabilizers were not preferred to be used in the content of the study.

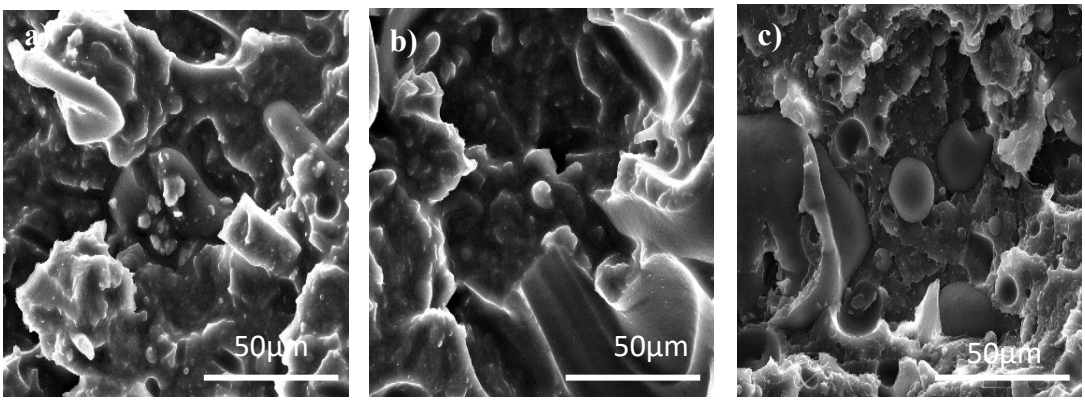

Figure 4.2 SEM Images of a) %1 TS-1/(70PLA/30ABS) b) %1 TS-2/(70PLA/30ABS) c) %0.5 TS-1+ %0.5 TS-2/(70PLA/30ABS) with 2000x Magnification.

4.1.1.2 Mechanical Properties

The mechanical properties including tensile strength, elastic modulus, elongation at break and the impact strength of PLA/ABS blends with 90/10, 70/30, and 50/50 ratios were investigated in this study. The tensile strength, the elastic modulus and the elongation at break values of the binary blends are given in Figures 4.3, 4.4 and 4.5, respectively. The average of test data and standard deviations can be seen in Table C.1. in Appendix C. Representative stress-strain curves are shown in Figure C.1 in Appendix C.

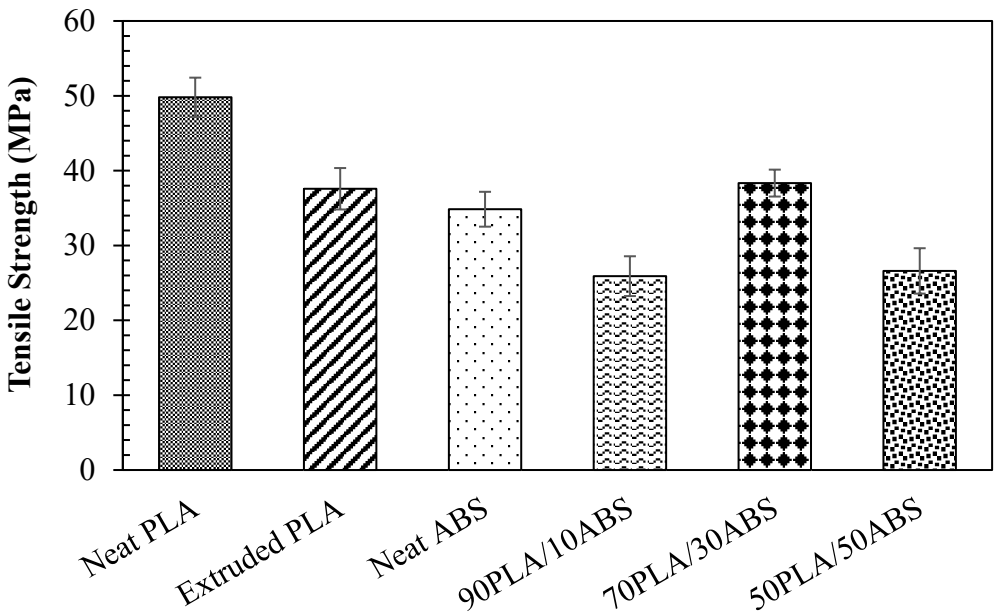

Figure 4.3 Tensile Strengths of Neat PLA, Extruded PLA, Neat ABS, PLA/ABS Blends.

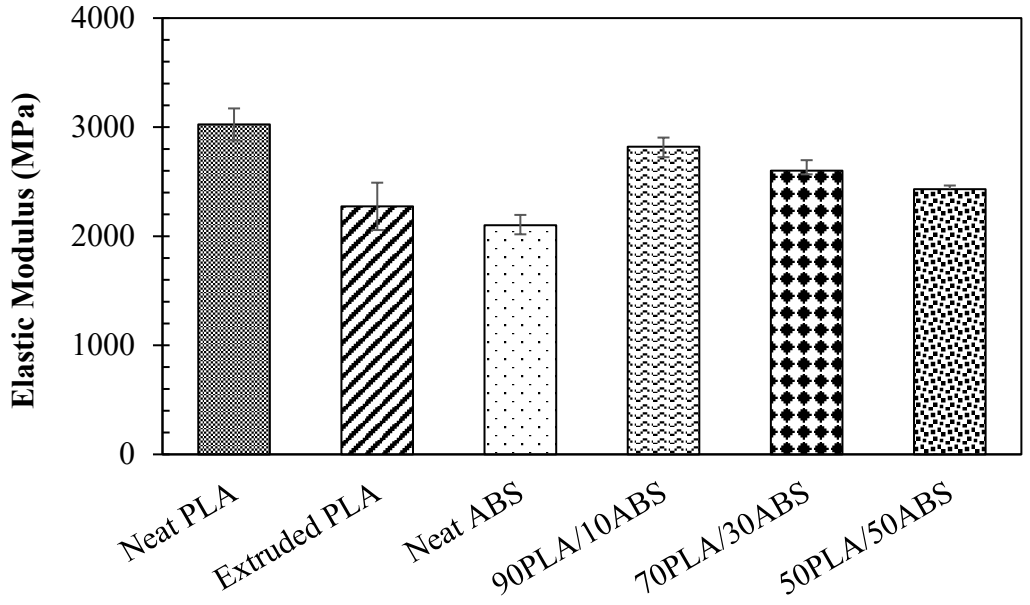

Figure 4.4 Elastic Moduli of Neat PLA, Extruded PLA, Neat ABS, PLA/ABS Blends.

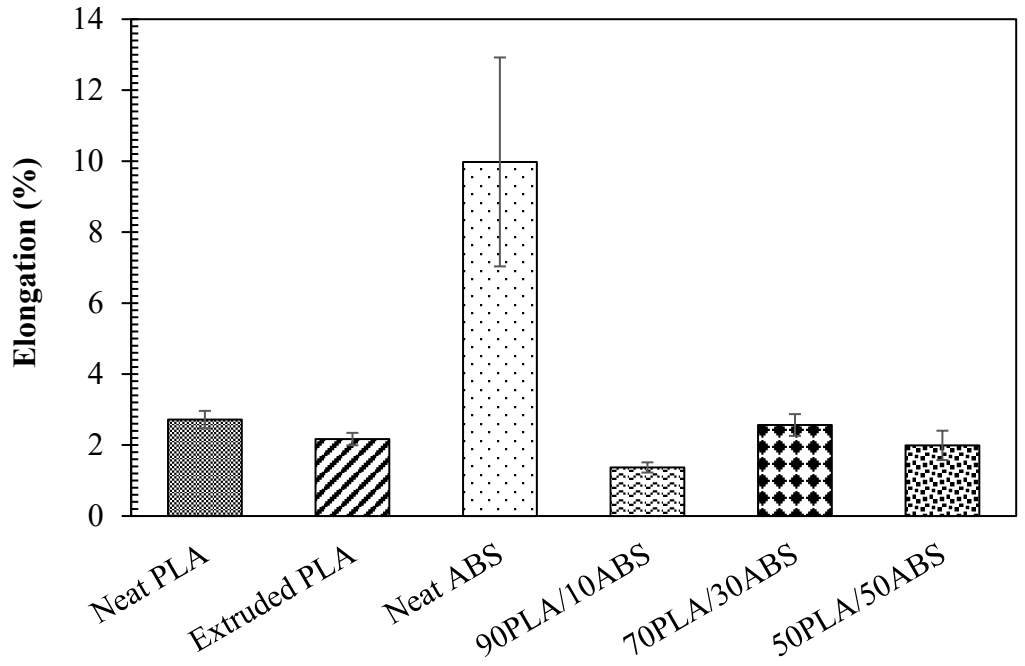

Figure 4.5 Elongation at Break of Neat PLA, Extruded PLA, Neat ABS, PLA/ABS Blends.

Temperature of 200°C is higher than the melting temperature of PLA (150-160°C) [37]. As PLA is exposed to second heating in injection molding after extrusion, the degradation occurs, and this leads to decrease in the tensile strength and modulus. The tensile strength of extruded PLA is 20% lower than tensile strength of neat PLA while the elastic modulus of extruded PLA is 25% lower than elastic modulus of neat PLA. While blending polymers it was expected to obtain mechanical properties between the values of neat polymers depending on the rule of mixture. In the case of mixing ABS with PLA, since the tensile strength and elastic modulus of neat ABS are lower than neat PLA, the drop in tensile strength and elastic modulus of PLA is consistent with the rule of mixture. However, for the blend ratios of 90PLA/10ABS and 50PLA/50ABS, the tensile strengths are around %30 lower than that of neat ABS. It is due to lack of miscibility between the PLA and ABS. As the content of ABS phase reaches the one in 70PLA/30ABS, the ABS domains are finely dispersed in PLA matrix which reduces the failures due to local stress concentrations causing tensile strength of 70PLA/30ABS blend to increase [48]. The decrease in tensile strength of 50PLA/50ABS blend can be attributed to two reasons. First, depending on the phase replacement between PLA and ABS, PLA is no longer the main matrix. This is also investigated in a study carried out by Hazer et al. [49], PLA and polycarbonate were blended in different ratios and mechanically characterized. It was stated that as the PLA amount increases, the properties of the blend are getting close to the properties of pure PLA. Second, as the content of ABS phase increases, it begins to contact each other forming coalescence. The coalescence of ABS domains prevents dispersion of external stresses through PLA matrix reducing the tensile strength. The elastic modulus results of PLA/ABS binary blends exhibit higher values than the modulus of extruded PLA and neat ABS.

The elongation at break results of PLA and PLA/ABS binary blends are lower than those of neat ABS. Since ABS has a rubbery nature, it shows the highest elongation at break. However, the incompatibility between PLA and ABS prevents the contribution of rubbery nature of ABS to elongation at break of binary blends. For

70PLA/30ABS binary blend, the elongation at break is relatively higher compared to the other blends. Because of incompatibility, the interfaces between spherical domains of ABS and PLA matrix might bring out slippage when the sample undergoes deformation [51]. When ABS content is increased to 50%, the ABS domains transfer to the co-continuous phase, the slippage under deformations becomes limited. At 10% ABS content, the amount of ABS domains is low to contribute slippage. Crazing is a deformation mechanism that forms a network between the cracks on the material under high tensile loads. It retards fracture in glassy polymers by the formation of microfibrils and voids [52]. The crazes occur parallel to applied stress causing elongation at break to increase. However, presence of ABS domains in PLA matrix restricts the formation of fine crazes causing decrease in elongation at break.

The impact strength values of neat PLA, neat ABS, extruded PLA and PLA/ABS blends are shown in Figure 4.6. The average values and the standard deviations of the test data are given in Table C.1. in Appendix C.

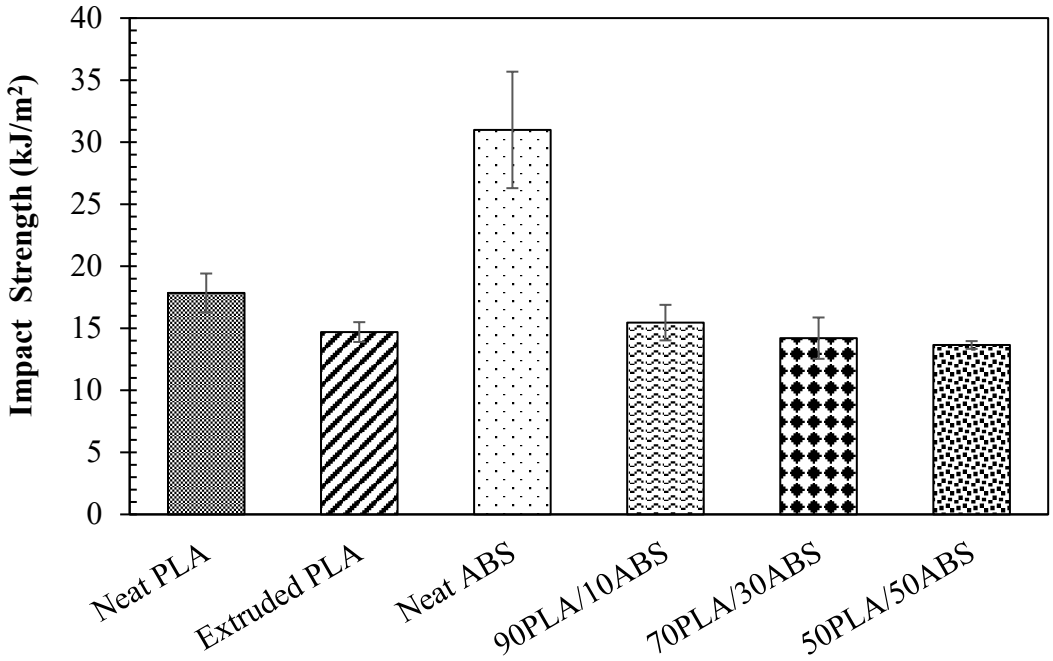

Figure 4.6 Impact Strengths of Neat PLA, Extruded PLA, Neat ABS, PLA/ABS Blends.

Enhancement in impact strengths of PLA/ABS binary blends is expected due to the fact that the butadiene content provides ABS a rubbery nature. However, the impact strengths of 90PLA/10ABS and 50PLA/50ABS binary blends are lowered with the addition of ABS due to the lack of compatibility. As stated by Kurtuluş [51], the presence of rubbery particles can control craze initiation and growth which contributes to the dissipation of impact energy. For 70PLA/30ABS binary blend, the presence of ABS domains dissipates the impact stresses through PLA matrix. When the ABS content reaches 50%, the ABS domains transfer to the co-continuous phase and the impact energy cannot be homogeneously dissipated through matrix by ABS domains, forming local stresses. At 10% ABS content, the particles are too small to dissipate impact energy.

For the determination of PLA/ABS ratio, the tensile strength is considered to be kept at maximum value as possible while keeping impact strength at an average value. The tensile strength of 70PLA/30ABS binary blend is approximately equal to

extruded PLA and there is not a significant difference among impact strengths of 90PLA/10ABS, 70PLA/30ABS and 50PLA/50ABS binary blends. In addition to mechanical properties, the morphology is taken into consideration for the determination of PLA/ABS ratio. In 70PLA/30ABS binary blend, ABS domains show more homogeneous dispersion than other binary blends without forming co-continuous phase morphology. For all these reasons, it is determined to continue with 70PLA/30ABS binary blend in further studies of the thesis.

The aim of using thermal stabilizers was to prevent any negative effect of process temperature on mechanical properties of the blends. The tensile and impact test results of 70PLA/30ABS blends with/without thermal stabilizers are given in Table 4.1.

Table 4.1 Tensile and Impact Test Results of Thermal Stabilizer/(70PLA/30ABS).

Samples	**Tensile Strength (MPa)**	**Elastic Modulus (MPa)**	**Elongation at Break (%)**	**Impact Strength (kJ/m^2)**
70PLA/30ABS	37.5±1.5	2601.3±96.1	2.5±0.2	14.2±1.7
1% TS-1/ (70PLA/30ABS)	27.1±1.1	2656.2±49.0	1.5±0.1	13.0±1.3
1% TS-2/ (70PLA/30ABS)	30.6±2.1	2544.6±83.2	1.8±0.2	12.1±1.1
0.5% TS-1+0.5% TS-2/ (70PLA/30ABS)	28.8±1.6	2631.2±100.6	1.6±0.2	13.4±0.5

In a study carried out by Amaro et al. [30], it was stated that around 200°C, PLA is thermally unstable and undergoes degradation due to hydrolysis. Since the blends were processed twice at 200°C through extrusion and injection molding before mechanical tests, there might be thermal degradation. To prevent degradation, phenolic and phosphite-based antioxidants as TS-1 and TS-2, respectively were introduced to 70PLA/30ABS binary blend. As seen from the table, there is not any positive contribution of the thermal stabilizers to the tensile strength and elongation at break results of the blends. Also, they do not cause a significant change in tensile moduli of the blends. On the other side, the impact strength of the blend is lowered with the addition of thermal stabilizer. When both morphology and mechanical test results are considered, it was decided not to use thermal stabilizers in the further parts of the study.

4.1.1.3 Thermal Properties

The effect of PLA/ABS ratios on thermal properties was determined with DSC analysis. The DSC thermograms are given in Figure 4.7. The average values and standard deviations of the test data are shown in Table 4.2. The degree of crystallinity values in Table 4.2 represent the maximum crystallinities which can be reached for the corresponding samples.

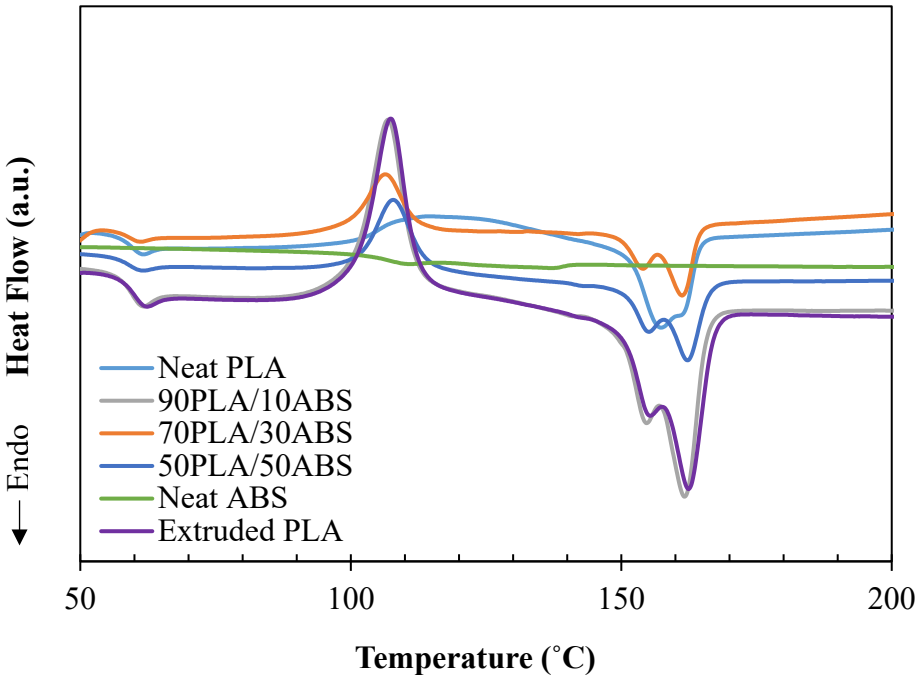

Figure 4.7 DSC Thermograms of PLA/ABS Blends.

Table 4.2 DSC Analysis Results of PLA/ABS Blends.

Samples	**Glass Transition Temperature (°C)**	**Melting Temperature (°C)**	**Heat of Melting (J/g)**	**Degree of Crystallinity (%)**
Neat PLA	58.5	157.3	38.4	41.0
Neat ABS	103.8	-	-	-
Extruded PLA	56.1	155.3/162.5	42.3	42.3
90PLA/10ABS	56.1	154.8/161.7	43.2	43.2
70PLA/30ABS	58.1	153.9/161.2	37.9	37.9
50PLA/50ABS	58.4	155.1/162.2	31.7	31.7

Since ABS is an amorphous polymer, it does not show melting peak in DSC curve, instead, at around 100°C, it is transferred from a glassy state to a rubbery state. While blending ABS with PLA, it was expected for glass transition temperature of binary blends to be higher than PLA because ABS has higher glass transition point than PLA. Considering the results in Figure 4.7, there is not a significant change in glass transition temperature and melting temperature of binary blends and extruded PLA. This stems from that the PLA and ABS are incompatible polymers. ABS become dispersed phase in PLA matrix not showing its characteristics. The glass transition and melting temperature of neat PLA slightly decrease when it is extruded before injection molding due to degradation of PLA at 200°C. In addition, the cold crystallization peak becomes apparent for extruded PLA and binary blends. It can be attributed to the rapid cooling of PLA during extrusion so that PLA has not enough time to crystallize. During injection molding of neat PLA, cooling is a relatively slow process when compared to extrusion. It provides time for PLA to recrystallize. Extruded PLA and binary blends show two melting peaks around 150°C and 160°C. The double melting behavior can be explained by melt-recrystallization model which describes melting of crystals, recrystallization and melting of recrystallizated crystals. Neat PLA has some less perfect crystal structures. Upon melting, the original crystals in the structure of neat PLA recrystallize [53]. The peak around 150°C shows the melting of original crystals while the peak around 160°C represents the melting of recrystallized crystals. 90PLA/10ABS blend shows the sharpest peak of cold crystallization when compared to 70PLA/30ABS and 50PLA/50ABS blends. The crystallization of polymers can be activated by the presence of other domains in the matrix since the domains provide nucleation sites by decreasing the nucleation energy barrier. The accelerated cold crystallinity is confined with increasing content of ABS due to the dilution effect [54]. Therefore, as the content of ABS increases the degree of crystallinity decreases. In addition, for 70PLA/30ABS and 50PLA/50ABS binary blends, ABS show its amorphous characteristic by dominating the highly crystalline structure of PLA. At lower contents of ABS, the enhanced kinetics may stem from the higher chain mobility. This situation can be

observed from Table 4.2. When the ABS content is 10% in the blend, the degree of crystallinity reaches its highest value among the other samples.

4.1.2 Characterization of Compatibilizer/PLA/ABS Blends and Determination of the Type of Compatibilizer and Ratio in PLA/ABS Binary Blend

In this part, to achieve compatibilization between PLA and ABS, different compatibilizers such as styrene ethylene butylene styrene terpolymer grafted with maleic anhydride (SEBS-MAH), ethylene-glycidyl methacrylate copolymer (E-GMA), styrene-maleic anhydride (SMA), and styrene-acrylonitrile glycidyl methacrylate (SAN-GMA) were blended with 70PLA/30ABS blend. Each compatibilizer was added to 70PLA/30ABS binary blend with concentrations of 5, 10, 15 wt.%. The most effective compatibilizer and its content were determined depending on FTIR analysis, SEM analysis, mechanical (tensile and impact tests) and thermal tests (DSC and TGA) results.

4.1.2.1 FTIR Analysis

FTIR analysis was performed to find evidence of interaction between the polymer matrix and the compatibilizers. Since the compatibilizers were selected considering their functional groups that can form a bridge between PLA and ABS, it is possible to figure out the interaction from the peak intensities, characteristic wavelengths, peak formations, and disappearances. The FTIR spectra of compatibilizer/(70PLA/30ABS) blends are given in Figure 4.8.

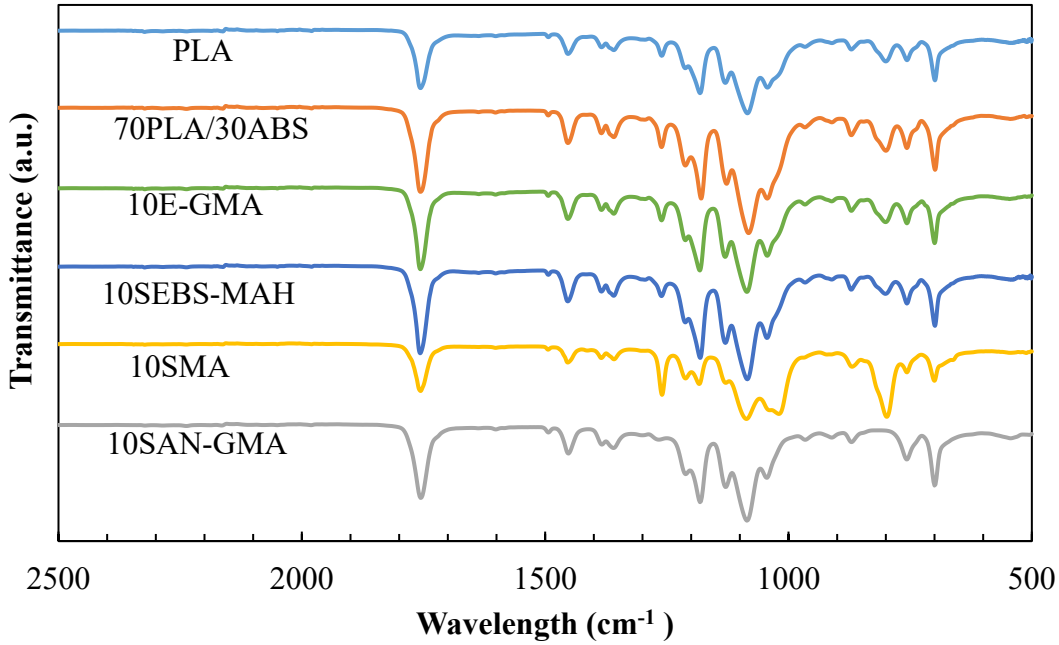

Figure 4.8 FTIR Spectra of Compatibilizer/(70PLA/30ABS) Blends.

Considering the FTIR curves in Figure 4.8, the major differences in characteristic peaks can be observed for the peaks of 10SMA blend and 10SAN-GMA blend indicating that their performances as compatibilizer are better among others. The decrease in peak intensities due to dilution effect with the addition of compatibilizers are taken into consideration by comparing the decrease in all peaks and investigating the noticeable peaks. For detailed analysis of the change in FTIR curve with the addition of SMA to the 70PLA/30ABS binary blend, the FTIR curves of SMA, 70PLA/30ABS and 10SMA are given in Figure 4.9.

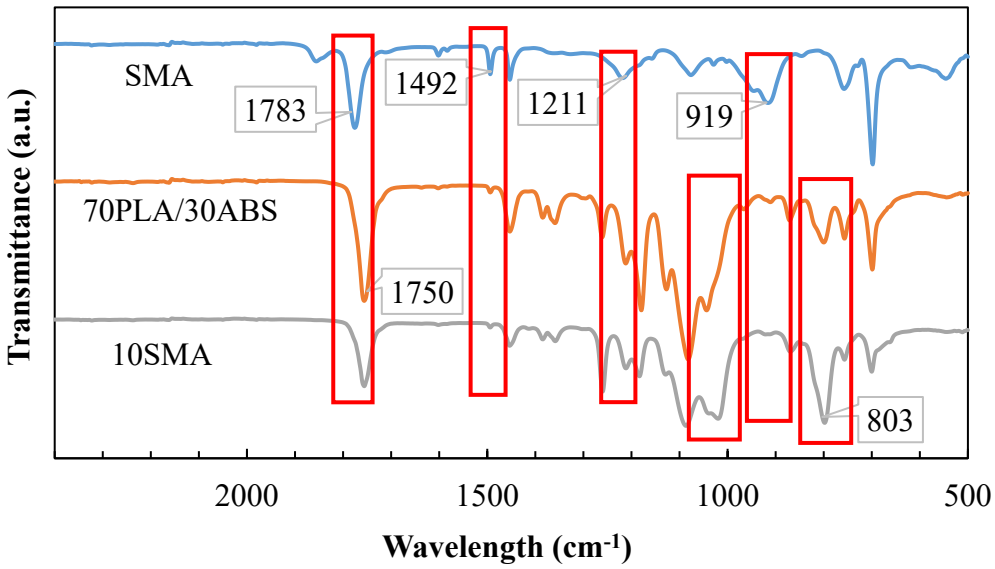

Figure 4.9 FTIR Spectra of Neat SMA, 70PLA/30ABS and 10SMA Blends.

As stated by Zhang et al. [55] ABS undergoes grafting reaction with MAH. It explains the loss in peak intensity around 1492 cm^{-1} which represents C=C bond in SMA structure. The peak of 70PLA/30ABS sample at 1042 cm^{-1} wavelength broadens with SMA addition indicating sp^3 C-N stretching in maleic anhydride grafted ABS. At wavelength of 803 cm^{-1}, the peak intensity increased with SMA which shows the C-H deformation in ABS structure. As stated by Zeng et al. [56], MAH functional group is also reactive with PLA forming ester structures from anhydride and hydroxyl group of PLA. Anhydride characteristic peaks exist at around 1780-1850 cm^{-1}, 1260 cm^{-1} and 919 cm^{-1} indicating C=O, C-O-C and C-H bonds, respectively. The peak at 1783 cm^{-1} in FTIR curve of SMA shifts to 1750 cm^{-1} which indicates the C=O bond in esters [57], and the other characteristic peak around 919 cm^{-1} disappears.

For detailed analysis of the change in FTIR curve with the addition of SAN-GMA to the 70PLA/30ABS binary blend, the FTIR curves of SAN-GMA, 70PLA/30ABS and 10SAN-GMA are given in Figure 4.10.

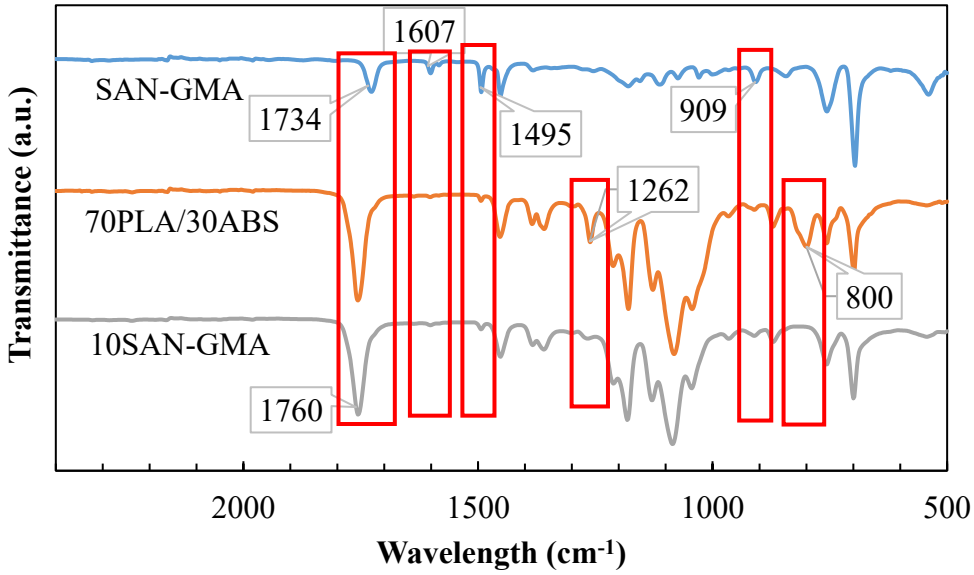

Figure 4.10 FTIR Spectra of Neat SAN-GMA, 70PLA/30ABS and 10SAN-GMA Blends.

Considering the reaction given in a study by Zeng et al. [56], the epoxy group undergoes reaction with carboxyl and hydroxyl functional groups of PLA. The intensity of epoxy characteristic peak at 909 cm^{-1} decreases when the SAN-GMA is added to the blend. The reaction can be proven by the disappearance of the peaks at 1262 cm^{-1}, 800 cm^{-1} respresenting C=O bending, C-C stretching in PLA, respectively. There is not any certain reaction that ABS undergoes with SAN-GMA. However, the decrease in peak intensities at 1734 cm^{-1}, 1607 cm^{-1} and 1495 cm^{-1} representing C=C bond in the acrylic moiety of GMA, carbonyl strecthing of GMA and C=C bond in styrene content of SAN-GMA, respectively, indicates potential interactions with ABS [58].

4.1.2.2 Blend Morphologies

SEM analyses were done to observe the effect of compatibilizer on blend morphology. SEM image of neat PLA, 70PLA/30ABS blend with and without compatibilizers are given in Figure 4.11.

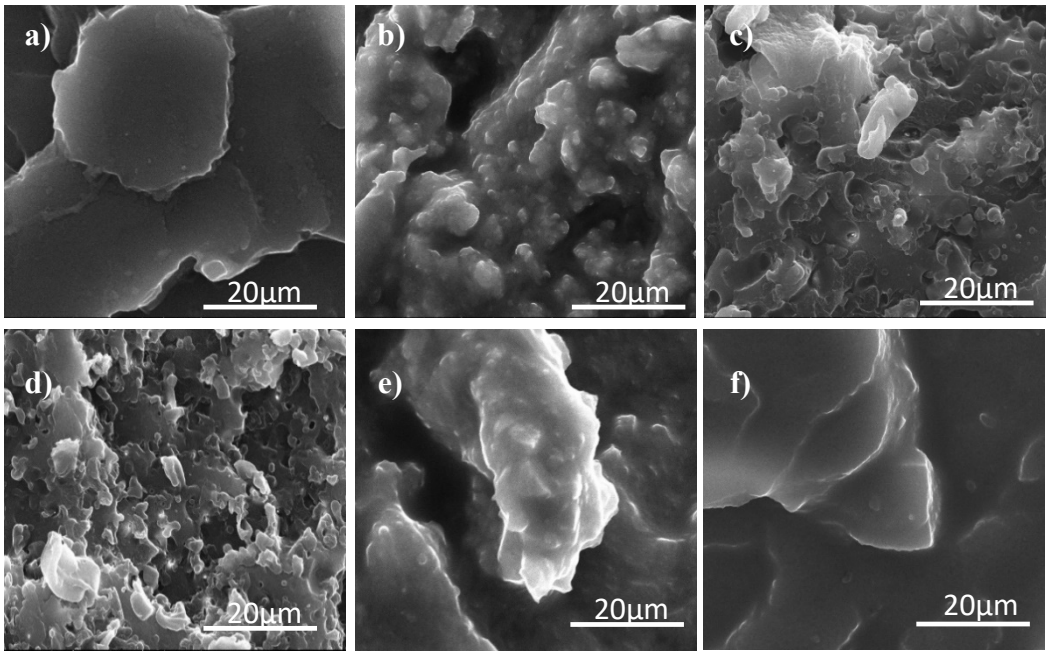

Figure 4.11 SEM Images of a) Neat PLA b) 70PLA/30ABS Blend c) 10E-GMA d) 10SEBS-MAH e) 10SMA f) 10SAN-GMA Containing 70PLA/30ABS Blends with 5000x Magnification.

When comparing the images of neat PLA and 70PLA/30ABS blend, it can be concluded that ABS is embedded in PLA matrix forming a secondary phase and there are apparent interfaces. With the addition of compatibilizers, the domain size decreases since the use of copolymers prevent ABS domain from coalescence. The presence of compatibilizer covers the surfaces of ABS domain decreasing its mobility [59]. Among the compatibilizers, SEBS-MAH is found to be less effective in decreasing the interfacial tension. When compared to SEBS-MAH, E-GMA looks more homogeneous in 70PLA/30ABS matrix due to its epoxy functionality that

might react with hydroxyl and carboxyl groups of PLA. For SMA, the shape of the ABS domain becomes irregular and the interfaces become unclear due to interactions proved by FTIR analysis but ABS domains are still visible in PLA matrix. It may be due to the high viscosity of ABS compared to PLA [60]. Considering the SEM image of blend with SAN-GMA, the ABS domains become invisible in PLA matrix forming a smooth texture. The use of SAN-GMA reduces the interfacial tension causing effective dispersion and stabilization of the blend [59]. The enhancement in morphology can be attributed to the high epoxy content of SAN-GMA which increases the possibility of reaction when compared to E-GMA and the SAN phase of SAN-GMA that is compatible with the ABS, resulting in a homogeneous blend.

4.1.2.3 Thermal Properties

The results of thermal analysis reveal information about material characteristics such as glass transition temperature which provides clues on toughness, degree of crystallinity and the possibility of the nucleation effect of compatibilizer [61]. The analysis results are given in Table 4.3.

Table 4.3 DSC Results of Compatibilizer/70PLA/30ABS Blends.

Samples	**Glass Transition Temperature (°C)**	**Melting Temperature (°C)**	**Heat of Melting (J/g)**	**Degree of Crystallinity (%)**
Neat PLA	58.5	157.3	38.4	41.0
Extruded PLA	56.1	155.3/162.5	39.7	42.3
70PLA/30ABS	58.1	153.9/161.2	24.8	37.9
10SMA	58.0	154.6/160.9	24.7	37.7
10SEBS-MAH	58.9	155.3/162.2	21.1	32.1
10E-GMA	58.6	155.2/161.9	21.6	32.9
10SAN-GMA	59.5	155.2/159.8	19.6	29.9

Considering the glass transition and melting temperatures, there are no significant differences between neat PLA, extruded PLA and ternary blends. The degree of crystallinity values in Table 4.3 represent the maximum crystallinities which can be reached for the corresponding samples. The percent crystallinity of PLA decreases with the addition of ABS and compatibilizers. Since ABS is an amorphous polymer, while blending with PLA, the content of crystalline structures decreases. The compatibilizers are used to interact with functional groups of polymers in the blend to enhance interfacial interactions. Since ABS is a more viscous polymer when compared to neat PLA, the presence of interaction between ABS and PLA increases the viscosity of the blend which retards the crystal growth [62]. The degree of crystallinities of the blends with compatibilizers except for 10SMA are lower than 70PLA/30ABS blend which proves that compatibilizers are effective at different levels. For compatibilizers having low interactions between the polymers of the blend, since the mobility is increased and there are fewer restrictions for alignment, the crystallinity increases. Besides, SAN-GMA is known as a chain extender which provokes the formation of long chains of PLA decreasing heat of melting [63]. This causes a decrease in degree of crystallinity which may be the clue of increased impact strength. These reasons prove that SAN-GMA is the most effective compatibilizer for 70PLA/30ABS blend among E-GMA, SEBS-MAH and SMA.

The TGA analysis curves of neat PLA, 70PLA/30ABS and compatibilizer/(70PLA/30ABS) blends are given in Figures 4.12 and 4.13. The numerical results are given in Table 4.4.

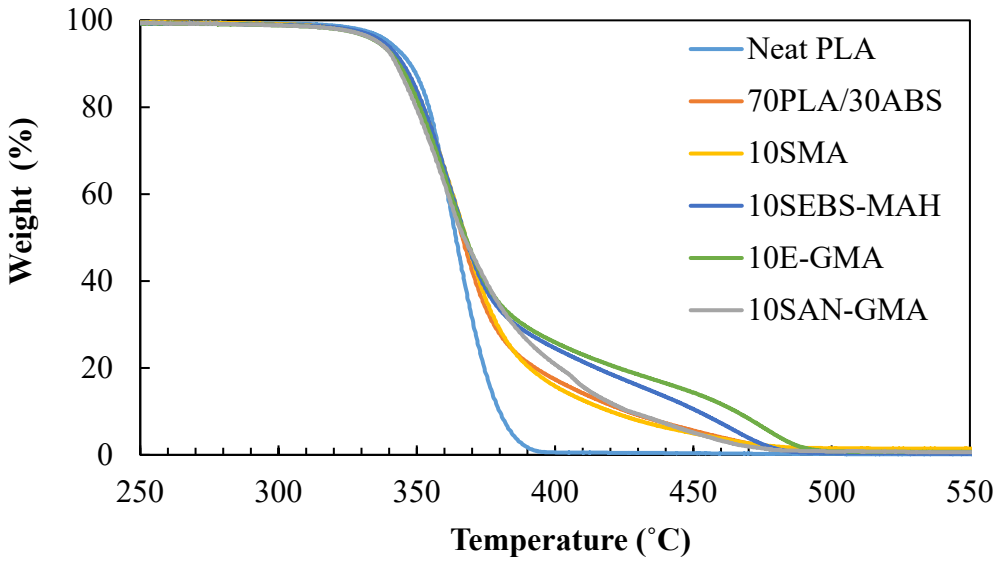

Figure 4.12 TGA Curves (Weight) of Compatibilizer/(70PLA/30ABS) Blends.

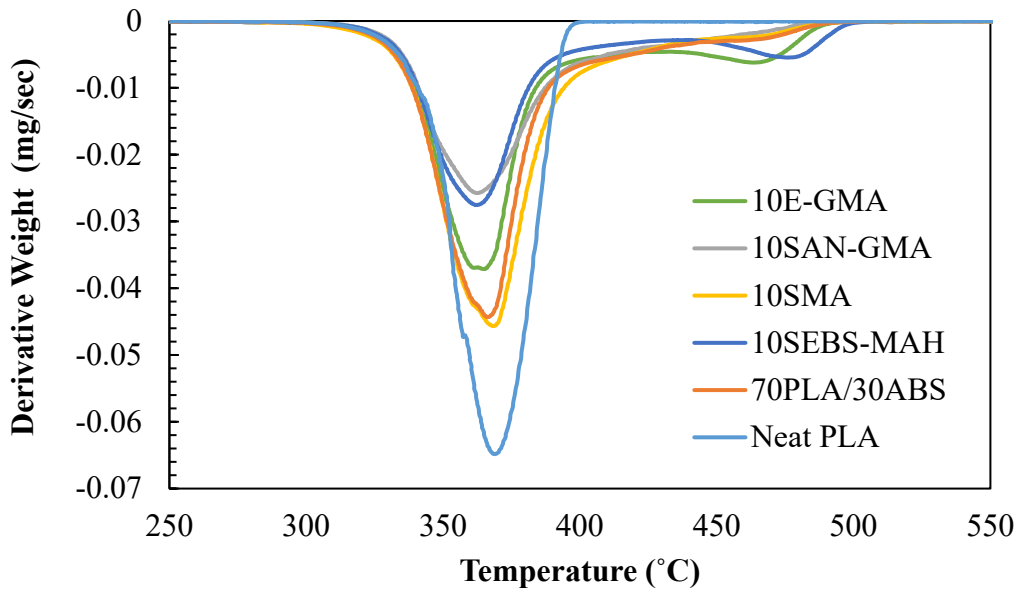

Figure 4.13 TGA Curves (Derivative Weight) of Compatibilizer/(70PLA/30ABS) Blends.

Table 4.4 TGA Results of Compatibilizer/(70PLA/30ABS) Blends.

Sample Codes	**Temperature at Maximum Weight Loss (°C)**	**Temperature at 10% Weight Loss (°C)**
Neat PLA	369.0	379.9
70PLA/30ABS	366.3	426.1
10SMA	368.6	419.9
10SEBS-MAH	364.9	451.4
10E-GMA	362.2	465.3
10SAN-GMA	362.2	426.7

As shown in Table 4.4, there is not any significant difference in the temperatures at maximum weight loss with the addition of both ABS and compatibilizers. But they have different temperatures at 10% weight loss. Comparing with neat PLA, the temperatures of binary and ternary blends at 10% weight loss are quite high. This may be due to the bio-degradable nature of PLA. In blends, PLA degrades first, and it is followed by the degradation of ABS and compatibilizers due to the higher process temperature of ABS which is around 230 - 260°C. The thermal stability of 70PLA/30ABS blend does not change with the addition of SMA and SAN-GMA due to the interaction formed with SAN-GMA and SMA between PLA and ABS. This may be due to combined effect of degradable nature of PLA and higher thermal stability of ABS. For the blends with E-GMA and SEBS-MAH, the %10 weight loss is reached at higher temperatures than SAN-GMA and SMA due to the lack of interaction between ABS and PLA.

4.1.2.4 Mechanical Properties

The mechanical properties of compatibilizer/(70PLA/30ABS) blend with 5%, 10%, 15% compatibilizer contents were investigated by tensile and impact tests. The tensile strength, elastic modulus and elongation at break values of the ternary blends are given in Figures 4.14-4.16, respectively. The average values and standard deviations of the test data can be seen in Table C.2. in Appendix C. Representative stress-strain curves are shown in Figure C.2 in Appendix C.

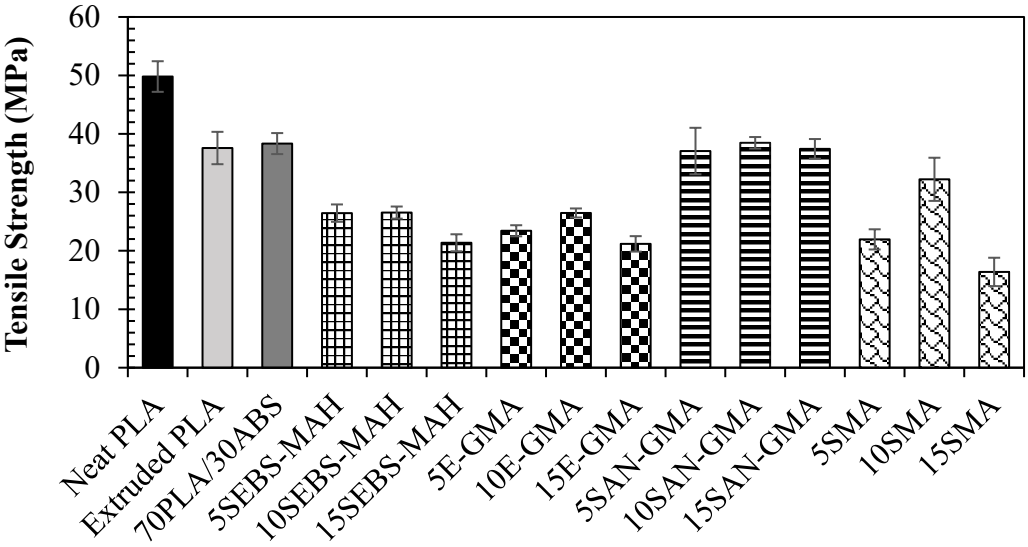

Figure 4.14 Tensile Strengths of Compatibilizer/(70PLA/30ABS) Blends.

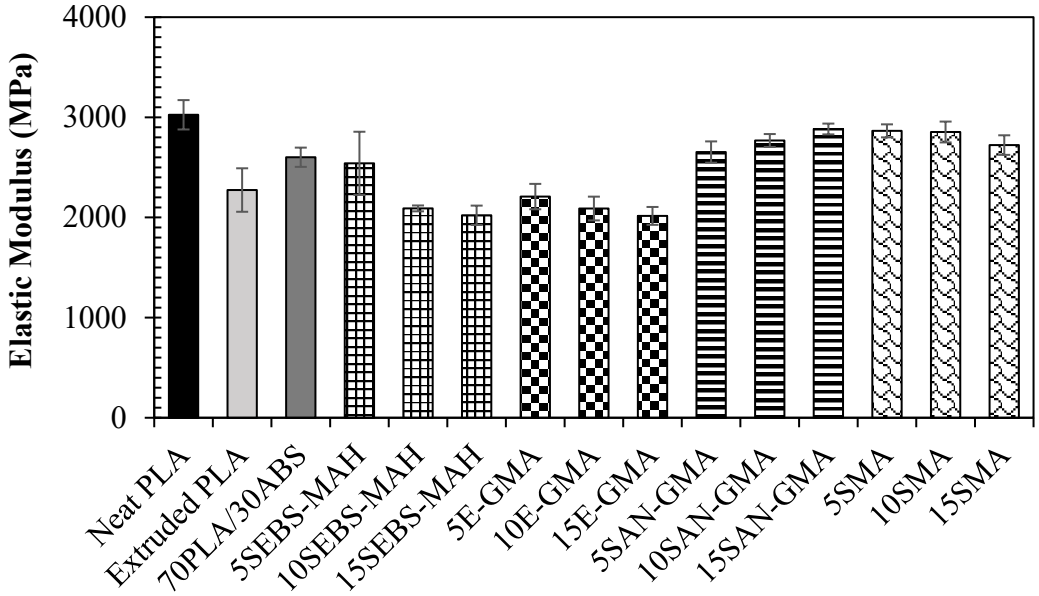

Figure 4.15 Elastic Moduli of Compatibilizer/(70PLA/30ABS) Blends.

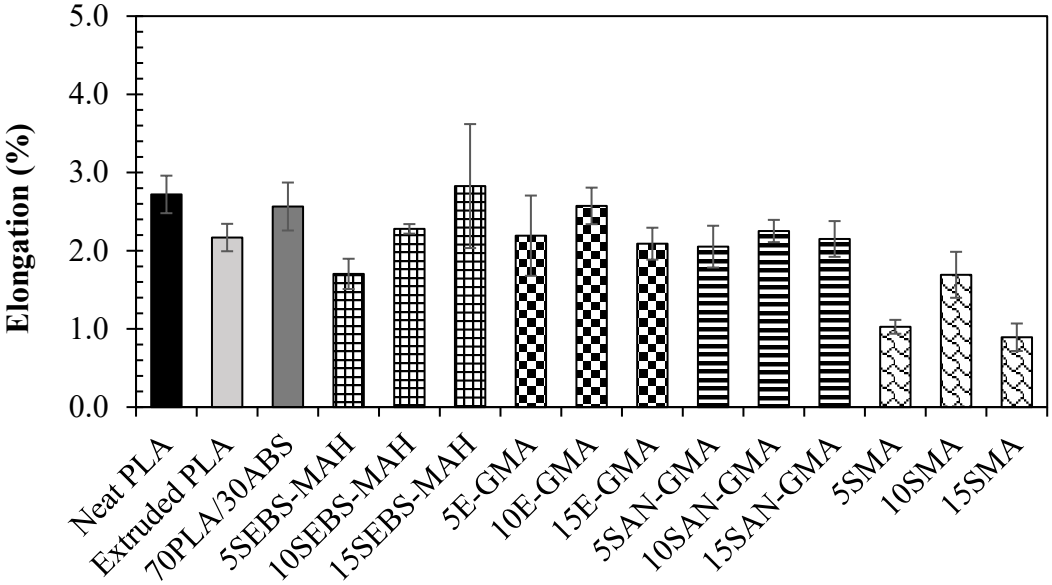

Figure 4.16 Elongation at Break of Compatibilizer/(70PLA/30ABS) Blends.

Tensile strength results shown in Figure 4.14 reveal that addition of SAN-GMA into the polymer blend matrix does not change the tensile strength of 70PLA/30ABS blend while there is a drop in tensile strength for other compatibilizers. There are two competing effects on the interfacial tension between PLA and ABS with the compatibilizers. Since ABS is a rubbery material having lower tensile strength when compared to neat PLA, it was expected that tensile strength decreases during polymer blending considering the rule of mixture. However, compatibilizers function as a bridge to transfer load between the phases. The better load transfer results in higher tensile strength. As can be proven with morphology analysis, the sharp interfaces between ABS domain and PLA matrix become invisible with the addition of SAN-GMA when compared to other compatibilizers. These reasons explain the similar tensile strengths of 70PLA/30ABS and 70PLA/30ABS compatibilized with SAN-GMA. For other compatibilizers, since the efficient load transfer cannot be achieved due to apparent ABS domains and there is the rubbery effect of ABS, the tensile strength is relatively low. More than 10% compatibilizer causes a drop in tensile strength. This can be attributed to the elastomeric behavior of compatibilizers [51]. While the compatibilizers decrease the interfacial tension, it also softens the PLA matrix. After 10% compatibilizer content, the softening effect can dominate which leads to a decrease in tensile strength.

Considering the elastic modulus results of all ternary blends in Figure 4.15, neat PLA has the highest modulus among them. This can be attributed to the highly crystalline structure of PLA. It is a semi-crystalline polymer that the amorphous areas are in glassy state [32]. The crystalline structure restricts the mobility of molecular chains by decreasing free volume, so it favors modulus. Another parameter affecting modulus is the presence of the rubbery phase. With the addition of ABS and compatibilizers, the elastic modulus of neat PLA is decreased. Considering the rule of mixture, a decrease in elastic modulus of PLA with the addition of ABS is expected since ABS has a relatively low modulus. However, there is not significant difference between the elastic modulus of extruded PLA and 70PLA/30ABS. This

situation stems from the incompatibility between PLA and ABS that ABS does not show its characteristics in PLA matrix. The decrease with the addition of compatibilizers can be explained by the plasticizing effect of compatibilizer. Among compatibilizers, SAN-GMA and SMA result in the high modulus of the blends, providing efficient load transfer by minimizing the ABS domains in PLA matrix.

Based on the elongation at break results given in Figure 4.16, it can be concluded that the elongation at break values decrease with the contribution of compatibilizers. The lack of interfacial adhesion has both promoting and demoting effects on elongation behavior. For 70PLA/30ABS specimen as shown in morphological analysis, ABS is dispersed as spherical particles in PLA matrix causing apparent interfaces. Under deformation, the interfaces between spherical ABS domains and PLA matrix provide slippage enhancing the elongation at break value. This reason explains why 70PLA/30ABS blend result in higher elongation values than extruded PLA. For the compatibilized blends, while the contribution of a rubbery phase increases the elongation at break, the slippage mechanism cannot contribute to elongation at break due to the minimized ABS domains.

The impact strengths of PLA and the blends are given in Figure 4.17. In accordance with morphology analysis, impact strength results reveal that interfacial adhesion accomplished by compatibilizers enhances the impact strength like a toughening agent. Compatibilizers also provide effective resistance to crack propagation [53]. This explains how the 10SAN-GMA blend reaches the maximum impact strength of 27.0 kJ/m^2 among other blends. The compatibilizers are rubbery materials. As stated in a study by Kurtuluş [51], rubbery materials are able to contribute craze growth by dissipating significant amount of impact energy. It can be observed that with the addition of compatibilizers up to 10%, there is an increasing trend of impact strength except for E-GMA. As mentioned in the tensile strength of the blends, when compatibilizer content is more than 10%, the softening effect of compatibilizer dominates the interfacial adhesion effect, decreasing the impact strength.

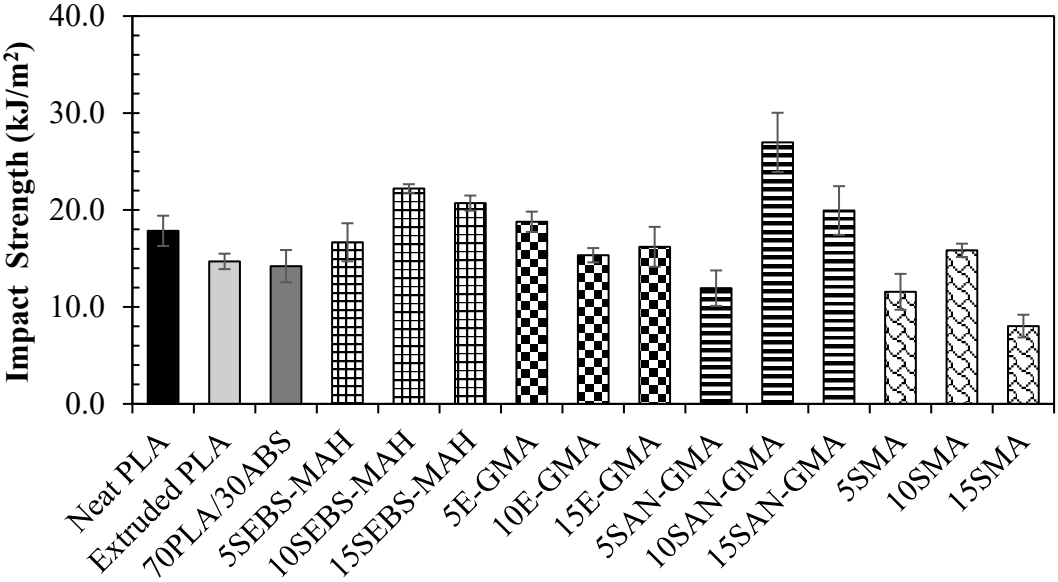

Figure 4.17 Impact Strengths of Compatibilizer/(70PLA/30ABS) Blends.

4.2 Effect of Process Temperature on Mechanical, Thermal Properties and Morphology of the Blends

4.2.1 Blend Morphologies

The morphology, FTIR analysis and mechanical test results revealed that among four different compatibilizers, SMA and SAN-GMA are more effective in compatibilization of PLA and ABS. Therefore, the effect of temperature analysis was studied with 70PLA/30ABS, 10SMA and 10SAN-GMA blends. Morphology analysis was carried out at both 200°C and 230°C. The SEM images for 70PLA/30ABS, 10SMA, and 10SAN-GMA blends are shown in Figure 4.18.

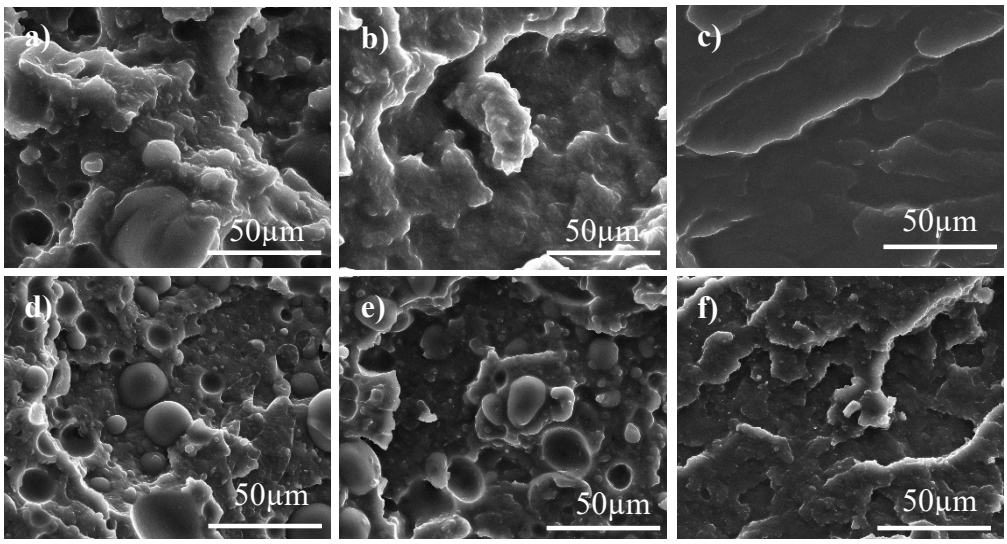

Figure 4.18 SEM Images of a) 70PLA/30ABS, and the Blends with b) 10SMA c) 10SAN-GMA Processed at 200°C d) 70PLA/30ABS and the Blends with e) 10SMA f) 10SAN-GMA Processed at 230°C with 2000x Magnification.

For 70PLA/30ABS and 10SMA blends, the increase in process temperature leads to an increase in the domain size. This phenomenon is known as the coalescence effect which involves the merging of dispersed phase domains into one larger domain [64]. At high temperatures, there is an increasing possibility for deformation and coalescence of ABS domains. For SAN-GMA, the sign of deformation on impact fractured surfaces become more visible at 230°C. The cavities on fracture surfaces stem from the removal of ABS particles during the impact test. Comparing the blends processed at 230°C between each other, SEM image of 10SAN-GMA blend show that the presence of compatibilizer reduces the coalescence, the ABS domains are invisible. However, ABS domains are apparent in SEM images of 70PLA/30ABS and 10SMA blend. For 10SMA specimen, the shape of ABS domains becomes ellipsoidal which indicates good interactions between the matrix and dispersed phase [61]. Based on the SEM image of the blend with SAN-GMA, it is concluded that SAN-GMA is very effective in decreasing the interfacial tension and stabilizing the phase morphology against coalescence.

4.2.2 Thermal Properties

The effects of process temperature on thermal properties were investigated by DSC and TGA analyses. The TGA analysis results at process temperatures of 200°C and 230°C, and representative derivative thermogravimetry curves at 230°C are given in Figures 4.19-4.21, respectively. The temperatures at maximum degradation and 10% weight loss are shown in Table 4.5.

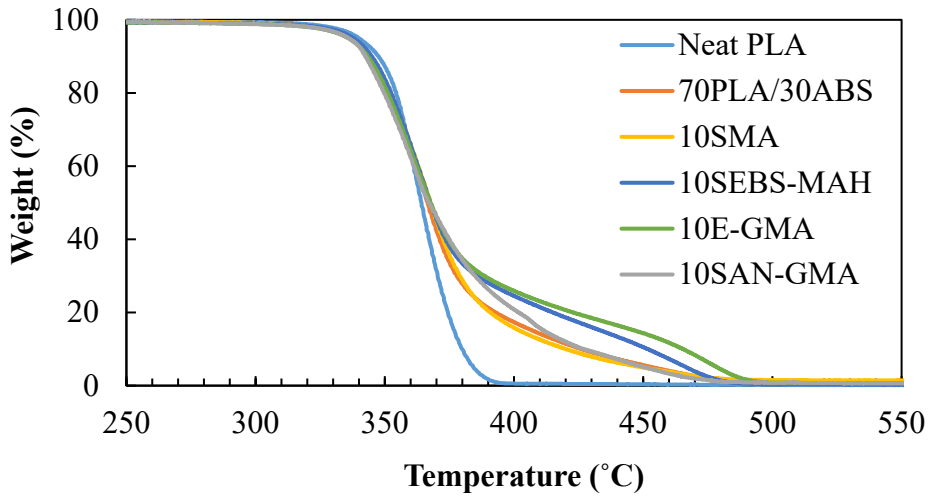

Figure 4.19 TGA Results (Weight) of 10Compatibilizer/(70PLA/30ABS) Blends Processed at 200°C.

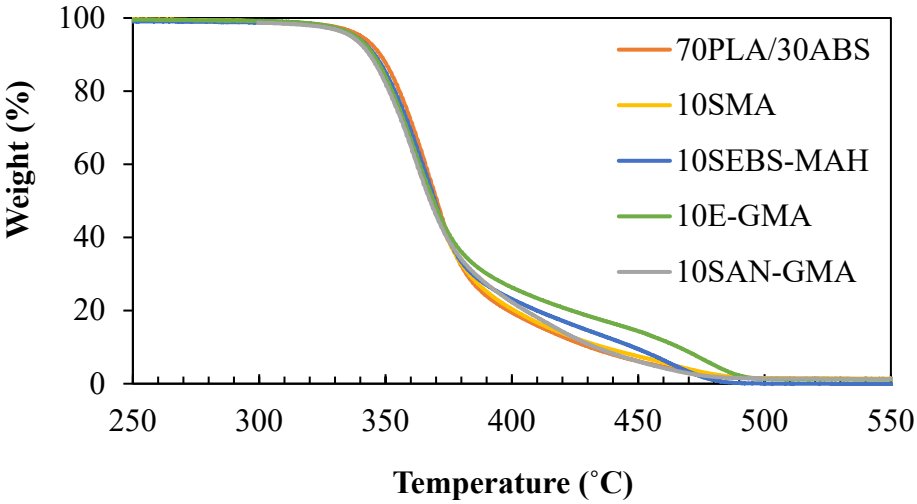

Figure 4.20 TGA Results (Weight) of 10Compatibilizer/(70PLA/30ABS) Blends Processed at 230°C.

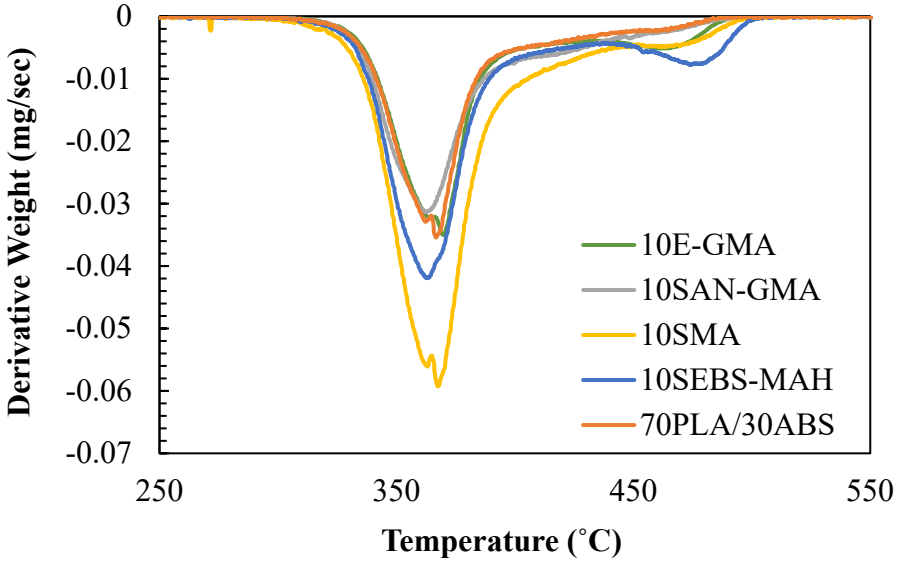

Figure 4.21 TGA Results (Derivative Weight) of 10Compatibilizer/(70PLA/30ABS) Blends Processed at 230°C.

Table 4.5 TGA Results of 10Compatibilizer/(70PLA/30ABS) Blends Processed at 200˚C and 230˚C.

Samples	**Temperature at Maximum Weight Loss (°C)**		**Temperature at 10% Weight Loss (°C)**	
	200°C	**230°C**	**200°C**	**230°C**
Neat PLA	369.0	-	379.9	-
70PLA/30ABS	366.3	366.7	426.1	427.3
10SMA	368.6	367.4	419.9	436.1
10SEBS-MAH	364.9	369.5	451.4	448.1
10E-GMA	362.2	362.9	465.3	465.9
10SAN-GMA	362.2	362.3	426.7	432.9

During processing, it was noticed that 230°C process temperature is not suitable for neat PLA. Due to its low viscosity at this temperature, it is not possible to process via extrusion. Therefore, it is not possible to observe the effect of process

temperature on neat PLA. The temperature at maximum weight loss and at 10% weight loss of the blends are not affected by 30°C increase in process temperature.

The DSC analysis results and the degree of crystallinities of ternary blends at 230°C and 200°C are given in Table 4.6. The glass transition temperature and the melting temperature of 70PLA/30ABS and ternary blends are not affected by the increase in process temperature. The degree of crystallinity values in Table 4.6 represent the maximum crystallinities which can be reached for the corresponding samples. At 230°C, there is not a significant change in degree of crystallinity of ternary blends except 10SEBS-MAH when compared to 70PLA/30ABS blends. When process temperature is increased, the mobility of PLA chains increases which leads to fewer restrictions for crystal structure. This explains the increase in degree of crystallinity of 70PLA/30ABS and 10SEBS-MAH. For 10SAN-GMA, the two melting peaks get close to each other yielding a single peak at 157.3°C. This situation can be attributed to low degree of crystallinity of 10SAN-GMA.

Table 4.6 DSC Results of 10Compatibilizer/(70PLA/30ABS) Blends Processed at 200°C and 230°C.

Samples	**Glass Transition Temperature (°C)**		**Melting Temperature (°C)**		**Degree of Crystallinity (%)**	
	200°C	**230°C**	**200°C**	**230°C**	**200°C**	**230°C**
Neat PLA	58.5	-	157.3	-	41.0	-
Extruded PLA	56.1	-	155.3/162.5	-	42.3	-
70PLA/30ABS	58.1	57.9	153.9/161.2	154.0/161.3	37.9	43.6
10SMA	58.0	57.8	154.6/160.9	154.7/161.8	37.7	36.6
10SEBS-MAH	58.9	58.0	155.3/162.2	154.2/161.1	32.1	38.9
10E-GMA	58.6	58.6	155.2/161.9	154.7/161.5	32.9	34.4
10SAN-GMA	59.5	60.2	155.2/159.8	157.3	29.9	29.8

4.2.3 Mechanical Properties

The effect of process temperature on mechanical properties was investigated based on tensile and impact test results. The tests were carried out under the same conditions that are given in Sections 2.7.1.1 and 2.7.1.2. Since PLA is not processable at 230°C, tests were done for 70PLA/30ABS and 10Compatibilizer/(70PLA/30ABS) blends.

The tensile strength values are shown in Figure 4.22. The average values and the standard deviations of test data are given in Table C.3. in Appendix C. Representative stress-strain curves are shown in Figure C.3. in Appendix C. Except for 10SAN-GMA blend, the tensile strengths show a decreasing trend with increasing temperature. As observed and discussed for SEM images, the ABS domain size becomes larger due to the coalescence of ABS domains, and interfacial tension is decreased at 230°C process temperature. The apparent interfaces inhibit the stress transfer reducing the tensile strength of the blend. In addition to these, deformation in PLA matrix is possible at high process temperature. It was also observed that neat PLA cannot be processed at this temperature. The tensile strength of 10SAN-GMA does not change significantly with process temperature. This situation can be attributed to the ability of compatibilizer to reduce interfacial tension producing a homogeneous blend as observed in morphology analysis at both temperatures.

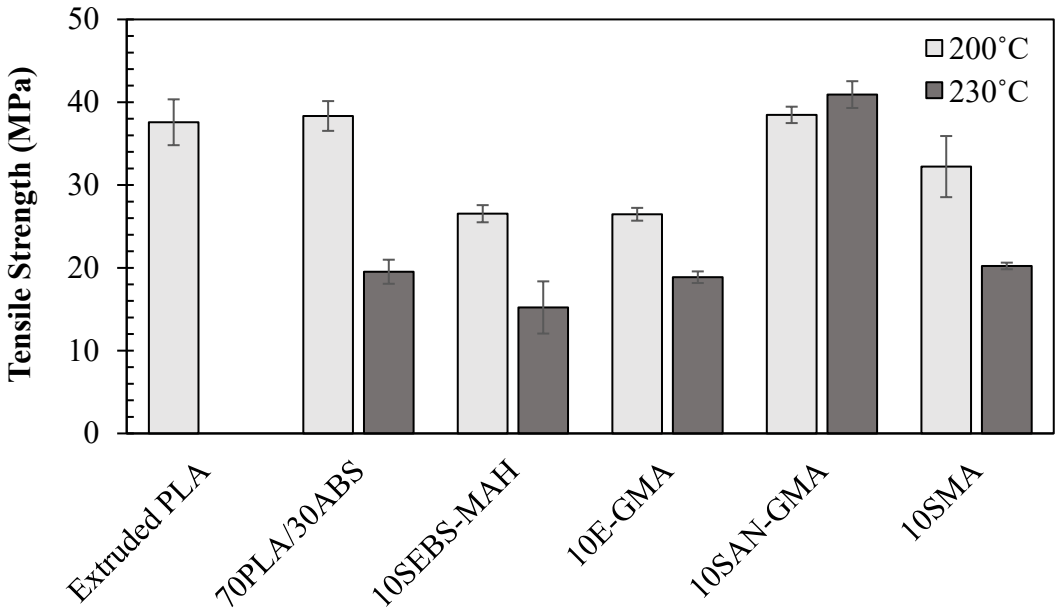

Figure 4.22 Tensile Strength Results of Blends Processed at 200˚C and 230˚C.

The main parameter affecting modulus is the binding energies of the atoms which are related to the use of compatibilizer [65]. The effect of compatibilizer on modulus at 200°C was discussed in the previous chapter. The effect of process temperature on modulus can be observed in Figure 4.23. The average values and the standard deviations of the test data are shown in Table C.3. in Appendix C. Based on the results, it can be concluded that the contribution of process temperature to elastic modulus can be neglected since there is not a significant change with increasing process temperature. In general, the modulus of elasticity for brittle polymers decreases with increasing temperature [66]. But it is not that sensitive to temperature change as it is sensitive to the presence of compatibilizer. For 10SEBS-MAH and 10E-GMA blends, with the addition of compatibilizer, the elastic modulus decreases by 20% while 30°C temperature range does not create a significant difference in elastic modulus of these ternary blends.

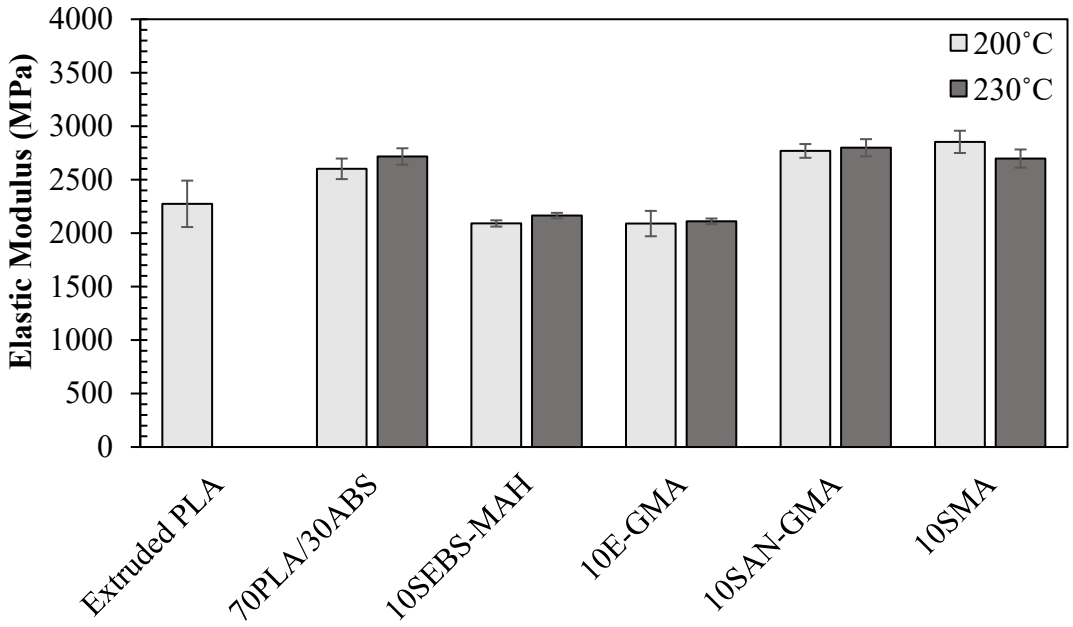

Figure 4.23 Elastic Modulus Results of Blends Processed at 200˚C and 230˚C.

The elongation at break values of blends processed at 230°C are given in Figure 4.24, the detailed test data are shown in Table C.3. in Appendix C. Considering the results, it can be concluded that the elongation at break values decrease with increasing temperature except for 10SAN-GMA blend. As observed in SEM images, interfaces between the dispersed phase and the matrix material become apparent indicating a lack of interfacial adhesion. In addition to that, the size of the dispersed phase is larger. These two reasons reduce the elongation values during tensile testing. Since SAN-GMA is known as chain extender, the chain extension can be combined with its plasticizing effect which do not decrease the elongation values at 230°C.

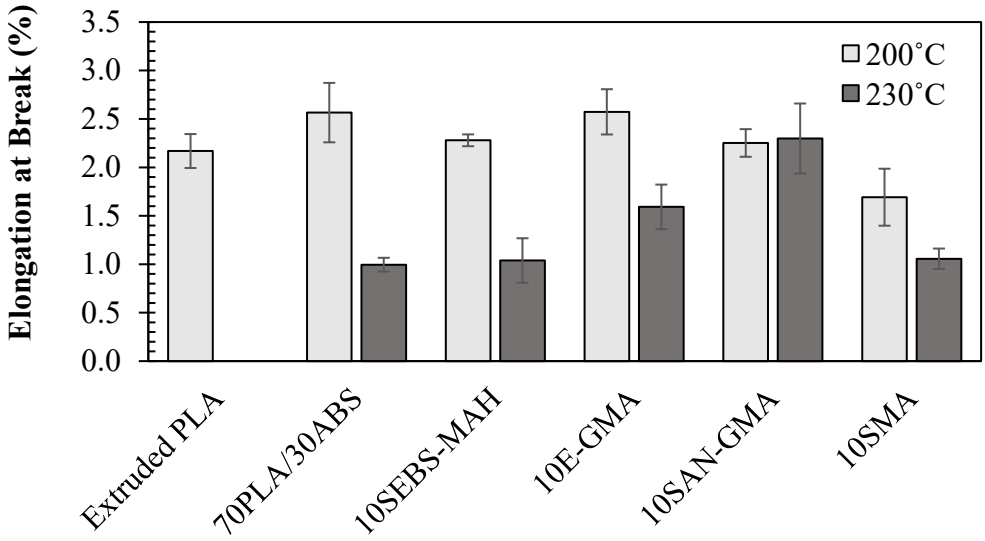

Figure 4.24 Elongation at Break Results of Blends Processed at 200˚C and 230˚C.

The impact test results are shown in Figure 4.25. The average values and the standard deviations of the test data are given in Table C.3. in Appendix C. In general, the impact strength decreases with increasing temperature. As mentioned before the presence of dispersed phase in droplet form can deflect the cracks, so the impact strength highly depends on the distribution and size of the dispersed phase [62]. Dispersed domains of ABS increase toughness by generating local stresses. The dispersion becomes limited with increasing domain size. When SEM images are considered, it is observed that the domain size of the dispersed phase increases at process temperature of 230°C. The cavities formed by the large domains cannot stop the crack propagation so the impact strength and toughness decrease.

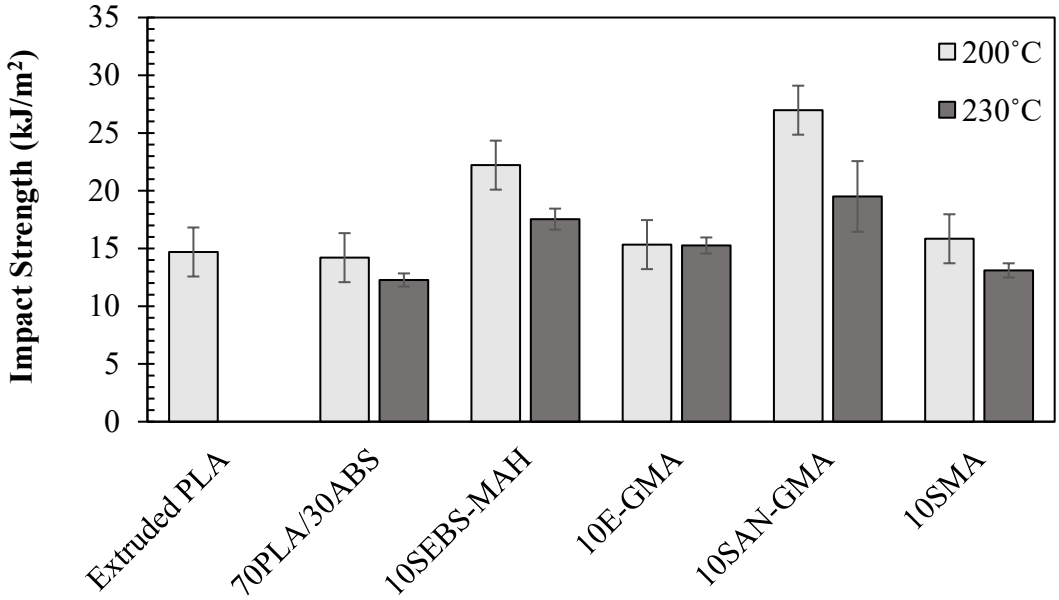

Figure 4.25 Impact Strength Results of Blends Processed at 200˚C and 230˚C.

4.3 Characterization of Carbon Fabric-Reinforced Polymer Composites

In this part, the characterization results of multilayer composites based on SEM analysis, tensile and flexural tests were discussed. Neat PLA, 70PLA/30ABS binary blend and 10SAN-GMA ternary blend were used as matrix materials. Carbon fabric was used as reinforcement material. The multilayer composites were prepared with one (1CF) and three layers of carbon fabric (3CFs) using compression molding at distinct parameters that are shown in Section 3.3.3. The effect of number of carbon fabric layer and type of polymer layer on morphology, tensile and flexural properties of the multilayer composites were investigated in this part.

4.3.1 Composite Morphologies

The morphology analysis of composites was carried out with SEM analysis. The images are taken from fracture surfaces of the representative test specimens. For tensile test specimens, the images are the top view of the area where the break occurs and they are shown in Figure 4.26.

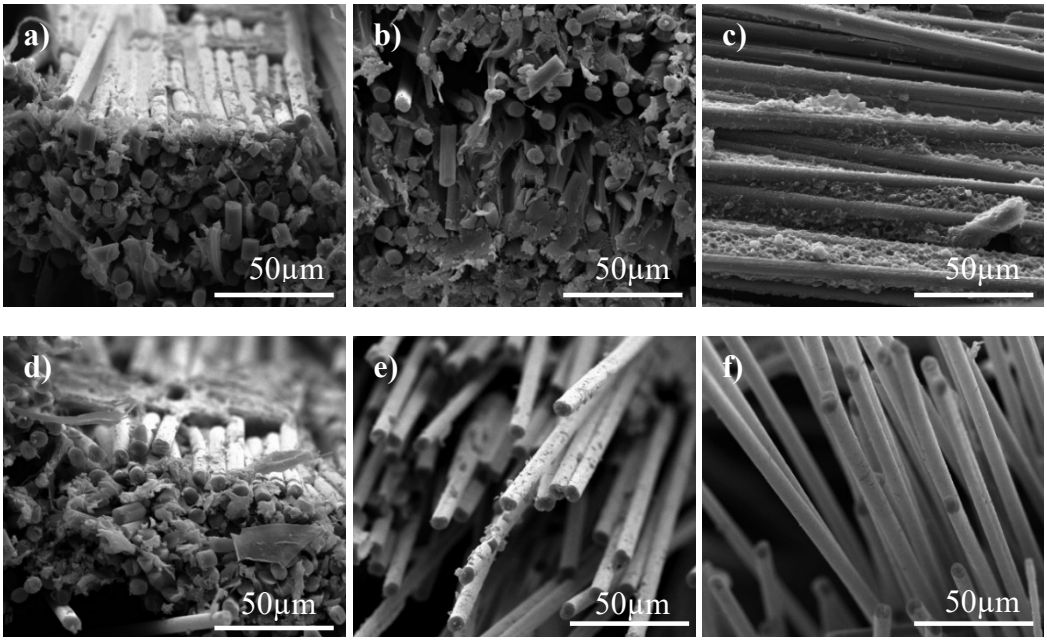

Figure 4.26 SEM Images of Tensile Test Specimens of 1CF Composite with a) Neat PLA b) 70PLA/30ABS c) 10SAN-GMA and 3CFs Composites with d) Neat PLA e) 70PLA/30ABS f) 10SAN-GMA with 2000x Magnification.

Considering the SEM images of tensile test specimens, it can be resulted that any of the blend composition with 1CF and 3CFs combinations show homogeneous structure. The interfacial adhesion determines the mechanical properties of the composite under tensile loading. When there is strong adhesion between the matrix and the reinforcement layer, the deformation takes place at the matrix near the interface. On the other hand, if the interfacial adhesion is weak, the fibers are directly

peeled off from the matrix which is called fiber pull out [67]. The images of neat PLA and 70PLA/30ABS show that the matrix deforms together with fibers and there are some cavities left by the fibers peeled off from the matrix. There are traces of matrix material on the fiber surface. This can be attributed to fiber wettability. The viscosity of neat PLA is considerably low compared to ABS. However, SEM images of 10SAN-GMA composites show clean fiber surfaces indicating lack of interaction between matrix and reinforcement material. The fibers are loosely held by the matrix.

For 70PLA/30ABS blend, since the polymer phases are incompatible, each phase shows its behavior distinctly in the blend. When the compatibilizer is introduced to blend, the viscosity increases since ABS is more viscous material than neat PLA. Higher surface free energy between matrix and reinforcement material enhances the fiber wettability resulting in better interfacial adhesion. The difference between the wetting behaviors of matrix materials can also be attributed to distinct free surface energies. These reasons explain why the impregnation of matrix material into CF layers is better for composites with neat PLA and 70PLA/30ABS blends when compared to composites with 10SAN-GMA blends. 10SAN-GMA as a polymer blend shows smooth surfaces at SEM images shown in Figure 4.18. However, in the multilayer composite prepared with 10SAN-GMA, the ABS domains become visible in PLA matrix. This behavior can proceed from the interaction between the epoxy functional group of SAN-GMA and carbon fabric. The commercial carbon fibers are generally coated with thin-film sizing agents [68]. Since the carbon fiber-epoxy composites are widely used in industry, sizing agents can be compatible with epoxy matrix. For this reason, the SAN-GMA can prefer to interact with carbon fabrics rather than to be a compatibilizer for ABS and PLA, and there can be less amount of SAN-GMA left in 70PLA/30ABS matrix.

The SEM images of flexural test specimens are given in Figure 4.27. The images were taken perpendicular to the width of the specimen to observe the failure modes at the interface between polymer and carbon fiber layers.

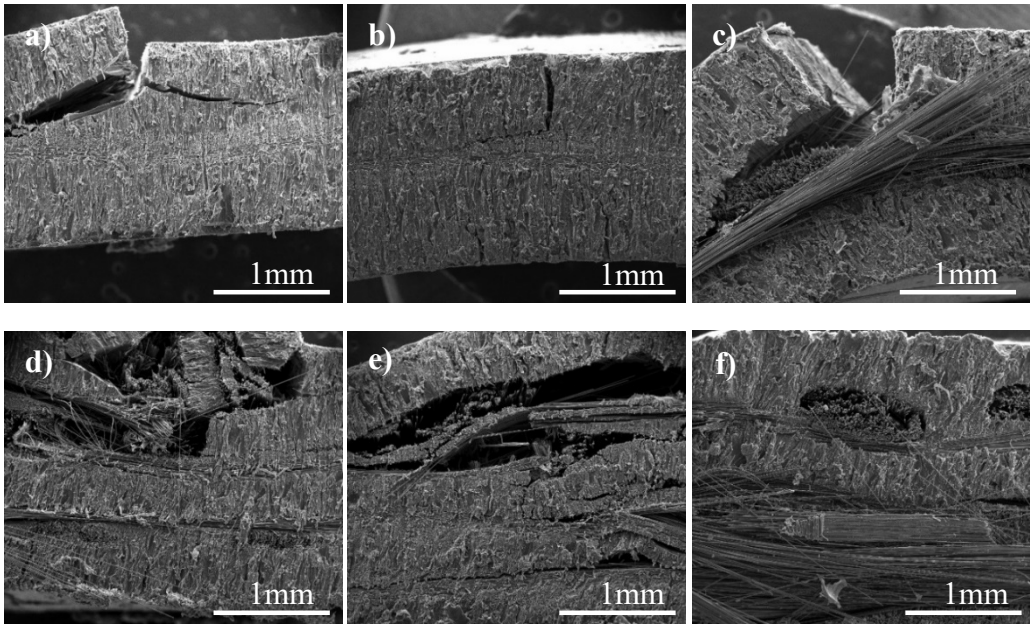

Figure 4.27 SEM Images of Flexural Test Specimens of 1CF Composite with a) Neat PLA b) 70PLA/30ABS c) 10SAN-GMA Blends and 3CFs Composite with; d) Neat PLA e) 70PLA/30ABS f) 10SAN-GMA Blends with 2000x Magnification.

During the flexural test, three different stress types were applied to the specimen. The upper layer suffers from compressive stress while the bottom layer is under tensile stress. At the mid-layers, these stresses are combined applying shear stress [69]. The composites with one CF layer generally deform from the bottom polymer layer. In 1CF composites, there are thicker polymer layers when compared to 3CFs specimens. So, when the load is applied, the bottom polymer layer is firstly exposed to tensile forces. In accordance with the tensile test specimen, for composite with 10SAN-GMA ternary blend, the carbon fibers are peeled off from polymer-carbon fiber interface while for neat PLA and 70PLA/30ABS binary blend, the fiber surfaces are covered with matrix material. The composites of neat PLA are fractured in brittle manner. The deformed surfaces of composites of neat PLA and 70PLA/30ABS are sharp, and the number of voids left by the pulled-out fibers is relatively low. As the number of CF layer increased from 1CF to 3CFs, the failure

modes changes. The deformations are the sign of compressive stresses and interlaminar shear. The shear effect is observable from the interfaces, especially for 3CFs composites with 10SAN-GMA ternary blend [69]. The voids left by the pulled-out fibers and delamination between layers can clearly be seen.

4.3.2 Mechanical Properties

In order to investigate the mechanical properties of 1CF and 3CFs composites both tensile and flexural tests were applied. The specimens were composed of carbon fabric as reinforcement, and neat PLA, 70PLA/30ABS, and 10SAN-GMA blends as polymer layer. The tensile strength results are shown in Figure 4.28. The average values and standard deviations of the test data are given Table D.1. in Appendix D. Representative stress-strain curves are shown in Figures D.1. and D.2. in Appendix D.

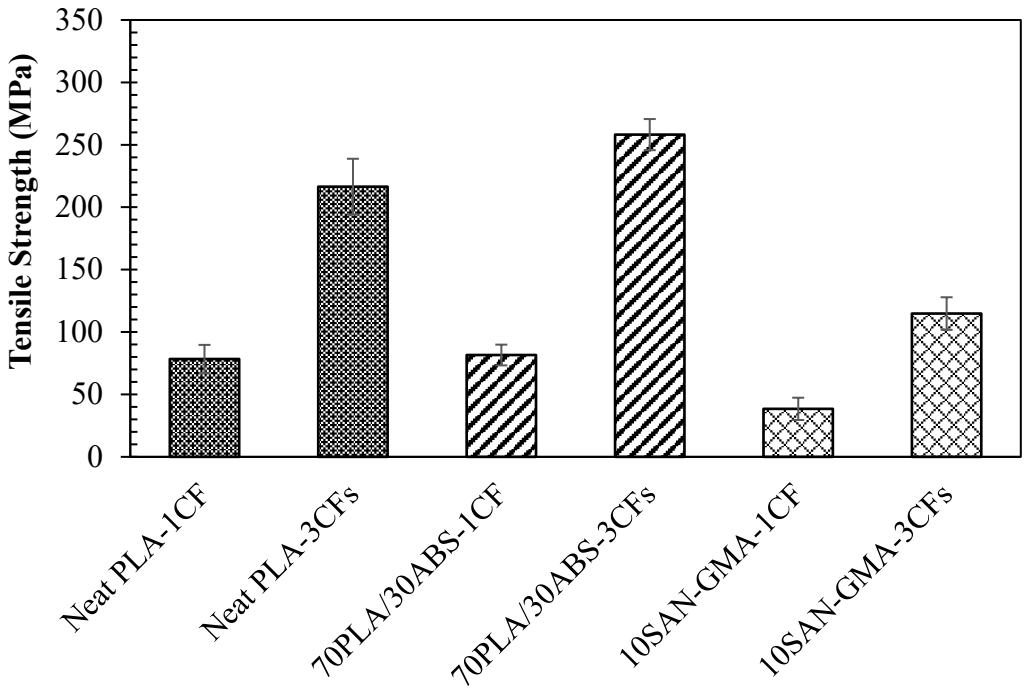

Figure 4.28 Tensile Strengths of 1CF and 3CFs Composites with Neat PLA, 70PLA/30ABS and 10SAN-GMA Blends.

The 1CF composites with neat PLA and 70PLA/30BS binary blend have similar tensile strength values in accordance with SEM results. In contrary to tensile strength results of blends, 70PLA/30ABS binary blend showed higher tensile strength than neat PLA in 3CFs multilayer composite form. PLA has low compatibility with carbon fibers [4]. Since ABS is commercially used with carbon fibers especially for car interiors, ABS can be more compatible with carbon fibers, resulting in higher tensile strength [33]. With the addition of SAN-GMA the tensile strength values dramatically decrease. This can be stem from rubbery nature of SAN-GMA, when compared to ABS and PLA. But most critically, this can be attributed to behavior of SAN-GMA in presence of carbon fibers. SAN-GMA may give interaction with the sizing agents on the carbon fibers instead of 70PLA/30ABS. When the SEM images of 10SAN-GMA in blend and composite forms are compared, it can be concluded that the PLA and ABS do not form a homogeneous blend in composite form which resulted in lack of efficient stress transfer.

From Figure 4.14, the blend forms of 70PLA/30ABS and 10SAN-GMA show similar tensile strength values. However, the tensile strengths of 10SAN-GMA in composite forms are even lower than the half of the composite form of 70PLA/30ABS. This can be explained as the smooth stress transfer in 10SAN-GMA ternary blend can compensate the plasticizing effect of SAN-GMA. But in composite form of 10SAN-GMA since it gives interaction with the sizing agents of carbon fibers rather than 70PLA/30ABS, the plasticizing effect cannot be compensated. For all composites, the tensile strength properties are enhanced with the increasing number of carbon fabric.

The tensile modulus values of multilayer composites are given in Figure 4.29. The average values and standard deviations of test data are shown in Table D.1. in Appendix D. Neat PLA-3CFs and Neat PLA-1CF show the highest values of modulus among other multilayer composites. Following the analysis of blend properties, the brittle nature of PLA can be observed through results. In composite forms of neat PLA, brittleness of PLA is combined with high strength carbon fibers

resulting in high modulus. Modulus determines the hardness of material, so it highly depends on the content of the rubbery phase in the blend. ABS and SAN-GMA decrease the modulus of the composites due to their rubbery nature. Another reason for the decrease in modulus for 70PLA/30ABS and 10SAN-GMA composites is the granular morphology of the blends between the layers providing ineffective stress transfer. The smooth surfaces of carbon fibers in SEM images of 10SAN-GMA composites support the low modulus results indicating the lack of interaction.

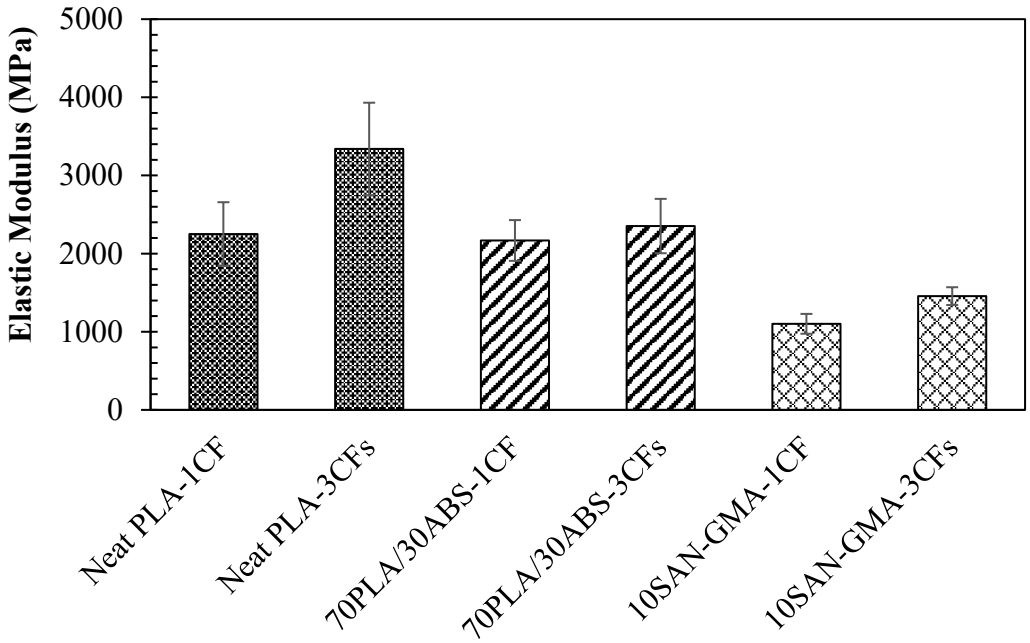

Figure 4.29 Elastic Moduli of 1CF and 3CFs Composites with Neat PLA, 70PLA/30ABS and 10SAN-GMA Blends.

The elongation at break results of composites are shown in Figure 4.30. The average values and standard deviations of the test data are given in Table D.1. in Appendix D. The increasing number of carbon fiber layer increases the elongation at break values because of a failure mechanism. When the tensile load is applied, since fiber ends are stress concentration points, cracks occur at the fiber ends. As time passes

cracks grow along fibers and disperse to the matrix [49]. During stress transfer, the interfacial adhesion becomes significant so the elongation at break results depend on the adhesion between layers. As observed in SEM images, the weakest interaction between fibers and the matrix is in the composites of 10SAN-GMA blend. The images are consistent with elongation at break results. Even there is not a significant difference between the fiber wetting capability of PLA and 70PLA/30ABS blends based on the SEM images, composites of 70PLA/30ABS blend result in higher elongation at break values. The increase in elongation at break values for composites of 70PLA/30ABS blend is due to the slippage between ABS and PLA phases and the effect of rubbery behavior of ABS in PLA matrix.

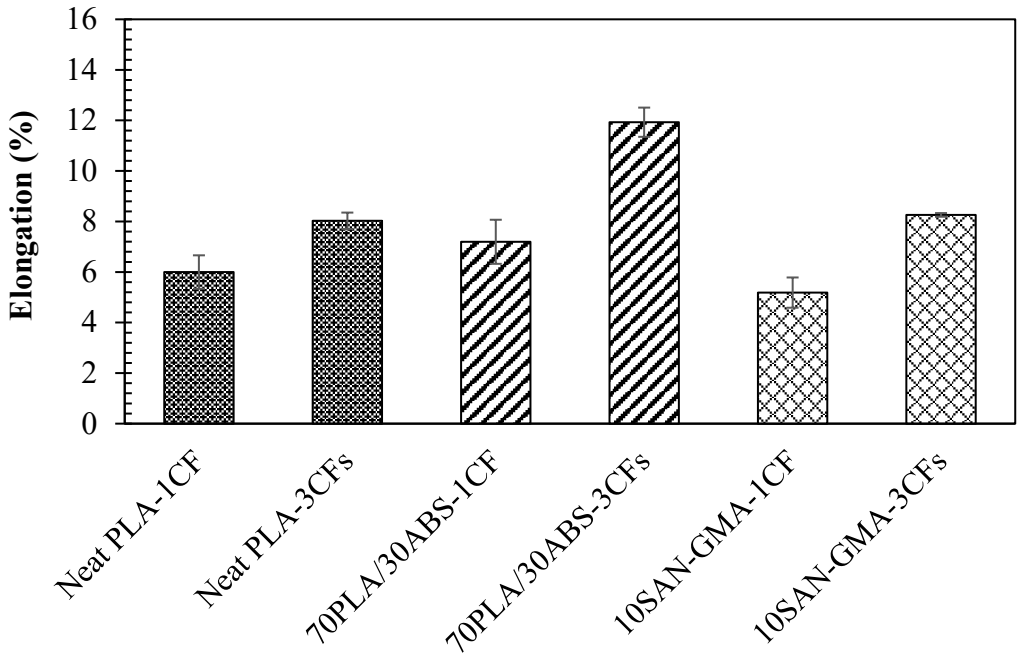

Figure 4.30 Elongation at Break of 1CF and 3CFs Composites with Neat PLA, 70PLA/30ABS and 10SAN-GMA Blends.

Flexural strengths of composites are shown in Figure 4.31. The average values and the standard deviations of the test data are given in Table D.2. in Appendix D. Representative stress-strain curves are shown in Figures D.3. and D.4. in Appendix D. The flexural test was carried out to investigate the interlaminar adhesion since the

test involves 3 modes of loading as tensile, compressive, and shear at the same time. The results of neat 1CF composites are approximately equal and among 3CFs composites, neat PLA has the highest flexural strength. Unlike tensile strength, due to shear loading, the adhesion between layers becomes more critical, especially for 3CFs composites. Considering the SEM images, low viscosity of PLA enables it to impregnate through carbon fibers causing an increase in the resistance of composite to shear loading. As expected, the 10SAN-GMA blend has the minimum flexural strength due to the lack of fiber wettability. In general, flexural strength is enhanced with the contribution of more carbon fiber layer. However, for the composites of 70PLA/30ABS and 10SAN-GMA, the percent increase in flexural strengths with increasing number of carbon fiber layer are lower than for the composites of neat PLA. As the number of carbon fiber layer increases, the bond line defects as voids and porosity increase, reducing the flexural strength [69].

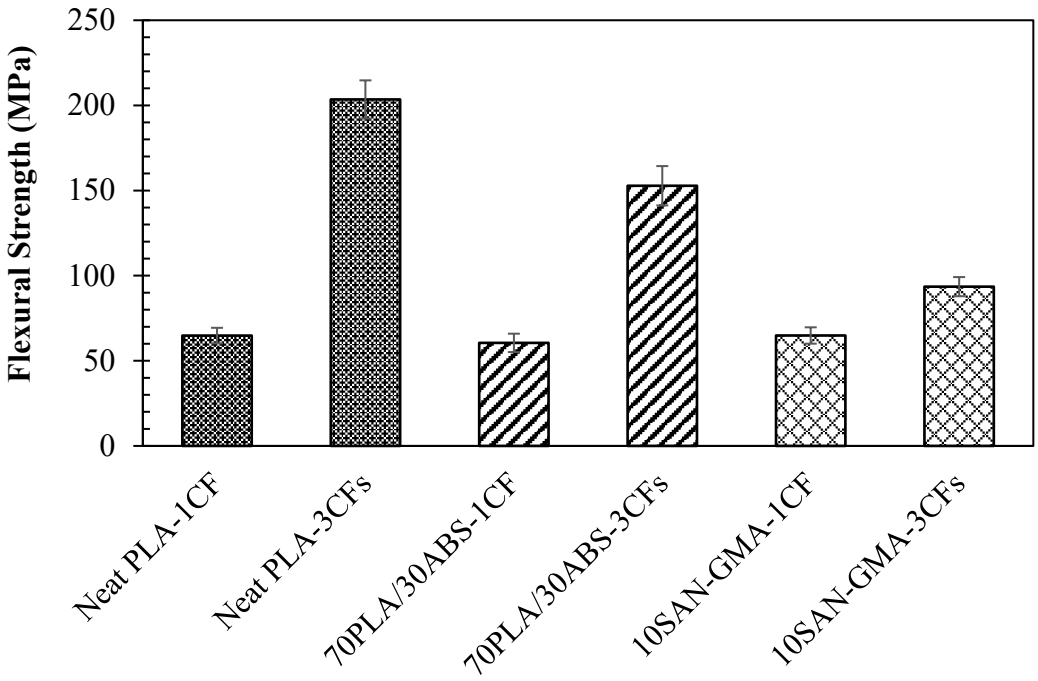

Figure 4.31 Flexural Strengths of 1CF and 3CFs Composites with Neat PLA, 70PLA/30ABS and 10SAN-GMA Blends.

The flexural modulus of 1CF and 3CFs composites are shown in Figure 4.32. The average values and the standard deviations of the test data are given in Table D.2. in Appendix D. For the composites with matrices of neat PLA and 70PLA/30ABS blends, the flexural moduli are approximately the same and increase with the increasing number of carbon fiber layers. It can be stated that the presence of ABS in the polymer matrix does not affect the flexural modulus of the composite. During the flexural testing, until the first failure occurs, a linear rising period appears in the stress-strain curve known as the Hookean region [69]. Among other composites, 10SAN-GMA composites show sharp breakage following the Hookean region. This reveals that the composite shows characteristic of 10SAN-GMA blend due to the lack of interfacial adhesion. The crack occurs at the polymer matrix and cannot be transferred through carbon fibers.

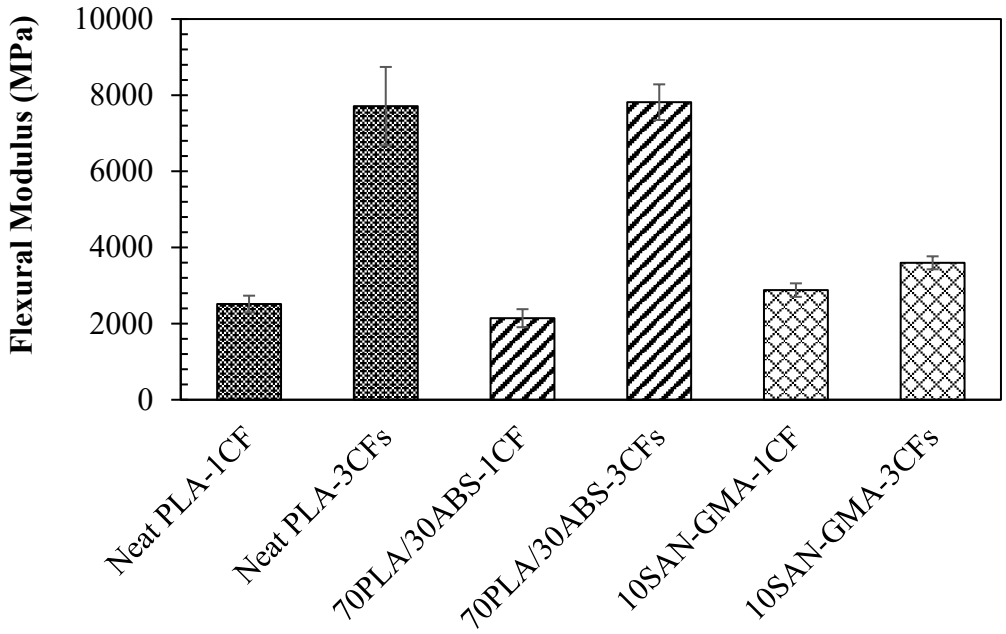

Figure 4.32 Flexural Moduli of 1CF and 3CFs Composites with Neat PLA, 70PLA/30ABS and 10SAN-GMA Blends.

The percent elongation at break results of the composites under flexural loading are shown in Figure 4.33. The average values and the standard deviations of the test data are given in Table D.2. in Appendix D. Since PLA is a highly brittle thermoplastic polymer when it is combined with high strength carbon fibers, the elongation at break becomes limited for their composites. This situation can also be observed from Figure 4.24. For the composites of 70PLA/30ABS and 10SAN-GMA, the ABS particles in the matrix leave pores under loading. Cavities left by the ABS domains can be observed from the SEM images. These cavities indicate the displacement of ABS domains by tensile stresses which improves toughness and the elongation at break value of the composite [4]. As the number of carbon fabrics increases the elongation at break is expected to decrease since the reinforcements resist to elongate. However, this case is different for the composites of 10SAN-GMA blend because of high standard deviations. It can be attributed to incompatibility between polymer layers and carbon fabric or the insufficient amount of compatibilizer to have high elongation before break [4].

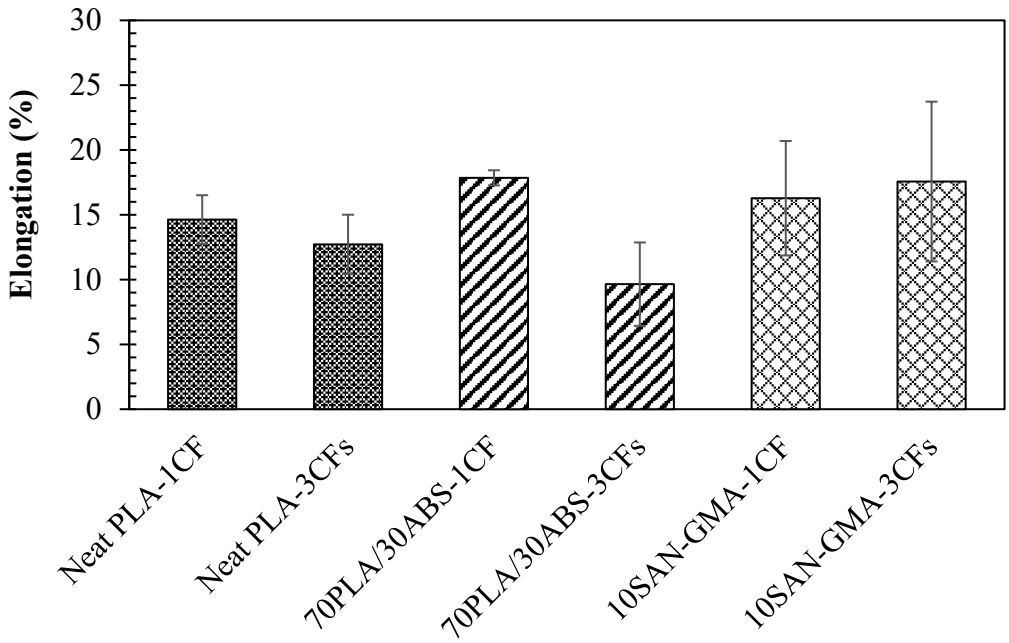

Figure 4.33 Elongation at Break of 1CF and 3CFs Composites with Neat PLA, 70PLA/30ABS and 10SAN-GMA Blends.

CHAPTER 5

CONCLUSIONS

Based on the experiments conducted within the scope of this thesis, following results were obtained;

1. Among 90PLA/10ABS, 70PLA/30ABS, and 50PLA/50ABS binary blends, 70PLA/30ABS shows the highest tensile strength while all blends have approximately equal impact strength values.
2. For binary blends, after 30% ABS content, ABS domains start to form coalescence increasing the domain size of ABS in PLA matrix.
3. Thermal properties such as glass transition and melting temperature are not affected by the presence of ABS but the degree of crystallinity depends on the content of ABS in PLA matrix.
4. PLA and ABS are incompatible polymers that require a suitable compatibilizer to obtain a homogeneous blend morphology.
5. The PLA/ABS blends processed at 200°C show better mechanical properties than PLA/ABS blends processed at 230°C.
6. The use of both phenolic and phosphate-based antioxidants as thermal stabilizers is not necessary for the blending of PLA/ABS at 200°C process temperature.
7. For SAN-GMA, the ability of giving interaction with PLA and ABS is found to be highest among E-GMA, SEBS-MAH, SMA, and SAN-GMA compatibilizers.
8. When the mechanical properties of SAN-GMA/(70PLA/30ABS) ternary blends with 5%, 10%, 15% compatibilizer contents are investigated, 10%

compatibilizer content is found to be the optimum since it increases the tensile and impact strengths of 70PLA/30ABS.

9. The behavior of compatibilizers in polymer blends can differ when they are used as matrix material in multilayer composites.
10. SAN-GMA compatibilizer is efficient in decreasing the interfacial tension of PLA and ABS. However, it is not that much efficient when used as matrix material in carbon-fabric reinforced composites.
11. The SEM images of multilayer composites acquired from the tensile and flexural test specimens show that there is a lack of interfacial adhesion between polymer layer and carbon-fabric of 10SAN-GMA composites. The interfaces are open to modifications in order to increase adhesion for better mechanical properties.
12. As the number of carbon fabric increases, both tensile and flexural strengths and moduli increase. The interfacial tension is lower for neat PLA-1CF composite so the increase in strength and modulus with the increasing number of carbon fabric is higher.
13. There are studies on enhancing the weak properties of PLA/ABS blends but there is a lack of study on investigation of PLA/ABS-based multilayer composites in literature. This study has an important contribution to literature on the development of environmentally friendly multilayer composites.

REFERENCES

[1] Polylactic acid or polylactide (PLA). Retrieved from https://bioplasticsnews.com/polylactic-acid-or-polylactide-pla/.

[2] S. Sridharan, Ed., Delamination Behaviour of Composites. Woodhead Publishing.

[3] R. Palazzetti and A. Zucchelli, Electrospun nanofibers as reinforcement for composite laminates materials – A review, Compos. Struct., vol. 182, no. June, pp. 711–727, 2017.

[4] C.T. Hsieh, Y.J. Pan, C.W. Lou, C.L. Huang, Z. I. Lin, J.M. Liao, and J.H. Lin, "Polylactic acid/carbon fiber composites: Effects of functionalized elastomers on mechanical properties, thermal behavior, surface compatibility, and electrical characteristics," Fibers Polym., vol. 17, no. 4, pp. 615–623, 2016.

[5] Acrylonitrile butadiene styrene (ABS) and its features. Retrieved from https://omnexus.specialchem.com/selection-guide/acrylonitrile-butadiene-styrene-abs-plastic.

[6] R. J. Spontak and J. J. Ryan, Polymer blend compatibilization by the addition of block copolymers. Elsevier Inc., 2019.

[7] X. M. Xie and X. Sui, Compatibilization of polymer blends by the addition of random copolymers. Elsevier Inc., 2019.

[8] V. Ambrogi, C. Carfagna, P. Cerruti, and V. Marturano, Additives in polymers. Elsevier Inc., 2017.

[9] M. Oliveira, E. Santos, A. Araújo, G. J. M. Fechine, A. V. Machado, and G. Botelho, The role of shear and stabilizer on PLA degradation, Polym. Test., vol. 51, pp. 109–116, 2016.

[10] S. J. Christian, Natural fibre-reinforced noncementitious composites (biocomposites). Elsevier, 2016.

[11] Scientific principles of composites. Retrieved from https://www.asminternational.org/documents/10192/1942084/composite.pdf/0eb5cca8-4613-482c-811c-993c58b42e92#:~:text=There are three main types,from environmental and physical damage.

[12] Materials & Processes: Fibers for composites. Retrieved from https://www.compositesworld.com/articles/the-fiber.

[13] A. K. Pathak, M. Borah, A. Gupta, T. Yokozeki, and S. R. Dhakate, Improved mechanical properties of carbon fiber/graphene oxide-epoxy hybrid composites, Compos. Sci. Technol., vol. 135, pp. 28–38, 2016.

[14] J. R. Fekete and J. N. Hall, Design of auto body: Materials perspective. Elsevier Ltd, 2017.

[15] T. Johnson, Understanding CFRP composites. Retrieved from https://www.thoughtco.com/understanding-cfrp-composites-820393.

[16] Degassing extruders. Retrieved from https://www.airtechusa.com/industries/plastics/degassing-extruders/.

[17] B. Cockram, The plastic extrusion process explained in 5 Steps, 2018. Retrieved from https://plastrading.com/2018/11/23/the-plastic-extrusion-process-explained-in-5-steps/.

[18] A. Shrivastava, Screw extruders, Introd. to Plast. Eng., 2018.

[19] What is injection molding? Retrieved from https://www.polyplastics.com/en/support/mold/outline/.

[20] M.N. Madiwale, Compression moulding process, no. 6, pp. 1615–1624, 2019.

[21] ISO 527-2, Plastics-Determination of tensile properties, Part 2: Test

conditions for moulding and extrusion plastics, 2012.

[22] ISO 527-4, Plastics-Determination of tensile properties, Part 4: Test conditions for isotropic ans orthotropic fibre-reinforced plastic composites, 1997.

[23] Difference between IZOD and charpy impact testing. Retrieved from https://www.testing-instruments.com/blog/difference-between-izod-and-charpy-impact-testing/.

[24] ASTM, D790-03-Standard test method for flexural properties of unreinforced and reinforced plastics and electrical insulation materials, ASTM Stand., pp. 1–11, 2015.

[25] R. Karoui, Food authenticity and fraud, Chem. Anal. Food Tech. Appl., pp. 499–517, 2012.

[26] Fourier dönüşümlü kızıl ötesi spektrometresi. Retrieved from https://merlab.metu.edu.tr/tr/fourier-donusumlu-kizil-otesi-spektrometresi.

[27] Scanning electron microscopy. Retrieved from https://www.nanoscience.com/techniques/scanning-electron-microscopy/#.

[28] K. Hamad, M. Kaseem, and F. Deri, Preparation and characterization of binary and ternary blends with poly(lactic acid), polystyrene, and acrylonitrile-butadiene-styrene, J. Biomater. Nanobiotechnol., vol. 03, no. 03, pp. 405–412, 2012.

[29] C. Thongpin, K. Chaemprasith, J. Teeralertpanich, P. Saensuk, and N. Kritape, In-situ reinforcement of PLA using Nylon 6 in PLA/Nylon 6 extrudate blend via twin-screw extrusion, Key Eng. Mater., vol. 659, pp. 428–435, 2015.

[30] L. P. Amaro, F. Cicogna, E. Passaglia, E. Morici, W. Oberhauser, S. Al-Malaika, N. T. Dintcheva, S. Coiai, Thermo-oxidative stabilization of poly(lactic acid) with antioxidant intercalated layered double hydroxides,

Polym. Degrad. Stab., vol. 133, pp. 92–100, 2016.

[31] C. Dubois and É. P. De Montréal, Thermal stabilization of high molecular weight L-polylactide Jérôme Burlet" , École Polytechnique de Montréal Marie-Claude Heuzey , École Polytechnique de Montréal Abstract Material and Structure Characterization, Polym. Degrad. Stab., pp. 1133–1137, 2005.

[32] J. Zhang, S. Wang, Y. Qiao, and Q. Li, Effect of morphology designing on the structure and properties of PLA/PEG/ABS blends, Colloid Polym. Sci., vol. 294, no. 11, pp. 1779–1787, 2016.

[33] M.Y. Jo, Y.J. Ryu, J.H. Ko, J.S. Yoon, Effects of compatibilizers on the mechanical properties of ABS/PLA composites, Wiley Online Libr., 2012.

[34] A. Galatas, H. Hassanin, Y. Zweiri, and L. Seneviratne, Additive manufactured sandwich composite/ABS parts for unmanned aerial vehicle applications, Polymers (Basel)., vol. 10, no. 11, 2018.

[35] M. Sharma, J. Bijwe, and P. Mitschang, Wear performance of PEEK-carbon fabric composites with strengthened fiber-matrix interface, Wear, vol. 271, no. 9–10, pp. 2261–2268, 2011.

[36] Thermoset vs. Thermoplastics. Retrieved from https://www.modorplastics.com/plastics-learning-center/thermoset-vs-thermoplastics/.

[37] Natureplast PLI 005 techical data sheet, 2018. Retrieved from https://omnexus.specialchem.com/product/t-natureplast-natureplast-pli-005.

[38] Xibond 920 technical data sheet. Retrieved from https://polymer-additives.specialchem.com/product/a-polyscope-xibond-920.

[39] Songnox 1680 technical data sheet. Retrieved from http://www.synergistixindia.com/Songwon Brochure_Antioxidants_Light_Stabilizers_Acid_Scavengers.pdf.

[40] T. Condition and T. Method, SONGNOX 1076 technical data sheet, 2020.

[41] ASTM D638 − 14, Standard test method for tensile properties of plastics, 2016.

[42] ISO179-1, Plastics-Determination of charpy impact properties, 2010.

[43] I. M. M. W.J. Sichina, DSC as Problem Solving Tool: Measurement of percent crystallinity of thermoplastics. Retrieved from https://www.perkinelmer.com/Content/applicationnotes/app_thermalcrystallinitythermoplastics.pdf.

[44] R. Z. Khoo, H. Ismail, and W. S. Chow, Thermal and morphological properties of poly(lactic acid)/nanocellulose nanocomposites, Procedia Chem., vol. 19, pp. 788–794, 2016.

[45] Standard test method for ash content in plastics. Retrieved from https://www.astm.org/Standards/D5630.htm.

[46] B. Erkmen, Polystyrene-based and carbon fabric-reinforced polymer composites containing carbon nanotubes: Preparation, modification and characterization, Ph.D. Thesis, Middle East Technical University, 2020.

[47] Ineos Styrolution, Novodur HD M203FC, vol. 49, no. 2133, pp. 49–51.

[48] C. W. Macosko, Morphology development and control in immiscible polymer blends, Macromol. Symp., vol. 149, pp. 171–184, 2000.

[49] S. Hazer, M. Coban, and A. Aytac, A study on carbon fiber reinforced poly(lactic acid)/polycarbonate composites, J. Appl. Polym. Sci., vol. 135, no. 48, pp. 1–9, 2018.

[50] Factors affecting young's modulus. Retrieved from https://omnexus.specialchem.com/polymer-properties/properties/young-modulus.

[51] C. Kurtuluş, Self reinforcement of poly(ethylene terephthalate) and polyethylene Blends, M.Sc. Thesis, Middle East Technical University, 2007.

[52] D. W. Van Krevelen and K. Te Nijenhuis, Mechanical properties of solid polymers. 2009.

[53] B. Xue, J. Bao, and J. Zhang, Ultrafine fly ash as a reinforcing filler in poly(lactic acid) matrix, J. Appl. Polym. Sci., vol. 133, no. 30, pp. 1–8, 2016.

[54] M. Hesami and A. Jalali-Arani, Cold crystallization behavior of poly(lactic acid) in its blend with acrylic rubber; the effect of acrylic rubber content, Polym. Int., vol. 66, no. 11, pp. 1564–1571, 2017.

[55] R. Zhang, K. Huang, S. Hu, Q. Liu, X. Zhao, and Y. Liu, Improved cell morphology and reduced shrinkage ratio of ETPU beads by reactive blending, Polym. Test., vol. 63, no. August, pp. 38–46, 2017.

[56] J. B. Zeng, K. A. Li, and A. K. Du, Compatibilization strategies in poly(lactic acid)-based blends, RSC Adv., vol. 5, no. 41, pp. 32546–32565, 2015.

[57] MERCK, Ir spectrum table by frequency range. Retrieved from https://www.sigmaaldrich.com/TR/en/technical-documents/technical-article/analytical-chemistry/photometry-and-reflectometry/ir-spectrum-table.

[58] L. B. Canto and L. A. Pessan, Determination of the composition of styrene-glycidyl methacrylate copolymers by FTIR and titration, Polym. Test., vol. 21, no. 1, pp. 35–38, 2002.

[59] N. Z. Tomić and A. D. Marinković, Compatibilization of polymer blends by the addition of graft copolymers. 2019.

[60] Y. Li and H. Shimizu, Improvement in toughness of poly(l-lactide) (PLLA) through reactive blending with acrylonitrile-butadiene-styrene copolymer (ABS): Morphology and properties, Eur. Polym. J., vol. 45, no. 3, pp. 738–746, 2009.

[61] E. Açık, Poly(lactic acid) based nanocomposites: mechanical, thermal and rheological properties and morphology, Ph.D. Thesis, Middle East Technical University, 2014.

[62] G. Özkoç, ABS/Polyamide-6 blends, their short glass fiber composites and organoclay based nanocomposites: Processing and characterization, Ph.D. Thesis, Middle East Technical University, 2007.

[63] A. S. M. Elhassan, H. A. M. Saeed, Y. A. Eltahir, Y. M. Xia, and Y. P. Wang, Modification of PLA with chain extender, Appl. Mech. Mater., vol. 716–717, no. December, pp. 44–47, 2014.

[64] M. Kuzmanović, L. Delva, L. Cardon, and K. Ragaert, The effect of injection molding temperature on the morphology and mechanical properties of PP/PET blends and microfibrillar composites, Polymers (Basel)., vol. 8, no. 10, pp. 13–18, 2016.

[65] Plastics & Elastomers. Retrieved from https://omnexus.specialchem.com/polymer-properties/properties/young-modulus#factors.

[66] K. Balani, V. Verma, A. Agarwal, and R. Narayan, Physical, thermal, and mechanical properties of polymers, Biosurfaces, pp. 329–344, 2015.

[67] P. Chen, C. Lu, Q. Yu, Y. Gao, J. Li, and X. Li, Influence of fiber wettability on the interfacial adhesion of continuous fiber-reinforced PPESK composite, J. Appl. Polym. Sci., vol. 102, no. 3, pp. 2544–2551, 2006.

[68] Q. Ma, Y. Gu, M. Li, S. Wang, and Z. Zhang, Effects of surface treating methods of high-strength carbon fibers on interfacial properties of epoxy resin matrix composite, Appl. Surf. Sci., vol. 379, pp. 199–205, 2016.

[69] X. Liu, B. Yang, L. Lu, Z. Wan, and Y. Tang, A thermoplastic multilayered carbon-fabric/polycarbonate laminate prepared by a two-step hot-press technique, Polymers (Basel)., vol. 10, no. 7, 2018.

[70] M. Yaşar, Performance of modified thermoplastic poly(ether)ester Elastomer in multilayer composites, M.Sc. Thesis, Middle East Technical University, 2014.

[71] CEAST Resil Pendulums -Series in Phase 3 – Out of production/Best effort support. Retrieved from https://www.instron.com/-/media/files/campaigns/product-life-cycle/productlifecyclenotice2017---phase-3-ceast-resil.pdf

APPENDICES

A. THEORETICAL CALCULATION OF ASH CONTENT IN MULTILAYER COMPOSITES

Volume of Multilayer Composites: 20x20x0.2 = 80 cm^3

Surface Area of Multilayer Composites: 20x20 = 400 cm^2 =0.04 m^2

CF Areal Density: 246 g/m^2

Weight of 1CF Layer: 0.04 m^2 x 246 g/m^2 = 9.84 g

For 1CF Multilayer Composites;

Two layers of polymer were used in 1 CF multilayer composites. Each layer was 40 gr. When polymer layers were compressed with CF, the percent CF content is calculated as;

$$\frac{9.84}{9.84+(2x40)} \text{ x } 100 = 11\ \%$$

For 3CFs Multilayer Composites;

Four layers of polymer were used in 3 CFs multilayer composites. Each layer was 20 gr. When polymer layers were compressed with CF, the percent CF content is calculated as;

$$\frac{9.84\text{x}3}{(9.84\text{x}3)+(4\text{x}20)} \text{ x } 100 = 27\%$$

B. ASH CONTENT ANALYSIS RESULTS OF MULTILAYER COMPOSITES

Table B.1. Ash Contents of Multilayer Composites.

Matrix Material	Number of CF	Analysis Result of Ash Content (wt.%)	Theoretical Calculation of Ash Content (wt.%)
Neat PLA	1CF	9.22 ± 0.34	11
	3CFs	24.08 ± 0.15	27
70PLA/30ABS	1CF	10.53 ± 0.1	11
	3CFs	25.73 ± 0.47	27
10SAN-GMA	1CF	9.71 ± 0.46	11
	3CFs	26.13 ± 0.38	27

C. TENSILE AND IMPACT TEST RESULTS OF POLYMER BLENDS

Table C.1. Tensile and Impact Test Results of PLA/ABS Blends.

Sample Codes	Mechanical Properties			
	Tensile Strength (MPa)	**Elastic Modulus (MPa)**	**Elongation at Break (%)**	**Impact Strength (kJ/m^2)**
Neat PLA	49.8 ± 2.6	3025.3 ± 146.6	2.7 ± 0.2	17.9 ± 1.6
Extruded PLA	37.6 ± 2.8	2273.9 ± 217.1	2.2 ± 0.2	14.7 ± 0.8
Neat ABS	34.8 ± 2.3	2101.2 ± 94.3	10.0 ± 2.9	31.0 ± 4.7
90PLA/10ABS	25.9 ± 2.7	2820.9 ± 83.5	1.4 ± 0.1	15.5 ± 1.4
70PLA/30ABS	38.3 ± 1.8	2601.3 ± 96.1	2.6 ± 0.3	14.2 ± 1.7
50PLA/50ABS	26.6 ± 3.0	2431.5 ± 33.6	2.0 ± 0.4	13.7 ± 0.3

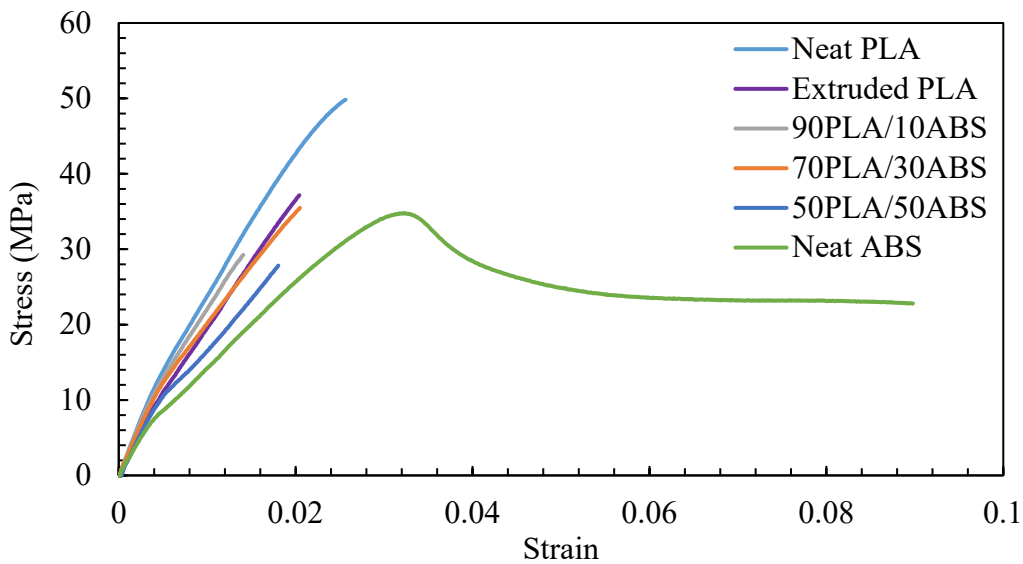

Figure C.1. Representative Stress-Strain Curves of PLA/ABS Blends.

Table C.2. Tensile and Impact Test Results of Compatibilizer/(70PLA/30ABS) Blends.

Sample Codes	Mechanical Properties			
	Tensile Strength (MPa)	**Elastic Modulus (MPa)**	**Elongation at Break (%)**	**Impact Strength (kJ/m^2)**
Neat PLA	49.8 ± 2.6	3025.3 ± 146.6	2.7 ± 0.2	17. 9 ± 1.6
Extruded PLA	37.6 ± 2.8	2273.9 ± 217.1	2.2 ± 0.2	14.7 ± 0.8
5SEBS-MAH	26.4 ± 1.5	2540.6 ± 315.3	1.7 ± 0.2	16.7 ± 2.0
10SEBS-MAH	26.5 ± 1.0	2090.5 ± 29.3	2.3 ± 0.1	22.2 ± 0.4
15SEBS-MAH	21.4 ± 1.5	2021.8 ± 96.6	2.8 ± 0.8	20.7 ± 0.8
5E-GMA	23.4 ± 0.9	2208.5 ± 126.8	2.2 ± 0.5	18.8 ± 1.0
10E-GMA	26.5 ± 0.8	2089.3 ± 118.6	2.6 ± 0.2	15.3 ± 0.7
15E-GMA	21.2 ± 1.3	2015.5 ± 89.3	2.1 ± 0.2	16.2 ± 2.1
5SAN-GMA	37.1 ± 4.0	2653.2 ± 106.3	2.1 ± 0.3	11.9 ± 1.8
10SAN-GMA	38.5 ± 1.0	2768.5 ± 64.4	2.3 ± 0.1	27.0±3.1
15SAN-GMA	37.4 ± 1.7	2883.4 ± 53.9	2.2 ± 0.2	19.9 ± 2.5
5SMA	22.0 ± 1.7	2864.9 ± 64.9	1.0 ± 0.1	11.6 ± 1.9
10SMA	32.2 ± 3.7	2853.3 ± 104.2	1.7 ± 0.3	15.8 ± 0.7
15SMA	16.4 ± 2.4	2722.8 ± 97.7	0.9 ± 0.2	8.0 ± 1.2

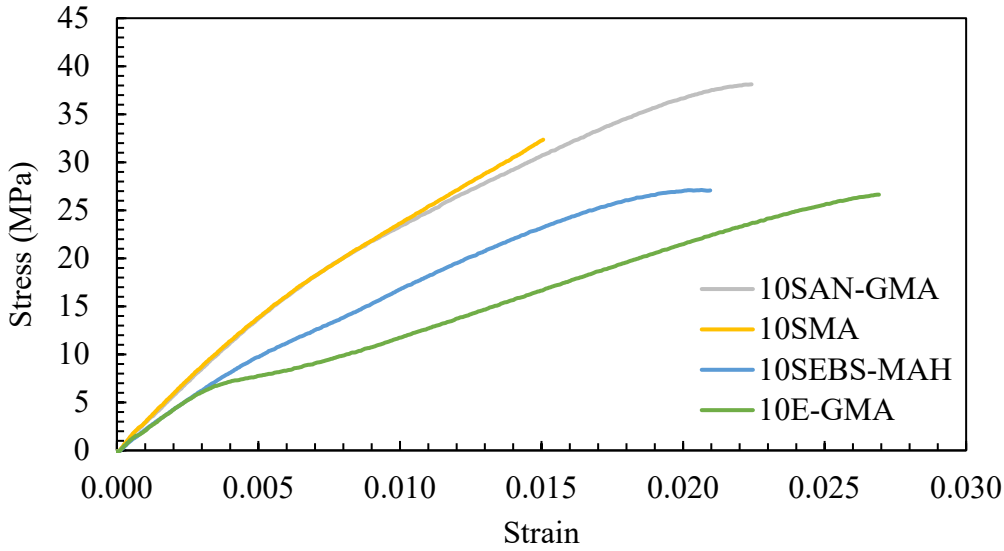

Figure C.2. Representative Stress-Strain Curves of Ternary Blends at 200°C.

Table C.3. Tensile and Impact Test Results of 10Compatibilizer/(70PLA/30ABS) Blends at 230°C.

Sample Codes	**Mechanical Properties**			
	Tensile Strength (MPa)	**Elastic Modulus (MPa)**	**Elongation at Break (%)**	**Impact Strength (kJ/m^2)**
70PLA/30ABS	19.5 ± 1.5	2716.7 ± 76.7	1.0 ± 0.1	12.3 ± 0.6
10SEBS-MAH	15.2 ± 3.2	2163.8 ± 25.6	1.0 ± 0.2	17.5 ± 0.9
10E-GMA	18.9 ± 0.7	2110.3 ± 26.5	1.6 ± 0.2	15.3 ± 0.7
10SAN-GMA	40.9 ± 1.6	2798.3 ± 80.3	2.3 ± 0.4	19.5 ± 3.1
10SMA	20.2 ± 0.4	2697.0 ± 85.5	1.1 ± 0.1	13.1 ± 0.6

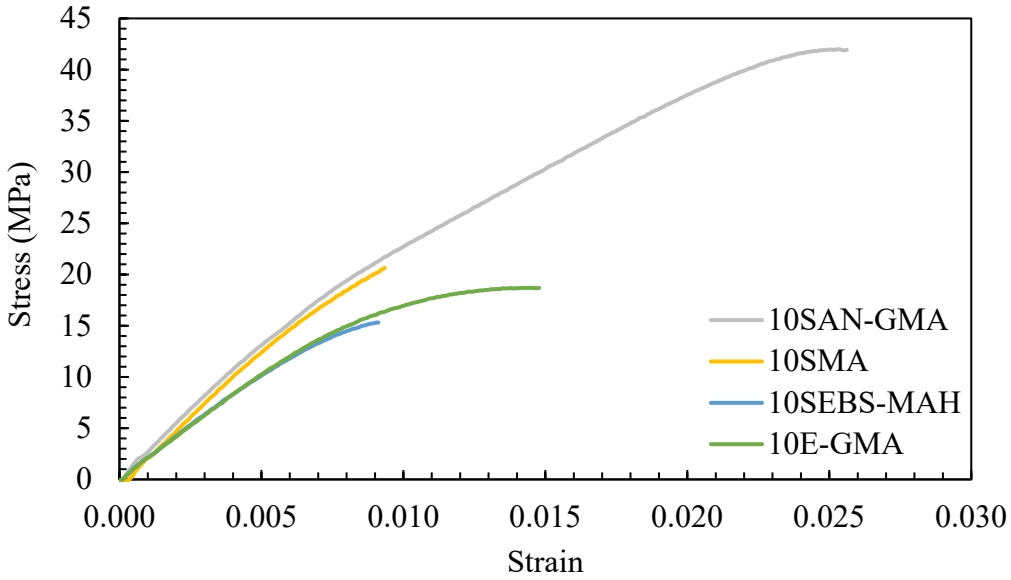

Figure C.3. Representative Stress-Strain Curves of Ternary Blends at 230°C.

D. TENSILE AND FLEXURAL TEST RESULTS OF MULTILAYER COMPOSITES

Table D.1. Tensile Test Results of Multilayer Composites.

Sample Codes	Mechanical Properties		
	Tensile Strength (MPa)	Elastic Modulus (MPa)	Elongation at Break (%)
Neat PLA-1CF	78.4 ± 11.3	2250.2 ± 407.6	6.0 ± 0.7
Neat PLA-3CFs	216.4 ± 22.4	3339.9 ± 591.2	8.0 ± 0.3
70PLA/30ABS-1CF	81.6 ± 8.3	2167.9 ± 260.9	7.2 ± 0.9
70PLA/30ABS-3CFs	258.2 ± 12.5	2352.6 ± 348.0	11.9 ± 0.6
10SAN-GMA-1CF	38.5 ± 8.9	1101.3 ± 127.1	5.2 ± 0.6
10SAN-GMA-3CFs	114.8 ± 13.0	1455.8 ± 113.8	8.3 ± 0.1

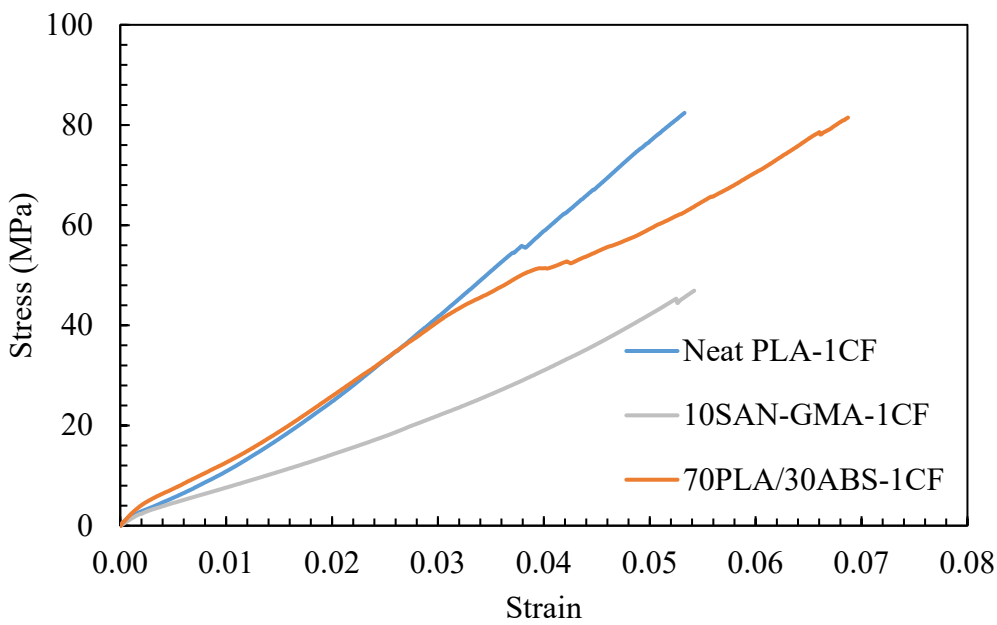

Figure D.1. Representative Stress-Strain Curves (Tensile Test) of Multilayer Composites (1CF).

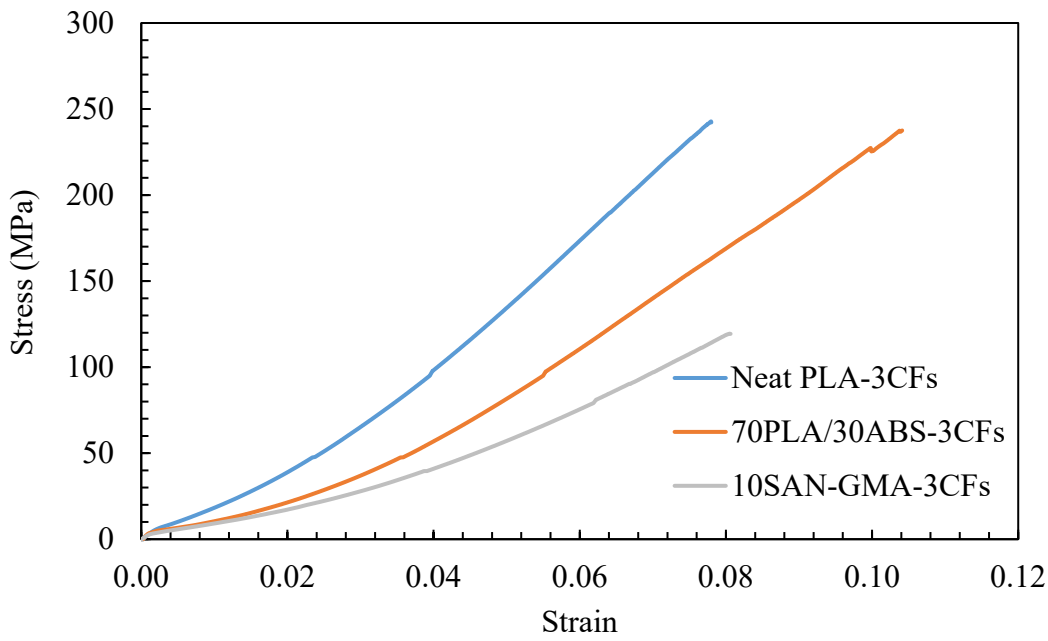

Figure D.2. Representative Stress-Strain Curves (Tensile Test) of Multilayer Composites (3CFs).

Table D.2. Flexural Test Results of Multilayer Composites.

Sample Codes	**Mechanical Properties**		
	Flexural Strength (MPa)	**Flexural Modulus (MPa)**	**Elongation (%)**
Neat PLA-1CF	64.8 ± 4.6	2514.6 ± 219.5	14.6 ± 1.9
Neat PLA-3CFs	203.5 ± 11.2	7711.5 ± 1030.1	12.7 ± 2.3
70PLA/30ABS-1CF	60.5 ± 5.4	2142.6 ± 236.8	17.8 ± 0.6
70PLA/30ABS-3CFs	152.8 ± 11.6	7816.5 ± 468.3	9.6 ± 3.2
10SAN-GMA-1CF	64.9 ± 4.8	2880.3 ± 177.4	16.3 ± 4.4
10SAN-GMA-3CFs	93.5 ± 5.6	3597.2 ± 170.5	17.6 ± 6.2

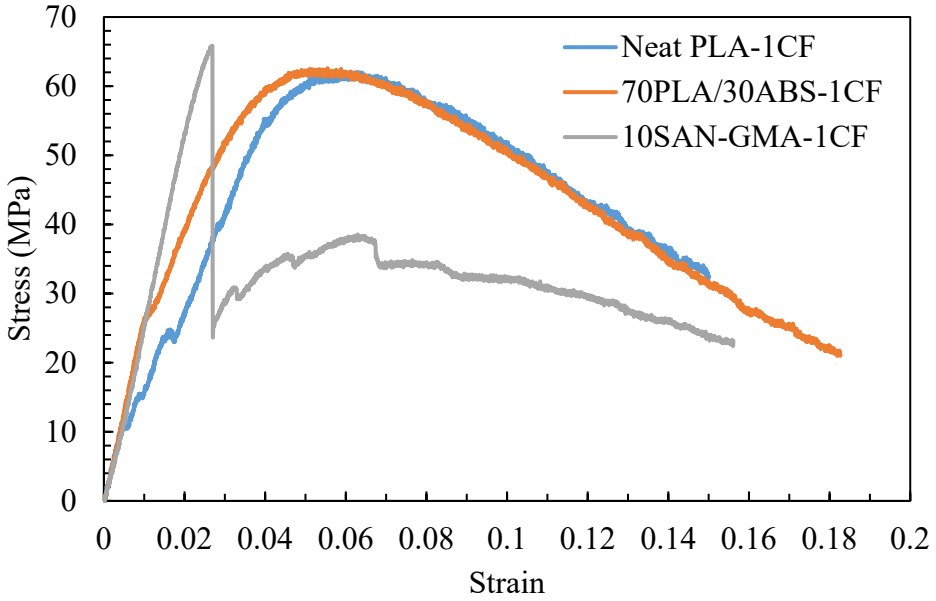

Figure D.3. Representative Stress-Strain Curves (Flexural Test) of Multilayer Composites (1CF).

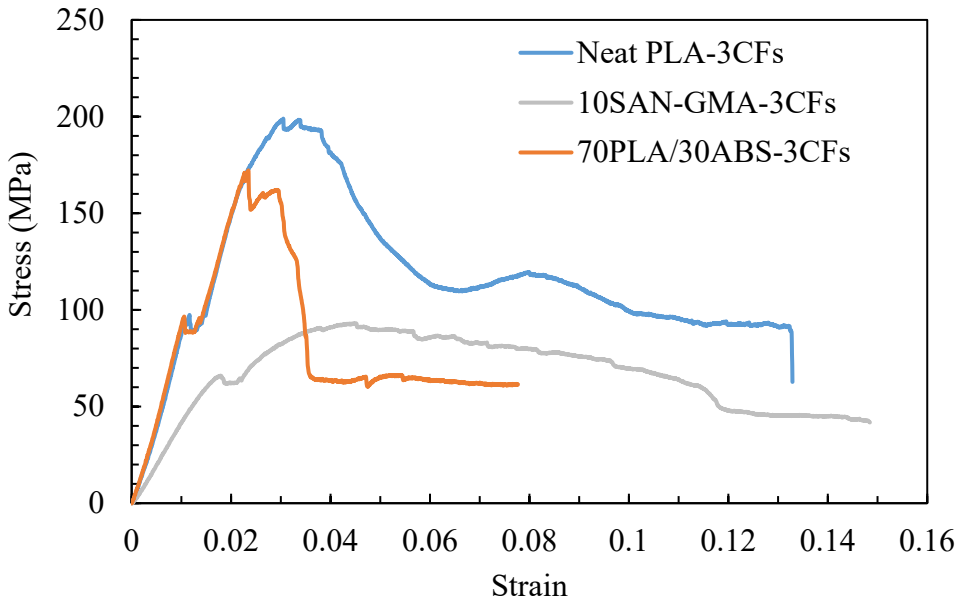

Figure D.4. Representative Stress-Strain Curves (Flexural Test) of Multilayer Composites (3CFs).